Human adipose tissue-derived multipotent mesenchymal stromal cells: focus on exosomes and their role in T cell modulation

Anastasia Cheng
Division of Experimental Medicine
McGill University, Montreal
January 2018

A thesis submitted to McGill University in partial fulfillment of the requirements of the degree of Master of Science in Experimental Medicine

Abstract

Background: Mesenchymal stromal cells (MSCs) possess immunosuppressive properties and are a promising candidate for treatment of immune mediated diseases. Previous work from our laboratory demonstrated that the inhibitory effects of MSCs on T cells decline with advancing age and co-morbidities including atherosclerosis and diabetes. The mechanisms underlying these age-associated changes remain undefined. We hypothesize that age and chronic inflammation alters the secretome of MSCs, specifically the quantity and cargo of exosomes, which may be responsible for the decline of their immunosuppressive effects.

Methods: MSCs, defined according to the International Society of Cellular Therapy, were isolated from adipose tissue of pediatric (PED) (15.9 ± 1.6 years, n=10), osteoarthritis (OA) (62.8±8.7 years, n=6) and atherosclerosis patients (ATH) (62.8±8.7 years, n=9). Extracellular vesicles (EVs) were harvested from resting and IFN-γ/TNF-α primed MSC CM by ultracentrifugation to enrich for exosomes. We quantified the size, distribution, and yield of EVs using nanoparticle tracking analysis and evaluated the cargo of the vesicles using mass spectrometry. The immunopotency of MSC exosomes was assessed in an *in vitro* assay that measured allogeneic MSC-mediated suppression of $CD4^+$ T cells activated with anti-CD3/CD28 coated beads. The expression of genes involved in vesiculation ('vesiculome') were measured using RT-qPCR.

Results: MSCs produced higher amounts of exosomes containing the anti-inflammatory protein TSG-6 upon licensing, and these vesicles were capable of inhibiting T cell proliferation *in vitro*. Licensing upregulated the expression of Rab GTPases (*RAB5A*, *RAB31, RAB27B*), tetraspanins (*CD63, CD82*) and the ESCRT-III component *CHMP4B*. Licensed MSCs obtained from adult donors (i.e., ATH and OA) produced lower amounts of exosomes compared to MSCs from young

healthy donors (i.e., PED). TSG-6 content in ATH MSC exosomes were also lower compared to PED. Analysis of the MSC vesiculome showed lower expression of *TSG101* and *RAB27B* in ATH MSCs suggesting defects in intraluminal vesicle formation and exosome release.

Conclusion: In response to activation (i.e., when exposed to an inflammatory environment), MSCs produce exosomes capable of inhibiting T cell proliferation. Donor age and disease status, specifically ATH, an age-related disease associated with chronic low-grade inflammation, reduces MSC exosome production and decreases their ability to suppress inflammation. Interventions aimed at improving exosome biogenesis may enhance the therapeutic effects of MSCs obtained from adult/elderly and ATH patients.

Résumé

Contexte: Les cellules stromales mésenchymateuses (CSM) possèdent des propriétés immunosuppressives et sont un candidat prometteur pour le traitement des maladies inflammatoires à médiation immunitaire. Les travaux de recherches précédant de notre laboratoire ont démontré que les effets inhibiteurs des CSM sur les lymphocytes T diminuent avec l'âge et les comorbidités tel que l'athérosclérose et le diabète. Les mécanismes associés à ces changements avec l'âge restent indéfinis. Nous émettons l'hypothèse que l'âge et l'inflammation chronique modifie le sécrétome des CSM, en particulier la quantité et la cargaison des exosomes de CSM, qui peuvent être responsables de la diminution des effets immunosuppresseurs des CSM.

Méthodes: Les CSM, définies selon la Société Internationale de Thérapie Cellulaire, ont été isolées à partir de tissu adipeux pédiatrique (PED) (15.9 ± 1,6 ans, n = 10), l'ostéoarthrite (OA) (62,8 ± 8,7 ans, n = 6) et patients atteints d'athérosclérose (ATH) (62,8 ± 8,7 ans, n = 9). Les vésicules extracellulaires (VE) ont été récoltées par ultracentrifugation à partir de CSM activée par IFN-y / TNF-α pour enrichir les exosomes. Nous avons quantifié la taille, la distribution et le rendement des VE en utilisant l'analyse de suivi individuel des nanoparticules et nous avons évalué la cargaison des vésicules en utilisant la spectrométrie de masse. L'immunosuppression des exosomes de CSM a été évaluée dans un essai in vitro qui a mesuré la suppression de prolifération des cellules T $CD4^+$ activées avec des billes revêtues d'anticorps anti-CD3/CD28 médiée par CSM allogène. L'expression des gènes impliqués dans la vésiculation («vésiculome») a été mesurée à l'aide de PCR en temps réelle.

Résultats: Les CSM ont produit des quantités plus élevées d'exosomes contenant la protéine anti-inflammatoire TSG-6 lors de l'activation, et ces vésicules étaient capables d'inhiber la prolifération des lymphocytes T *in vitro*. L'activation a augmenté l'expression des GTPases Rab (*RAB5A, RAB31, RAB27B*), des tétraspanines (*CD63, CD82*) et la composante *CHMP4B* de ESCRT-III. Les CSM activées obtenues des donneurs adultes (c'est-à-dire OA et ATH) ont produit moins d'exosomes que les CSM provenant de jeunes donneurs sains (c'est-à-dire PED). La teneur en TSG-6 des exosomes ATH CSM était également inférieure à celle de la PED. L'analyse du vésiculome des CSM montrent une expression plus faible de *TSG101* et *RAB27B* dans les CSM ATH suggérant des défauts dans la formation de vésicules intraluminales et la libération d'exosomes.

Conclusion: En réponse à l'activation (c'est-à-dire lorsqu'ils sont exposés à un environnement inflammatoire), les CSM produisent des exosomes capables d'inhiber la prolifération des cellules T. L'âge des donneurs et l'état de la maladie en particulier l'ATH, une maladie liée à l'âge associée à une inflammation chronique de basse intensité, réduit la production d'exosomes des CSM, ce qui diminue leur capacité à supprimer l'inflammation. Les interventions visant à améliorer la biogenèse de l'exosome peuvent améliorer les effets thérapeutiques des CSM obtenues chez des patients âgés et des patients atteints d'ATH.

Acknowledgements

First and foremost, I want to thank my supervisor Dr. Inés Colmegna for her guidance during my research and writing of this thesis. Inés has challenged me to work my hardest since day one. Thank you for your patience and for being such a knowledgeable, enthusiastic, and dedicated mentor.

I am sincerely grateful to my laboratory members Dr. Maximilien Lora, Dr. Özge Kizilay Mancini, and Natalia de França Shimabukuro. Not only am I thankful for their many insightful conversations and their co-operation during the development of this thesis, but also for their encouragement whenever I was in need.

I consider it an honor to have worked with Dr. Janusz Rak and his laboratory members, Laura Montermini, Dr. Esterina D'Asti and Dr. Dong Sic Choi, who continuously lend their expertise in exosome research and technical assistance. I am gratefully indebted to their collaboration and feedback during the course of this project.

I would like to also thank Dr. Francis Rodier and his laboratory members at Le Centre Hospitalier de l'Université de Montréal; and Dr. Ursula Stochaj and her laboratory members at McGill University for their continuing collaboration on MSC characterization and secretome analyses.

My thesis committee guided me through my MSc. I would like to thank my academic advisor Dr. Jun-Li Liu and committee members Dr. Martin Olivier, Dr. Bertrand Jean Claude, and Dr. Dominique Shum-Tim for their insightful comments and encouragement.

I must express my very profound gratitude to Dr. Joyce Rauch who helped me complete the writing of this thesis. Joyce always offered an open ear for discussion whenever I had difficulties with writing.

It has been a pleasure to work in the Infectious Diseases and Immunity in Global Health Program (IDIGH) at the Research Institute of the McGill University Health Center (RI-MUHC). The IDIGH not only provided me access to the equipment used in this project but also opportunities to discuss this work with other researchers and students in the immunology field.

I would also like to thank Sylvain Chaperon from the MUHC for drawing the blood used in the immunosuppression experiments.

This thesis is dedicated to family, thank you for always supporting me throughout my endeavors.

Preface and Contribution of Authors

All samples included in the experiments that I have performed were obtained through ERB approved protocols (GEN-10-107 and A01-M05-12A 'The effects of aging on human mesenchymal stem cells'). Samples were obtained from patients recruited at the (1) Jewish General Hospital (JGH), (2) Shriners Hospital for Children (SHC), and (3) Royal Victoria Hospital (RVH). Dr. Hudson (JGH), Dr. Hamdy (SHC) and Dr. Shum-Tim (RVH) provided the samples from adults with osteoarthritis (OA), healthy children (PED), and adults with atherosclerosis respectively (ATH).

All experiments presented in this thesis were performed by Anastasia Cheng under the supervision of Dr. Colmegna except:

(1) Isolation and phenotype characterization of MSCs: were performed by Anastasia Cheng and previous members of Dr. Colmegna's laboratory (Dr. Lora, Dr. Kizilay Mancini, and Natalia de França Shimabukuro) (Figure 1).

(2) Nanoparticle tracking analysis and RT-PCR experiments were performed by Anastasia Cheng with technical assistance from Laura Montermini and Dr. D'Asti from Dr. Rak's laboratory (Figure 8, 12, 14, and 17).

(3) The transmission electron microscopy (EM) images were obtained at the McGill University EM facility by Dr. Lira Filho from Dr. Olivier's laboratory (Figure 8).

(4) The proteomic analysis of the exosome cargo was performed at the Proteomics Platform at the RI-MUHC by Lorne Taylor and analyzed by Anastasia Cheng (Figure 10, 15).

Table of Contents

Abbreviations

Atomic Force Microscopy	AFM
Adipose Tissue Derived MSCs	aMSCs
Atherosclerosis	ATH
Amyloid Beta Protein	Aβ
B Cell Receptor	BCR
Bone Marrow	BM
Coronary Artery Bypass Graft	CABG
Cellular Adhesion Molecule	CAM
Cluster of Differentiation	CD
Carboxyfluorescein Diacetate Succinimidyl Ester	CFSE
Conditioned Medium	CM
Concanavalin A	ConA
Cytotoxic T-Lymphocyte Associated Protein 4	CTLA-4
Database for Annotation, Visualization and Integrated Discovery	DAVID
Dendritic Cells	DCs
DNA Damage Response	DDR
Dynamic Light Scattering	DLS
Deoxyribonucleic Acid	DNA
Eukaryotic Translation Elongation Factor 1A1	EEF1A1
Enzyme-linked Immunosorbent Assay	ELISA
Enolase	ENO
Endosomal Sorting Complexes Required for Transport	ESCRT
Extracellular Vesicles	EVs
Fas Ligand	FasL
Fibroblast Growth Factor	FGF
Gene Ontology	GO
Glyceraldehyde 3-phosphate dehydrogenase	GAPDH
Graft-Versus-Host Disease	GVHD
Hepatocyte Growth Factor	HGF
Hypoxia-Inducible Factor	HIF
Human Leukocyte Antigen	HLA
High Performance Liquid Chromatography	HPLC
Intercellular Adhesion Molecule 1	ICAM-1
Indoleamine 2,3 Dioxygenase	IDO
Interferon-Gamma	IFN-γ
Interleukin	IL-
Intraluminal Vesicles	ILVs

International Society for Cellular Therapy	ISCT
International Society for Extracellular Vesicles	ISEV
Integrin	ITG
Lipopolysaccharide	LPS
Myocardial Infarction	MI
Mixed Lymphocyte Reaction	MLR
Myelin Oligodendrocyte Glycoprotein	MOG
Multiple Sclerosis	MS
Mesenchymal Stromal Cells	MSCs
Multivesicular Body	MVB
Microvesicles	MVs
Molecular Weight Cut Off	MWCO
N-Acetyl-L-Cysteine	NAC
Natural Killer	NK
Nanoparticle Tracking Analysis	NTA
Osteoarthritis	OA
Peripheral Blood Mononuclear Cells	PBMCs
Programmed Death Ligand 1	PD-L1
Platelet Derived Growth Factor	PDGF
Polyethylene Glycol	PEG
6-phosphofructo-2-kinase/fructose-2,6-biphosphatase 3	PFKFB3
Prostaglandin E2	PGE_2
Phosphoglycerate Kinase	PGK
Phosphoglucomutase	PGM
Phytohemagglutinin	PHA
Phosphoinositide 3-kinase	PI3K
Pyruvate Kinase M2	PKm2
Protein Organic Solvent Precipitation	PROSPR
Size Exclusion Chromatography	SEC
Soluble N-ethylmaleimide-sensitive factor attachment protein receptors	SNAREs
Superoxide Dismutase 3	SOD3
Type 2 Diabetes	T2D
Transmission Electron Microscopy	TEM
Transforming Growth Factor Beta	TGF-β
T Helper Cell	Th
Transgolgi Network	TGN
Tumor Necrosis Factor Alpha	TNF-α
TNF-related apoptosis-inducing ligand	TRAIL
Regulatory T Cells	Treg
Tumor suppressor-activated pathway 6	TSAP-6

Tumor Necrosis Factor Stimulated Gene 6	TSG-6
Tumor Susceptibility Gene 101	TSG101
Ultrafiltration	UF

Chapter 1. Background

Section 1: Mesenchymal Stromal Cells (MSCs): Key Players in Immune Tolerance

1.1.1 MSCs: Definition and Biological Significance

MSCs are non-hematopoietic plastic-adherent cells most commonly isolated from the bone marrow (BM) and adipose tissue. They are also present in most other adult tissues, feto-maternal interface tissues (i.e., amniotic fluid, amniotic membrane, umbilical cord, placenta); and embryonic-fetal tissues [1-6]. MSCs were initially called 'mesenchymal stem cells'. However, a lack of evidence demonstrating the self-renewal capacity of MSCs *in vivo* (a defining feature of stem cells) lead to the current term 'multipotent mesenchymal stromal cells' by the International Society for Cellular Therapy (ISCT) [7]. Multipotency refers to the ability of MSCs to differentiate *in vitro* into multiple mesodermal lineages including osteoblasts, chondroblasts and adipocytes, which generate bone, cartilage and fat respectively [8]. The term 'mesenchymal' alludes to the origin of this cell type, the mesenchyme, a crucial tissue that forms most of the connective tissues in the body during embryonic development. Although the mesenchyme does not exist after development, MSCs persist throughout the body to maintain and repair tissues. MSCs are called 'stromal cells' because they are found in the stromal compartment of resident tissues [7].

MSCs have a broad range of functions, including: attenuation of tissue injury [9], inhibition of fibrotic remodeling [10], angiogenesis [11], reduction of oxidative stress [12] and modulation of the innate (i.e., dendritic cells [DCs], neutrophils, macrophages and natural killer [NK] cells) and adaptive (i.e., T and B cells) arms of the immune system [13-19]. These functional properties provide the rationale for using MSCs for the treatment of tissue injury and inflammatory conditions. A proof of concept demonstrating the therapeutic value of MSCs was reported in 2004, describing the successful treatment of a patient with grade IV acute graft-versus-host disease

(GVHD) [20]. This case lead to the use of MSCs in clinical trials. Currently, there are over 800 trials evaluating the therapeutic efficacy of MSCs (https://clinicaltrials.gov/ct2/results/details?term=mesenchymal), making MSCs the most commonly studied cell type for therapy. Notably, many of these trials have yielded suboptimal outcomes and several have failed to meet their primary endpoint of efficacy. In order to reliably assess the therapeutic effects of MSCs and advance MSC-based therapies beyond the experimental phase, two important challenges need to be resolved: (1) standardizing cell isolation (Section 1.1.2 – Standardization and Heterogeneity of MSCs), and (2) increasing the effectiveness (potency) of MSCs by defining metrics to predict the therapeutic effects of these cells (Section 1.1.3 – Elucidation of MSC Effects) [21, 22].

1.1.2 Standardization and Heterogeneity of MSCs

The cell preparations administered to patients in different clinical trials vary widely in their preparation and characteristics, and this may explain the inconsistent results in the therapeutic efficacy of MSCs. This is, in part, due to the lack of specific markers to identify MSCs. To address this issue, the ISCT proposed three minimal criteria to define MSCs and thus standardize the work between researchers in this field [1]. The three criteria defining MSCs are: (1) ability to adhere to plastic under standard culture conditions; (2) surface expression of MSC markers (CD90, CD73, and CD105), and absence of leukocyte (CD45), hematopoietic progenitor (CD34), monocyte (CD14 or CD11b), B cell (CD19 or CD79) and activation (HLA-DR) markers; and (3) capacity to differentiate to osteoblasts, chondrocytes and adipocytes (demonstrated by staining of MSCs cultured *in vitro*) [1]. *Following these recommendations, the MSCs used in my experiments fulfill the ISCT minimal criteria (Figure 1).*

There are several factors that can lead to heterogeneity in the preparation of MSCs [23]:

1) **Tissue Source:** MSCs obtained from different tissue sources vary in their proliferative capacity. Therefore, it cannot be assumed that all tissue-derived MSCs will display equivalent functional properties [23]. BM and adipose tissue are the two most commonly used sources of MSCs in ongoing clinical trials. Because adipose derived human MSCs (aMSCs) are more abundant, can be expanded to larger numbers, and can be obtained through less invasive procedures compared to BM, *all of my experiments use MSCs obtained from subcutaneous adipose tissue* [3, 24-26].

2) **Donor Selection:** The donor from whom the MSCs are derived has been shown to affect the immunomodulatory properties of the cells, thus influencing their therapeutic potential. Our laboratory previously reported that age and age-associated chronic inflammatory conditions, such as type 2 diabetes (T2D) and atherosclerosis (ATH), affect the immunoregulatory function of MSCs [27]. *To assess the age and disease-associated changes underlying the reduced immunosuppressive abilities of MSCs, I have compared MSCs from three patient populations:*

    1- *Young healthy individuals (PED, n=10; age 15.9 ± 1.6 years) undergoing programmed orthopedic surgery. Indications for surgery in these patients included: ligament reconstruction and excision of benign tumors.*

    2- *Adults without systemic inflammatory diseases (OA, n=6; age 62.8 ± 8.7 years) undergoing programmed orthopedic surgery. The indication for surgery in these patients was osteoarthritis and the type of surgery was hip or knee joint replacement.*

    3- *Adults with a systemic inflammatory disease (ATH, n=9, age 65.2 ± 11.9 years) undergoing programmed cardiovascular surgery. The indication for surgery in*

these patients was coronary artery disease and the type of surgery was coronary artery bypass graft (CABG).

The selection of these three patient populations allows the comparison of the effect of age in MSC-exosomes (PED vs OA); as well as the effect of chronic inflammation on MSC-exosomes (OA vs ATH age-matched). We acknowledge that the ideal comparator group for the effect of age in PED MSCs would have been healthy individuals undergoing surgeries for similar indications than the PED group. However, practically those patients would have been younger and not age-matched to the ATH group. Of relevance, patients with OA have degenerative joint disease without evidence of systemic inflammation. The demographic characteristics of the MSCs donors of my experiments are summarized in Table 1.

3) **Cell Culture Techniques:** The conditions used during the expansion of MSCs *in vitro* can affect cellular function. These extrinsic factors include: basal medium (e.g., glucose content) [28]; growth supplements (e.g., serum, growth factors) [29, 30]; environment (e.g., density, hypoxia, mechanical strain) [31-33]; and passage number [34]. *In my experiments, these conditions were carefully optimized and controlled to limit the impact of ex vivo culture on MSC function (Section 2.1.2 – Isolation and Expansion of aMSCs).*

1.1.3 Elucidation of MSC Effects

The effective translation of MSCs into clinical care requires functional predictors of the effects of MSCs and an understanding of their mechanisms of action. T cell suppression assays are considered a reproducible surrogate measure of the immunomodulatory capacity of MSCs [35]. T cells play a key role in inflammation, therefore suppressing inappropriate T cell activity is crucial

to restoring immune tolerance and tissue homeostasis. *Our laboratory uses an in vitro potency assay that evaluates T cell proliferation as a readout of MSC suppressive ability* [27, 36]. *We have taken into consideration several aspects suggested by the ISCT during the design of the potency assay* [23, 37]. *For instance, we utilize monocyte-depleted peripheral blood mononuclear cells (PBMCs) obtained from a single healthy donor to limit the inter-donor variability which can affect the reproducibility of the potency assay [27]. The PBMCs are also depleted of monocytes because differences in monocyte content between PBMC preparations can cause inter-assay variability. Moreover, in the assay, the PBMCs are stained with carboxyfluorescein diacetate succinimidyl ester (CFSE) and the T cells within the PBMCs are stimulated to proliferate with anti-CD3/CD28-coated beads (ratio: 1 bead: 1 PBMC). These beads activate T lymphocytes in a physiologically relevant manner similar to antigen-presenting cells. The final read-out of the assay is the proliferation of viable $CD4^+$ T cells after a 4 day co-culture with MSCs or cell culture supernatant (i.e., MSC conditioned media or 'MSC CM') (Section 2.1.6 – MSC CM Preparation), which is assessed by measuring cell division (flow cytometry)* [38].

In vitro potency assays, such as ours, have shown that both cell contact-dependent and -independent mechanisms contribute to the immunosuppressive effects of MSCs. *In my experiments, we focused on contact-independent effects (contact-independent mechanisms are summarized in Table 2)*. Di Nicola and colleagues were the first to show that the inhibitory effects are greatest when MSCs and T cells are in direct contact, but MSCs still suppress T cell proliferation in the absence of cell contact (i.e., using a transwell system) [28]. Using neutralizing antibodies, they demonstrated that transforming growth factor beta (TGF-β) and hepatocyte growth factor (HGF) released by MSCs inhibit T cells synergistically [17]. Subsequently, Djouad et al. reported that the supernatant collected from MSC and T cell co-cultures, but not from MSCs

alone, is capable of suppressing T cell proliferation. These findings suggest that MSCs are not constitutively immunosuppressive, and that this property is triggered in response to specific stimuli (i.e., MSC licensing) [39]. *In my project, we investigate the effect of MSC licensing on the secretion of factors involved in T cell suppression, in particular exosomes.*

1.1.4 The Importance of Licensing MSCs

MSCs polarize towards enhanced inhibitory functionality upon exposure to various pro-inflammatory cytokines, such as interferon (IFN)-γ, tumor necrosis factor (TNF)-α, IL-1α or IL-1β. This process is known as 'MSC licensing' or also as 'MSC priming' in the literature; thus, these terms are used interchangeably in this thesis. IFN-γ, one of the first cytokines to be released by T cells upon activation and an important driver of the expansion of surrounding lymphocytes, is key for MSC licensing. IFN-γ enhances the suppressive ability of MSCs by inducing the expression and/or secretion of immunomodulatory factors, including indoleamine 2,3 dioxygenase (IDO), prostaglandin E2 (PGE_2), HGF, IL-10 and TGF-β1 [40, 41]. TNF-α is another pro-inflammatory cytokine that influences the suppressive ability of MSCs. TNF-α is synthesized by macrophages and is involved in the acute phase of systemic inflammation. This cytokine increases the expression of chemokine receptors on MSCs, resulting in enhanced migration towards chemokine attractants. MSC homing efficiency has been shown to be improved by TNF-α licensing prior to transplantation [42]. In addition to enhancing the migratory capacity of MSCs, TNF-α licensing increases the release of TNF-α-induced protein 6 (TSG-6). This secreted glycoprotein induces anti-inflammatory M2 macrophages and reduces T cell proliferation [43-45]. Compared to priming with IFN-γ or TNF-α alone, priming MSCs with a combination of these two cytokines greatly enhances the inhibitory effects of MSCs through the production of immunomodulatory factors (i.e., PGE_2, IDO, programmed death ligand 1 [PD-L1], and superoxide

dismutase 3 [SOD3]) [46-49]. This 'synergistic licensing effect' achieved by the concomitant use of TNF-α and IFN-γ is recommended by the ISCT because it not only stimulates the immunomodulatory functions of MSCs, but also recapitulates the environment that MSCs are exposed to upon transfer into patients with dysregulated immune responses or systemic inflammation [23]. *Since measurable immunological features of MSCs, both at the phenotypic and functional levels, depend on their activation status at the time of interaction with effector cells, comparing resting and licensed MSCs (treated with IFN-γ + TNF-α) is most informative. Accordingly, my experiments have included these two conditions when appropriate.*

1.1.5 Involvement of MSC Extracellular Vesicles (EVs) in Immune Regulation

The therapeutic effects of MSCs were initially thought to depend on the migration, engraftment and differentiation of these cells in/to damaged tissues [50]. However, transplantation studies using animal models of myocardial infarction (MI) demonstrated that long term engraftment is not necessary for MSCs to exert their therapeutic effects [51, 52]. In fact, MSC CM alone can reproduce the effects of the cells [53, 54]. The current consensus is that the trophic factors secreted by MSCs are capable of modulating the microenvironment and influencing the activity of resident cells [54]. These factors include cytokines, growth factors, and hormones that alter the activity, viability and proliferation of cells in the vicinity leading to tissue regeneration and immunomodulation [55, 56]. Current research aims to elucidate, augment and harness the factors secreted by MSCs, and to determine whether these paracrine mechanisms alone can be used as a cell-free therapy for immune mediated and inflammatory diseases.

Although a variety of factors secreted by MSCs contribute to their immunomodulatory ability, no single element alone is capable of reproducing the effects of the MSC secretome. Recently, EVs have been proposed to be the 'ideal vehicle' for mediating the therapeutic effects

of MSCs [57]. EVs are organelles enclosed by a lipid bilayer that are capable of containing and protecting inhibitory factors secreted by MSCs, carrying them to target cells. In animal models of MI, MSC-derived exosomes (hereafter referred to as "MSC exosomes") are considered the main therapeutic component released by MSCs and are able to reproduce the effects of the cells themselves [12]. On this basis, MSC exosomes were first used in 2014 to treat a patient with therapy-refractory GVHD [58]. Prior to transfer, the immunomodulatory properties of the MSC exosomes were assessed using an *in vitro* MLR assay and shown to be capable of reducing the pro-inflammatory cytokine response of the patient's PBMCs [58]. Administration of these vesicles to the patient resulted in a significant improvement in the GVHD symptoms within two weeks, which was maintained for 4 months [58]. *Although MSC exosomes could be a promising alternative to cellular therapy, the actual contribution of these vesicles to MSC potency and the mechanisms mediating the effects of exosomes are poorly defined and are the focus of my research (Section 1.3.2 – T cell suppression by MSC Exosomes).*

Section 2: EVs: Key Mediators of Cell-to-Cell Communication

1.2.1 EVs: Definition and Biological Significance

Communication between cells and the environment is essential for the survival of unicellular and multicellular organisms. Cells have developed different strategies of communication to monitor the surrounding environment and co-ordinate their activities. These strategies consist of direct physical contact between cells, including receptor-mediated interactions and cellular junctions, and the secretion of soluble factors (such as cytokines, chemokines and growth factors). During the past 10 years, EVs have been recognized as an important mode of intercellular communication, participating in normal physiological (e.g., immune regulation, pregnancy) and pathological processes (Table 3). Typical EVs are composed of a lipid bilayer containing transmembrane proteins and cytosolic components such as proteins, lipids, DNA, messenger RNA (mRNA), microRNA (miRNA), and long noncoding RNA from the cell of origin (Figure 2) [59, 60]. The lipid membrane protects the internal cargo of EVs from enzymatic degradation in the extracellular space, allowing these vesicles to act as efficient vehicles of communication between cells. The contents and the functional properties of EVs are heterogeneous and dynamic, differing between cellular sources; changing with the cell's activation state; and responding to environmental conditions.

1.2.2 EV Subtypes

Three subgroups of EVs have been defined based on the mode of EV biogenesis, internal contents, and membrane constituents, (summarized in Table 3):

1. **Apoptotic bodies** are membrane enclosed vesicles released by cell blebbing during apoptosis. Whereas microvesicles and exosomes are produced by living cells, apoptotic bodies are only formed during programmed cell death. These vesicles are very large (1-4 μm in diameter) and

carry tightly packed organelles and DNA fragments [61]. Due to their size, apoptotic bodies can be separated from other types of EVs by low speed centrifugation. Apoptotic bodies are recognized for clearance by macrophages via phosphatidylserine, thrombospondin (CD36), and vitronectin receptors (αVβ3 integrin) [62, 63].

2. **Microvesicles** (MVs), also called ectosomes or microparticles, are released from cells by direct budding of the plasma membrane. Membrane budding/vesicle formation is a result of phospholipid asymmetry initiated by the sustained increase of cytosolic Ca^{2+} and subsequent phosphatidylserine translocation to the outer-membrane leaflet. The resulting phospholipidic imbalance is co-ordinated by phospholipidic pumps: an inward-directed pump (flippase); an outward-directed pump (floppase); and a lipid scramblase, responsible for non-specific redistribution of lipids across the membrane [64]. This budding process is then completed by actin-myosin interactions, leading to the contraction of the cytoskeleton. Unlike exosomes, which are formed internally, MVs are formed on the surface of the cell and thus have an unrestricted size ranging from 100 to 1,000 nm in diameter. Although the size of MVs can overlap with exosomes, their mode of biogenesis differs. As a result, MVs carry different membrane constituents and internal contents. For example, unlike exosomes, MVs are devoid of transferrin receptors, which traffic between the cell surface and early endosomes [65]. MVs have also been suggested to carry specific cellular components, particularly those involved in cell-matrix interactions and matrix degradation [66].
3. **Exosomes** are the smallest (50-150 nm in diameter) and most homogeneous population of EVs. Whereas apoptotic bodies and MVs originate from membrane blebbing or shedding, exosomes are formed internally through the endolysosomal pathway (discussed in Section 1.2.3 – Exosome Biogenesis). Proteomic analyses of EV subtypes have shown that exosomes carry a

specific subset of proteins from their cell of origin, as well as a distinct set of proteins that are found in most exosomes regardless of cell type (exocarta.org/exosome_markers_new) [67]. Owing to their endosomal origin, exosomes contain proteins involved in a number of cellular processes including: membrane transport and fusion (e.g., Rab GTPases, annexins); multivesicular body (MVB) biogenesis (e.g., ALIX, TSG101, "soluble N-ethylmaleimide-sensitive factor attachment protein receptors" [SNAREs], clathrin); and lipid microdomains (e.g. flotillin, tetraspanin proteins CD63, CD9, CD81 and CD82) [68-72].

Although these three types of EVs have been defined, the current methods do not allow for the isolation of a pure preparation containing a single type of vesicle. In our work, we studied MSC-derived EVs that were enriched in exosomes (referred to as MSC exosomes). Technical and biological aspects relevant to EV isolation and characterization are reviewed in Section 1.2.5 – Exosome Isolation.

1.2.3 Exosome Biogenesis

Exosomes originate from the endosome, an organelle that is important for the recycling and degradation of extracellular ligands and cellular components. As endosomes mature into late endosomes, their membrane buds internally, forming intraluminal vesicles (ILVs) that contain specific subsets of proteins, lipids and cytosol. Following maturation, these MVBs can fuse either with lysosomes (for degradation) or with the plasma membrane (releasing their vesicles into the extracellular milieu as exosomes). MVB and ILV formation is co-ordinated by the "endosomal sorting complex required for transport" (ESCRT) machinery, which is composed of approximately 30 proteins assembled into four complexes (ESCRT-0, -I, -II and -III) with associated proteins (VPS4, VTA1, ALIX). These four complexes are responsible for recognizing and recruiting ubiquitin-tagged proteins and/or receptors to the endosome; clustering these ubiquitin-tagged

proteins; generating cargo containing vesicles; and membrane constriction/scission leading to vesicle cleavage [68]. ILVs can also be formed in an ESCRT-independent manner involving lipid metabolism (sphingomyelinases) and tetraspanin proteins (CD9, CD82, CD63) [73-76]. The subsequent fusion of MVBs with the plasma membrane and release of exosomes is regulated by several mechanisms including intracellular calcium changes; Rab GTPases (Rab 11, Rab27, Rab35); and SNAREs [77-81]. *My research has investigated the impact of MSC licensing and donor age/chronic inflammatory disease (ATH) on the expression of genes regulating exosome biogenesis and release (i.e., the 'vesiculome')* [82].

1.2.4 Exosome Production as an Inducible Process

Exosome production is both a constitutive and inducible process, depending on the environmental conditions and the cell type being investigated. For example, tumor cell lines, DCs and macrophages do not require stimulation to secrete exosomes, and can release vesicles constitutively. However, some cell types require stimulation (i.e., receptor crosslinking, stress [e.g., irradiation, hypoxia], and pro-inflammatory cytokines) to produce exosomes. For example, resting B cells secrete exosomes following the activation of cell surface receptors [83, 84]. B cell receptor (BCR) triggering not only increases exosome quantities but also alters the protein composition of the isolated vesicles [83]. BCR-induced exosome production is associated with enhanced MVB formation, as a consequence of intracellular calcium flux and PI3K (phosphoinositide 3-kinase) activation. Cell stress induced by irradiation has been shown to induce exosome production; in a study using splenocytes, irradiation-induced DNA damage activates the transcription factor p53, leading to an increase in exosome production in a tumor suppressor-activated pathway 6 (*TSAP6*) dependent manner [85]. These induced exosomes were proposed to be an important mechanism for cells to expel proteins that are not necessary for survival [85]. Cell

stress induced by hypoxia has also been shown to enhance the release of exosomes in breast cancer cell lines via the oxygen-sensitive hypoxia-inducible factor (HIF) pathway [86]. These exosomes carry elevated levels of mir-210 and miR-135b, which are important for promoting endothelial cell tubulogenesis and resolving hypoxia [86, 87].

Inflammation is another mechanism capable of inducing exosomes. Primary mast cells can be stimulated to secrete exosomes with the pro-inflammatory cytokine IL-4 [88]. The exosomes obtained from these stimulated mast cells possess the capacity to induce B and T lymphocyte proliferation and Th1 cytokine production (IL-2, IFN-γ, and IL-12) [88]. Recent evidence in mouse astrocytes suggests that the pro-inflammatory cytokine TNF-α stimulates the release of EVs that may play a role in neuroinflammation [89]. Furthermore, the addition of the antioxidant N-acetyl-l-cysteine (NAC) blocks TNFα-stimulated EV release, indicating a role of oxidative stress in this process [89]. IFN-γ stimulation has not been shown to alter exosome quantity, but has been demonstrated to affect the cargo of exosomes produced by DCs [90]. Indeed, IFN-γ-stimulated DC-derived exosomes carry microRNA species involved in myelin production and anti-inflammatory responses, and thus may be a potential therapy for demyelinating syndromes such as multiple sclerosis (MS) [90]. These studies support the concept that exosome quantity and cargo are modulated in cells following cell activation by pro-inflammatory cytokines. To our knowledge, the effect of MSC licensing with IFN-γ and TNF-α on exosome biogenesis and proteomic cargo has not yet been reported. *As part of my work, I assessed the effect of MSC licensing (by IFN-γ and TNF-α) on exosome secretion.*

1.2.5 Exosome Isolation

Various methods for exosome isolation have been described, but there is currently no accepted (“gold standard”) method to isolate and/or purify exosomes. The most efficient methods

depend on: (a) the specific scientific question asked, and (b) the downstream applications used. Ultracentrifugation has been the most widely used methodology but rapid methods, including Size Exclusion Chromatography (SEC) and/or the addition of precipitating agents such as Polyethylene glycol (PEG) or PRotein Organic Solvent PRecipitation (PROSPR) have also emerged [91, 92]. Other approaches include filtration and immunological separation. The advantages and limitations of each of these methods are discussed below.

- **Affinity chromatography** uses antibodies against exosome-specific surface proteins (e.g. CD81, CD63, CD9) or EV-binding molecules, such as heparin and heat shock protein-binding peptides, to isolate exosomes. However, in this method, intact vesicles are difficult to detach from the affinity matrix, thus limiting subsequent analyses of EV function [93].
- **Size exclusion chromatography (SEC)** separates EVs based on size. As the biological fluid/CM passes through Sepharose beads, larger molecules that cannot pass through the pores of the beads are eluted more quickly than smaller molecules that enter the beads because of differences in path length [94, 95]. SEC is typically performed using gravity flow to preserve the structure, integrity and the biological activity of the isolated EVs; as a result, this method is slow [96]. Despite this, SEC has several advantages, including its low cost, high reproducibility, and ability to separate exosomes from contaminating proteins and other vesicle types [96].
- **Ultrafiltration** drives biological fluids/CM through filters of specific pore size to eliminate larger vesicles, concentrate exosomes and eliminate contaminating proteins based on size or molecular weight. UF is fast, highly reproducible, and does not require special equipment [97]. However, exosomes can adhere to filtration membranes, or become damaged or deformed during the UF process.

- **Polymer-based precipitation** involves incubating the biological fluid with a polymer-containing precipitation solution such as PEG (e.g. ExoQuick™) to collect exosomes [98]. This method is rapid, but may precipitate other molecules besides exosomes. Moreover, the presence of polymer material may interfere with downstream functional analyses.
- **Density Gradient Ultracentrifugation** involves loading EVs on an iodixanol (Optiprep) or sucrose density gradient/cushion [99, 100]. This method can be used to prepare relatively pure preparations of exosomes by separating these molecules based on their densities and eliminating proteins and other vesicles. Exosomes typically float at a density of 1.13 to 1.19 g/ml in sucrose solutions. *In my research, MSC exosomes were collected by differential centrifugation. Their density was assessed after separation with an iodixanol cushion (Section 2.1.8 – Isolation of Exosomes from MSC CM)*.
- **Differential Ultracentrifugation** is the most widely used technique for separating EVs and collecting exosomes from biological fluids and CM [101]. Most published studies of exosomes apply this method to concentrate or partially purify exosomes. The International Society for Extracellular Vesicles (ISEV) published a position paper on EV isolation which states that large (i.e., MVs) and small EVs (i.e., exosomes) can be separated by centrifugal forces of 10,000-20,000g and 100,000-120,000g respectively [102]. *For my project, I have collected MSC exosomes by ultracentrifugation following the differential centrifugation protocol established by Théry et al.* (Section 2.1.8 Isolation of Exosomes from MSC CM) [103]. This method is summarized in Figure 3 and the rationale for each step is as follows:
    1) **Low speed centrifugation** eliminates cells, cellular debris and apoptotic bodies;
    2) **Filtration (0.22 µm filter)** removes MVs;

3) **Ultracentrifugation** (110,000xg for 2 hours) enriches for exosomes;
4) **Final washing and ultracentrifugation step** removes any contaminating proteins that may have co-precipitated with the exosomes [104].

1.2.6 Exosome Characterization

Following isolation, exosome preparations need to be characterized in terms of size and purity according to EV subtype markers. Currently there is no single marker that can uniquely identify each vesicle subtype. Therefore, it is necessary to combine multiple techniques. In 2014, ISEV published a position statement on the minimal experimental requirements to claim the presence of EVs in isolates [105]. These requirements are:

1. To present the general protein composition of the harvested exosomes, and to determine whether other types of EVs or subcellular products may have been co-isolated in the final product. This is done by evaluating at least one protein of each of the following categories:

   Category 1: Transmembrane or lipid-bound extracellular proteins, such as tetraspanins (i.e., CD9, CD63, CD81), integrins (i.e., ITG), growth receptors and adhesion molecules (i.e., CAM). These proteins are enriched in EVs and exosomes.

   Category 2: Cytosolic proteins with membrane or receptor-binding capacity, such as endosome or membrane-binding proteins (i.e., TSG101, annexins, Rabs), and signal transduction or scaffolding proteins (i.e., syntenin). These proteins are enriched in EVs and exosomes.

   Category 3: Intracellular proteins associated with compartments other than plasma membrane or endosomes, such as endoplasmic reticulum (i.e., calnexin), mitochondria (i.e., cytochrome C), and nucleus (i.e., histones) associated proteins.

These proteins are absent or under-represented in exosomes, but are present in other types of EVs.

Category 4: Extracellular proteins that bind specifically or non-specifically to membranes and may co-isolate with exosomes, such as cytokines, growth factors, and matrix metalloproteinases. These proteins have variable association with EVs.

2. To characterize the single vesicles in a mixture using transmission electron microscopy (TEM) or atomic force microscopy (AFM). Visualizing the size and morphology of individual vesicles provides an indication of the heterogeneity in the exosome preparation. In addition to microscopy, nanoparticle tracking analysis (NTA) and dynamic light scattering (DLS) can be used to measure the distribution of size in the population of vesicles isolated.
3. To demonstrate a dose-response relationship between the isolated exosomes and the *in vitro* function being investigated. The starting fluid and quantity of cells used to isolate the exosomes should be stated, and EV-depleted CM should be included as a negative control because it provides insight into the level of activity caused by the soluble versus the EV-associated components secreted by the cells. The ISEV also emphasizes the importance of ensuring the absence of serum-derived EVs, as they may co-isolate with the exosomes produced by the cells of interest and confound the resulting functional effect being measured.

In accordance with the ISEV's position statement, we characterized MSC exosomes isolated under serum free conditions by: (1) evaluating at least one protein of each category (1, 2 and 3) present and absent in exosomes in a semi-quantitative manner (i.e. Western blot); (2) visualizing and measuring the size distribution of the isolated exosomes with TEM and NTA; and

(3) assessing the T cell inhibitory effects of MSC exosomes at different concentrations (0,25, and 125 µg/ml). We have included MSC CM as a negative control for all experiments when necessary. We compared the protein isolates of our MSC exosomes with those reported in the Vesiclepedia database [106]. We acknowledge that although our preparations fulfill the ISEV's criteria to claim the presence of exosomes, we cannot call them 'purified exosomes' but rather 'exosome-enriched EVs'. In this thesis, we use the term 'MSC exosomes' to refer to 'exosome-enriched EVs from MSCs'.

1.2.7 Exosome Interaction with Targeted Cells

Exosomes exert their biological effects on targeted cells through the following mechanisms:

1. **Adhesion:** Exosomes may not need to be internalized by target cells to elicit cellular responses. Proteins on the surface of exosomes can interact with adhesion molecules or receptors on target cells, initiating downstream signaling cascades. Follicular DC-derived exosomes have been shown to display peptide-loaded MHC class II molecules on their surface that can activate immune cells upon interaction [107]. Moreover, Fas ligand (FasL) and TNF-related apoptosis-inducing ligand (TRAIL) on the surface of exosomes can trigger apoptosis via juxtacrine signalling [108]. Several proteins on the surface of exosomes are involved in vesicle attachment to target cells, including intercellular adhesion molecule 1 (ICAM-1), integrins (β1, α3, and αv), and lactadherin [109-111].
2. **Uptake:** More than one mechanism of exosome uptake has been reported (Figure 4) [112], including: receptor- (clathrin) mediated endocytosis involving a ligand on the exosome surface engaging specific receptors on the target cell [113]; lipid raft-

(caveolae) mediated endocytosis relying on the presence of sphingolipid-rich microdomains in the plasma membrane; and phagocytosis and micropinocytosis by the target cell [113, 114]. Regardless of the mechanism, exosomes uptaken by endocytosis deposit their vesicular cargo in the endosomal pathway of the recipient cell. These proteins are then sorted, and either targeted for degradation by lysosomes or redirected back to the plasma membrane.

3. **Fusion:** The exosome membrane can directly fuse with the plasma membrane of the target cell [115]. Following fusion, the exosomal cargo (microRNA, mRNA, proteins) is released into the cytoplasm, leading to stimulation of specific signalling pathways and changes in the transcriptome and phenotype of the recipient cells. As an example, exosomes from metastatic melanoma cells have been shown to fuse with the plasma membrane of target cells, transferring tumor-associated proteins (such as caveolin-1) [115].

1.2.8 General Functions of Exosomes and EVs

Exosomes have been shown to act as important vehicles for physiological (e.g., immune regulation) and pathological processes (e.g. tumor progression and neurodegenerative diseases):

- **Immune regulation:** Many studies have shown the importance of EVs in regulating immune cell activity. In fact, one of the earliest studies in the EV field obtained vesicles from B cells and showed that they were capable of presenting antigenic peptides to T cells and stimulating their proliferation [116]. Following this discovery, exosomes were harvested from tumor peptide-loaded DCs and shown to prime specific antitumor cytotoxic lymphocyte responses, which could inhibit the growth of established tumors *in vivo* [117]. In addition to their ability to stimulate an anti-tumor response, exosomes

have also been used to treat infectious diseases. Exosomes obtained from DCs pulsed with antigens from the obligate intracellular parasite *Toxoplasma gondii* were demonstrated to be an effective vaccine against *T. gondii* infection in mice [118]. Accumulating evidence suggests that MSC exosomes possess immunosuppressive properties and could represent a useful tool for treating immune-mediated diseases (described in Section 1.3.2 – T cell Suppression by MSC Exosomes).

- **Tumor progression:** EVs promote tumor progression and are involved in the evasion of immune surveillance. For example, highly metastatic melanoma cells have been shown to confer their metastatic properties to non-metastatic tumor cells through the transfer of Met72 expressing exosomes; these exosomes conferred to recipient cells the capacity to form metastatic tumor lung colonies. [119]. Similarly, EVs from human brain tumor (glioma) cells can transfer the oncogenic receptor EGFRvIII to surrounding cells [120]. In the context of immune evasion, EVs from patients with advanced melanoma, but not healthy controls, carry melanoma antigen gp100 and promote the generation of suppressive myeloid cells [121].
- **Neurodegenerative diseases:** Exosomes may be important vehicles for spreading toxic aggregates (i.e., mutated or misfolded proteins that can serve as template for oligomer formation) between neurons in the brain, leading to neurodegenerative diseases such as Parkinson's, Alzheimer's and prion-related diseases. Indeed, exosomes can carry α-synuclein and amyloid beta protein (Aβ) aggregates, which are implicated in the pathogenesis of Parkinson's and Alzheimer's disease respectively [122, 123]. Pathogenic prion proteins have also been observed to transfer between cells via exosomes [124].

Besides the above described exosomal functions, new evidence suggests a key role of these nanoshuttles, in short- and long-distance intercellular communication in the context of cardiovascular diseases (e.g., restoring cardiac function, attenuating cardiac fibrosis, stimulating angiogenesis, and modulating miRNA expression) [125]. Furthermore, exosomes have been proposed as potential diagnostic markers in post-MI [12]; and as therapeutic cell products for cardiac disease [126]. *My work, has characterized the impact of aging and chronic inflammation (ATH) on exosome production. My results will inform studies assessing MSC exosomes for diagnostic and therapeutic purposes, as well as attempting their functional modulation.*

Section 3: MSC Exosomes: Therapeutic Applications and Mechanisms of Action

1.3.1 Proteomic Cargo of MSC Exosomes

There is increasing interest in administering MSC exosomes as an alternative to cell therapy [58, 127]. However, the specific contents of these vesicles and their mechanism(s) of action remain unclear. So far, only three studies have characterized the proteome of MSC exosomes by mass spectrometry [128-130]; two of these studies (reviewed below) utilized the proteomic data to identify exosomal components that may be responsible for the observed effects.

1. Myocardial ischemia and reperfusion injury – Lim and colleagues demonstrated the cardioprotective effects of MSCs derived from human embryonic stem cells in models of myocardial ischemia and reperfusion injury [12, 128]. Using mass spectrometry and antibody arrays, they showed that MSC exosomes carried over 857 unique gene products (http://www.exocarta.org/) [128, 131]. They were able to identify 20S proteasome in MSC exosomes, which could reduce oligomerized protein levels in a mouse model of MI [128]. The

proteolytic activity of MSC exosomes may participate in ameliorating tissue damage by degrading soluble peptides in extracellular fluids and preventing potentially pathogenic protein aggregation. Their group further showed that, in addition to their proteolytic effects, MSC exosomes also carried gene products involved in the adenosine triphosphate (ATP)-generation stage of glycolysis (e.g., glyceraldehyde 3-phosphate dehydrogenase [GAPDH]), phosphoglycerate kinase (PGK), phosphoglucomutase (PGM), enolase (ENO), pyruvate kinase m2 isoform (PKm2) and phosphorylated 6-phosphofructo-2-kinase/fructose-2,6-biphosphatase 3 (PFKFB3) [132]; these proteins may be responsible for restoration of ATP and NADH levels in the ischemic/reperfused myocardium after treatment with MSC exosomes [132].

2. *Peripheral artery disease* – Human BM-derived MSC exosomes have been shown to induce tubule formation in human umbilical vein endothelial cells (HUVECs) via the NF-κB pathway [130]. The authors identified 1927 proteins associated with human BM MSC exosomes, of which 457 were not detected in the MSC proteome, suggesting specific enrichment of the latter proteins in exosomes [130]. These proteins were related to functions including angiogenesis, vasculogenesis, cell migration, and endothelial cell proliferation. Upon exposure to ischemic culture conditions (i.e., hypoxic and low serum), MSCs increased their secretion of exosomes, with cargo that was enriched in proteins related to canonical angiogenesis-associated pathways (i.e., cadherin; epidermal growth factor receptor [EGFR]; fibroblast growth factor [FGF]; and platelet-derived growth factor receptor [PDGFR]) [130]. This study suggests that MSCs exposed to ischemic conditions stimulate angiogenesis through the secretion of exosomes, leading to localized tissue healing.

In my research, we assessed the immunosuppressive capacity of MSC exosomes from pediatric, adult and ATH donors, and performed mass spectrometry to identify candidate molecules within the cargo of these vesicles that may be responsible for the observed effects.

1.3.2 T cell Suppression by MSC Exosomes

Several studies have previously evaluated the immunomodulatory properties of MSC exosomes, in particular their effect on proliferating T cells (Table 5). The majority of these studies (seven of 11) reported that MSC exosomes are able reproduce the T cell suppressive effects of their parental cells. However, the number of MSCs required to obtain the amount of exosomes exerting an equivalent suppressive effect (equipotency) to the starting cells is extremely large (approximately 40-fold). Therefore, it is clear that the MSC-derived exosomes are not as efficient as the cells themselves [133]. In addition to demonstrating the suppressive ability of MSC exosomes, many of these studies showed that MSC exosomes induce T cell apoptosis and/or promote Treg generation.

Importantly, exosomes obtained from licensed MSCs (treated with IL-1β, IFN-γ, or IFN-γ + TNF-α) functioned differently than their resting counterparts, and contained a significantly altered cargo [134-136]. IL-1β primed murine BM MSCs were shown to produce exosomes expressing higher levels of PD-L1, Gal-1 and TGF-β on their surface; these vesicles inhibited the proliferation of experimental autoimmune encephalomyelitis (EAE) mouse splenocytes to a greater extent than exosomes from resting MSCs [134]. Exosomes from IFN-γ primed human umbilical cord blood MSCs expressed MHC I and carried a more complete proteasome complex. Since these vesicles were enriched in unique Rab proteins, compared to exosomes from resting cells, the authors hypothesized that IFN-γ induces a separate route of exosome production [136]. Administration of MSC exosomes from resting cells ameliorated kidney ischemia-reperfusion

injury in rats, while exosomes from primed MSCs did not [136]. IFN-γ + TNF-α licensing lead to the release of EVs that were capable of inducing an immunophenotypic switch in resting MSCs (i.e., increased ICAM-1, MHC I and MHC II on the cell surface) and enhancing their suppressive effects on T cells (but not on NK and B cells) [135]. These findings suggest that licensed MSCs produce EVs that trigger surrounding resting MSCs to become immunosuppressive towards T cells.

Four of the studies reviewed did not observe an immunosuppressive effect of MSC exosomes. The discrepancy between these four 'negative' and the seven 'positive' studies can be attributed to differences in the culture conditions used to generate the MSCs, EV isolation, and the assessment of immunopotency. Inconsistencies between exosome preparations and functional readouts may explain why there is no clear consensus on the biologic effects of exosomes.

Both MSCs and derived exosomes are naturally occurring biological products, however exosomes offer many advantages over administering cells. For example, exosomes are non-viable and metabolically inactive, thus they are much more stable during long term storage (–80 °C) and safer because they do not pose risk for tumor formation [137]. Also there is the possibility of using of exosomes as a vehicle for drug design [138]. However, it is critical to elucidate the mechanisms underlying their potential therapeutic benefit. *To address the mechanisms involved in MSC suppression of T cell proliferation, my research assessed the: 1) effect of licensing on MSC exosome biogenesis; 2) relationship of MSC exosome cargo with the immunomodulatory effects of exosomes (i.e., T cell suppression); and 3) effect of chronological aging, a known factor that impairs the function of MSCs, on exosome production and function (see Section 1.4.1 – 'Aging' of MSCs).*

Section 4: Age-associated functional changes of MSC Exosomes

1.4.1 'Aging' of MSCs

Aging is the progressive loss of physiological integrity and function that occurs over time, increasing the vulnerability for chronic diseases, disability and death [139]. A key factor during aging is the functional decline of stem and progenitor cell activity (i.e., MSCs), which reduces the tissue's homeostatic and regenerative capacities [140]. Direct consequences of MSC aging include: (1) reduced capacity for tissue repair, (2) altered hematopoiesis, and (3) impaired immunomodulatory responses (i.e., pro-inflammation [141]). At a molecular level, aging affects several critical cellular processes, including but not limited to telomere maintenance (resulting in telomere attrition); DNA repair (leading to genomic instability); mitochondrial function (promoting oxidative stress); protein regulation (increasing aggregated/misfolded/unfolded proteins); and intercellular communication (senescence associated secretory phenotype) [139]. Abnormalities involving each of the above described molecular effectors of aging have been shown in human MSCs (Table 6). *The adult/elderly aMSCs included in my experiments have been previously characterized in our laboratory and proven to display the following hallmarks of aging:*

1. Shorter telomere lengths (Rodier et al., unpublished data)
2. Impaired DNA damage response (DDR) and increased DNA damage accrual [36, 142, 143]
3. Increase of intracellular ROS and impaired mitochondrial integrity [144]
4. Defects in the unfolded protein response (UPR) (Stochaj et al., unpublished data)
5. A pro-inflammatory secretome and an impaired ability to inhibit inflammatory T cell activity [145, 146]

In addition, we have observed other phenotypic changes typical of senescent MSCs in samples from adult/elderly donors, including morphological changes (i.e., enlarged and flattened

cell morphology) [36, 145]; decreased proliferation rates (i.e., doubling rates) and overall proliferative capacity (i.e., total population doublings) [147-149]; reduced number of CFU-F; and shifts in the differentiation capacity of the MSCs (i.e., reduced chondrogenic/osteogenic and increased adipose commitment) [146, 149, 150]. *These well-characterized MSC samples have been included in my work to evaluate the effect of age on aMSC exosome quantity, biogenesis and content.*

1.4.2 Implications of Aging on MSC Exosome Biogenesis

We recently reported that MSCs from adult/elderly donors are less efficient at suppressing allogeneic T cell proliferation (reduced immunopotency) due to their secretion of higher levels of 'senescence-associated' pro-inflammatory cytokines [145]. Although exosomes are key components of the MSC secretome, to date, only three studies have investigated whether exosome production or function is impacted by age. A comparison between human embryonic stem cell- and umbilical cord-derived MSCs reported an inverse correlation between exosome production and developmental maturity (i.e., age) [151]. Almost 10-fold more exosomes could be obtained per liter of immortalized embryonic stem cell-derived MSC CM compared to umbilical cord MSC CM (1282 μg versus 177 μg) [151]. Similar efficacy was achieved using the same exosome dose (regardless of the MSC source- embryonic vs umbilical cord) in a murine model of acute myocardial ischemia and reperfusion injury. These results support a negative correlation between the number of qualitatively similar exosomes released by MSCs and the developmental maturity of the donor.

Contrary to the previous study, Fafián-Labora et al. showed that the amount of protein derived from each MSC exosome decreases with donor age in rats; conversely, the quantity of exosomes released by each cell increases [152]. More importantly, miRNAs (miR-146a, miR-132

and miR-155) involved in regulating inflammatory cytokines and inhibiting the pro-inflammatory response of immune cells were decreased in elderly MSC exosomes [152]. These results suggest that exosomes obtained from elderly MSCs have an impaired capacity to induce anti-inflammatory cytokines and have reduced immunosuppressive activity.

Recently, aging has been shown to reduce the ability of BM MSC exosomes to inhibit tumor angiogenesis [137]. Although the size and quantity of exosomes produced by young and elderly BM MSCs were shown to be similar, a subset of 12 miRNAs was significantly downregulated in older BM MSC exosomes [137]. Replenishing older BM MSCs with these miRNAs (i.e., miR-340 and miR-365) restored the ability of these vesicles to inhibit tumor angiogenesis [137].

To our knowledge, these are the only three studies that have investigated whether aging impacts the quantity, cargo, and function of MSC exosomes. Importantly, none of these papers have examined whether age affects the mechanisms of exosome biogenesis in MSCs. *In my research, we have evaluated the biogenesis of exosomes, and the quantity and cargo of exosomes from young and adult/elderly human aMSCs. Moreover, we investigated whether changes in exosome production contribute to the age-associated decline of T cell suppression by MSCs.*

In summary, the effect of aMSC licensing, on exosome biogenesis has not been previously investigated. Furthermore, the cargo of aMSC exosomes that may be responsible for the immunoregulatory properties of exosomes remains to be elucidated. Although donor age and disease status is associated with altered MSC secretome and reduced immunopotency, it is not known whether exosome production is impacted. We hypothesize that changes in the quantity and cargo of exosomes occur following MSC priming; and that qualitative/quantitative differences in exosomal content could underlie the decline of MSC immunopotency observed during aging and age-associated conditions (i.e., ATH). To investigate these hypotheses, the specific aims of my research project are to:

1. Characterize MSC exosomes and assess their effects on $CD4^+$ T cell proliferation
2. Determine the effect of MSC licensing on exosome quantity and cargo
3. Compare the exosomes derived from MSCs of young and adult/elderly donors
4. Investigate the genes involved in the biogenesis of MSC exosomes, and whether gene expression changes occur with advancing donor age (i.e., PED versus OA) or chronic inflammatory diseases (i.e., OA versus ATH)

Chapter 2: Methods

2.1.1 Study Subjects

Study approval was obtained by the McGill University Health Center Ethics Review Board and participants provided written informed consent. Subcutaneous adipose tissue was obtained from a total of 18 patients, including ten young healthy individuals (PED, age 15.9 ± 1.6 years) undergoing elective orthopedic surgery, nine adults undergoing programmed cardiovascular surgery for ATH (ATH, age 65.8 ± 14.2 years), and six adults (OA, age 62.8 ± 8.7 years) undergoing elective orthopedic surgery for OA. The justification for the selection of these specific patient groups was discussed in page 16. Table 1 summarizes the demographic characteristics and cardiovascular risk factors of the study participants.

2.1.2 Isolation and Expansion of aMSCs

The human subcutaneous adipose tissue samples were washed with phosphate-buffered saline (PBS). The tissue was minced with surgical scissors, and digested with 0.05% collagenase (Millipore Sigma, Etobicoke, ON) in Hank's balanced salt solution (HBSS) (Invitrogen, Carlsbad, CA). The enzyme was then neutralized with 5% Gibco® MSCs Qualified fetal bovine serum (FBS, Thermo Fisher Scientific, Waltham, MA). The dissociated cells were collected by centrifugation (4˚C, 800 g for 5 min) and re-suspended in complete medium (1.0g/L glucose, with L-glutamine & sodium pyruvate Dulbecco's modified Eagle's medium [DMEM, WISENT Inc., St. Bruno, QC]) supplemented with 10% FBS and 1% penicillin/streptomycin (10,000 units/mL penicillin, 10,000 mg/mL streptomycin, WISENT Inc., St. Bruno, QC). MSCs were seeded at 1 gram of tissue/flask and cultured under standard conditions (5% carbon dioxide, 37°C) in 75cm^2 tissue culture flasks. Two days after the initial isolation, non-adherent cells were washed off and complete media was replaced. When MSCs reached 80% confluency, the cells were detached with

0.25% Trypsin-EDTA (37°C for 5 minutes) and re-seeded at a density of 5,000 cells/cm^2. Passage 1 MSCs were stored in liquid nitrogen. P4 MSCs were used for all experiments.

2.1.3 MSC Surface Markers

The expression of surface markers on MSCs was determined by multiparametric flow cytometry (BD LSRII; Becton Dickinson Co, Mountain View, CA). P2 MSCs were stained with the following fluorochrome-conjugated monoclonal antibodies (BD Biosciences, San Jose, CA): fluorescein isothiocyanate (FITC)-conjugated anti-CD90 (555595) and anti-CD45 (555482); phycoerythrin (PE)-conjugated anti-CD73 (555749); allophycocyanin (APC)-conjugated anti-CD34 (555824), anti-CD19 (555415) and anti-HLA-DR (560896); peridinin chlorophyll (PerCP)-conjugated anti-CD105 (560819), and anti-CD14 (562692). Data analysis was performed using FlowJo software 9.7.2.

2.1.4 MSC Tri-Lineage Differentiation

To assess the osteogenic and adipogenic potential, P4 MSCs were seeded in 24-well plates at a density of 5,000 cells/cm^2. After four days, the media was replaced with differentiation medium (Gibco™ StemPro® adipogenesis or osteogenesis differentiation kit, Thermo Fisher Scientific, Waltham, MA) or complete medium, and replenished every 3-4 days for 20 days. MSCs were fixed with 4% formaldehyde and stained with Alizarin Red S or Oil Red O (Electron Microscopy Sciences, Hatfield, PA) to evaluate osteogenesis and adipogenesis respectively. For chondrogenic differentiation, a micromass pellet of 250,000 MSCs was expanded in a 24-well plate for 20 days with Gibco™ StemPro® chondrogenesis differentiation medium (Thermo Fisher Scientific, Waltham, MA), fixed, sectioned (1 μm), and stained with Alcian Blue.

2.1.5 MSC Potency Assay

Peripheral blood mononuclear cells (PBMCs) were isolated from one unrelated donor (24-year-old non-smoking healthy female) using Lymphocyte Separation Medium through density gradient centrifugation (Mediatech, Inc., Corning, Manassas, VA). For monocyte depletion, PBMCs were cultured in Rosewell Park Memorial Institute medium (RPMI-1640) (WISENT Inc., St. Bruno, QC) supplemented with 10% FBS and 1% Penicillin Streptomycin overnight. The efficacy of monocyte depletion (95%) was verified by flow cytometry (Supplementary Figure S1).

Monocyte depleted PBMCs were stained with carboxyfluorescein succinimidyl ester (CFSE, Millipore Sigma, Etobicoke, ON) and stimulated with CD3/CD28 antibody coated beads (1 bead/cell) (Dynabeads® Human T-Activator CD3/CD28, Life Technologies, CA). CFSE stained, $2x10^6$ activated PBMCs (100µl) were added to either (a) $2.5x10^4$ MSCs in cell-cell contact dependent or independent (transwell) conditions, (b) MSC CM, or (c) MSC exosomes (25 or 125 µg/ml). CFSE stained, activated PBMCs cultured in complete medium or in exosome collection medium (maximal proliferation), and CFSE stained non-activated PBMCs (minimal proliferation) served as controls. After four days, the PBMCs were collected and stained with Annexin V (556421), 7-Aminoactinomycin D (7-AAD) (559925), and CD4-APC (555349) (BD Biosciences, San Jose, CA). The Expansion Index (EI) of Annexin $V^-/7AAD^-/CD4^+$ cells (viable $CD4^+$ T cells) was determined with FlowJo software. The immunopotency of MSCs (i.e., the proportion of non-proliferating $CD4^+$ T cells in the presence of MSCs) was calculated with the following formula:

$$CD4^+T\ cell\ Inhibition\ (\%) = 100 - \left(\frac{x - control}{maximal\ proliferation - control} \times 100\%\right)$$

Where:

x = EI of stimulated $CD4^+$ T cells in the presence of MSCs or derived products

Control = EI of non-stimulated $CD4^+$ T cells

Maximal proliferation = EI of stimulated $CD4^+$ T cells alone (without MSCs)

2.1.6 MSC CM Preparation

MSCs ($2.5x10^5$ cells/ml) were stimulated ('primed') or not ('resting') for 72 hours with 100 IU/mL (10 ng/mL) IFN-γ and 15 ng/mL TNF-α (R&D Systems, Minneapolis, MN) in exosome collection medium (phenol red-free low glucose DMEM containing 1% insulin-transferrin-selenium (ITS, Thermo Fisher Scientific, Waltham, MA). At 72 hours, MSC CM was collected and centrifugation was used to remove cells and larger MVs (4°C, 13,000g for 30 min) prior to storage at -80°C.

2.1.7 MSC Secretome Analysis

Soluble factors in resting and primed MSC CM were quantified with Meso Scale Discovery immunoassay kits (Meso Scale Diagnostics, Rockville, MD) according to manufacturer's instructions. Readouts were those involved in pro-inflammatory processes (i.e., IFN-γ, IL-10, IL12p70, IL-13, IL-1β, IL-2, IL-4, IL-6, IL-8), cytokines (i.e., GM-CSF, IL-12, IL-15, IL-16, IL-1α, IL-5, IL-7, TNF-β), chemokines (i.e., Eotaxin-1, Eotaxin-3, IP-10, MCP-1, MCP-4, MDC, MIP-1α, MIP-1β, TARC), angiogenesis (i.e., bFGF, Flt-1, PlGF, VEGF, VEGF-C) and vasculogenesis (i.e., CRP, ICAM-1, SAA, VCAM-1).

IDO activity of resting and primed MSC CM was quantified using a spectrophotometric assay measuring kynurenine concentration (product of IDO). Briefly, 50 µl of resting or primed MSC CM was mixed with an equal volume of 30% trichloroacetic acid (BioShop Canada Inc., Burlington, ON) and incubated at 50°C for 30 minutes. After centrifugation (3,000g for 10 min), the supernatant was mixed with an equal volume of Ehrlich's reagent (2% w/v 4-dimethylamino benzaldehyde in glacial acetic acid, Millipore Sigma, Etobicoke, ON) in a 96-well plate. The absorbance was read at 490 nm using Opsys MR™ Microplate Reader (Dynex® Technologies,

Chantilly, VA). The concentration of kynurenine was calculated based on a standard curve of commercially-available kynurenine (Millipore Sigma, Etobicoke, ON).

2.1.8 Isolation of Exosomes from MSC CM

Exosomes were obtained from MSC CM as previously described with some modifications [103]. MSCs were grown in T75 cm^2 flasks with complete medium until they reached 80% confluency. MSCs were then washed with PBS and cultured an additional three days in exosome collection medium with or without cytokines for priming. Cells and debris were eliminated from the CM by centrifugation at 800g for 5 min and 2,000g for 10 min. The CM was then filtered using 0.22-mm pore filters (Millipore Sigma, Etobicoke, ON) to eliminate large MVs. Exosomes were harvested from the CM by ultracentrifugation at 110,000g (Type 70Ti fixed angle, Beckman Coulter, Brea, CA) for 2 hours at 4°C. The exosome pellet was washed in 18 ml of PBS prior to a second ultracentrifugation step (4°C, 110,000g for 2 hours). The pellet was re-suspended in 100 µl of exosome isolation medium or PBS and stored in 10 µl aliquots at -80°C. The protein concentration of exosome preparations was quantified using Micro BCA™ Protein Assay Kit (Thermo Fisher Scientific, Waltham, MA). To assess the density of isolated exosomes, the exosomes were loaded in a gradient consisting of 2.5 ml 5%, 3 ml 20% and 4.5 ml 30% iodixanol (OptiPrep™ Density Gradient Medium, Millipore Sigma, Etobicoke, ON) prepared in diluent (0.25 M sucrose, 150 mM NaCl, 20 mM HEPES, pH 7.4). The gradient was subject to centrifugation in an SW-41 Ti rotor (Beckman Coulter, Brea, CA) (4°C, 200,000g for 2 hours. 1 ml fractions were collected, 8 µl per fraction was retained for nanoparticle tracking analysis. A second gradient column without exosomes was used in parallel to measure the refractive index values and calculate the densities of each respective fraction.

2.1.9 NTA

The size and concentration of EVs in MSC CM and exosome preparations was measured using NanoSight NS500 (NanoSight, Amesbury, UK)[153]. EVs of 50-150 nm in diameter were quantified as exosomes as per definition. The Nanosight NS500 system is equipped with a 405-nm violet laser that illuminates the nanoparticles within the CM loaded into the sample chamber. The light scattered from all the particles in the field of view were then visualized using a conventional optical microscope and captured using a complementary metal-oxide semiconductor (CMOS) camera (Hamamatsu Photonics, Hamamatsu City, Japan). Five- 30 second videos were captured at room temperature for each sample, and then processed using NTA software; this software identifies and tracks each particle on a frame-by-frame basis and uses this data to calculate the size and concentration of particles based on their Brownian motion. More specifically, the software calculates particle size using the velocity of particle movement by applying the two-dimensional Stokes-Einstein equation [153]:

$$< x, y >^2 = \frac{K_B T_{ts}}{3\pi\eta d_h}$$

where $<x,y>^2$ is the mean squared displacement, K_B is Boltzmann's constant, T is the temperature of the solvent, *ts* is the sampling time, η is the viscosity, and d_h is the hydrodynamic diameter.

2.1.10 TEM

Exosomes purified by ultracentrifugation were suspended in exosome buffer (137 mM NaCl, 20 mM HEPES, pH 7.5) and fixed onto carbon coated grids with glutaraldehyde. After fixation, the grids were stained with uranyl acetate and visualized by TEM as previously described [154].

2.1.11 Western Blot Analysis

MSC lysate (10^7 MSCs/mL) was prepared in RIPA buffer (50 mM Tris-HCl, 150 mM NaCl, 1% NP-40, 0.5% sodium deoxycholate, and 0.1% SDS, pH 7.4; Boston Bioproducts, Ashland, MA) and 1X Protease Arrest™ (G-Biosciences, St. Louis, MO). Fifty micrograms of MSC lysate, or exosomes enriched from MSC CM were loaded into a standard 12% SDS-PAGE, transferred to a PVDF membrane, and incubated with 1:1000 mouse anti-human CD81 antibody (Thermo Fisher Scientific, Waltham, MA), 1:1000 mouse anti-human CD9 antibody (Santa Cruz Biotechnology, Dallas, TX), 1:250 mouse anti-human ALIX antibody (Santa Cruz Biotechnology, Dallas, TX), 1:1000 rabbit anti-human calnexin antibody (Abcam, Toronto, ON), 1:5000 rabbit anti-human RAB27b (Proteintech Group, Chicago, IL) or 1:100 mouse anti-human TSG-6 antibody (Santa Cruz Biotechnology, Dallas, TX). The secondary antibodies used were 1:5000 peroxidase AffiniPure rabbit anti-mouse IgG or Peroxidase AffiniPure donkey anti-rabbit IgG (Jackson ImmunoResearch Labs, West Grove, PA). Rabbit anti-human β-actin antibody (Santa Cruz Biotechnology, Dallas, TX) or mouse anti-human GAPDH antibody (Santa Cruz Biotechnology, Dallas, TX) were used as loading control antibodies. Page Ruler™ Prestained Protein Ladder (Thermo Fisher Scientific, Waltham, MA) was used as molecular mass standard. Immunoreactive proteins were visualized with Amersham™ ECL Prime Western Blotting Detection Reagent (GE Healthcare Life Sciences, Amersham, UK), and imaged using Omega Lum™ C Imaging System (Aplegen®, San Francisco, CA).

2.1.12 Flow cytometry For Surface Markers on MSC Exosomes

The expression of surface markers on MSC exosomes was determined by multiparametric flow cytometry (CytoFLEX, Beckman Coulter, Pasadena, CA) as previously described [155]. Briefly, MSC exosomes were suspended in 0.02 μm-filtered PBS and stained with a combination

of the following fluorochrome-conjugated monoclonal antibodies (BD Biosciences, San Jose, CA): FITC-conjugated anti-CD90 (555595); PE-conjugated anti-CD73 (555749) or anti-CD63 (557305); and APC-conjugated anti-CD81 (561958). The samples were incubated in the dark for 15 minutes before centrifugation to remove excess antibodies (2,000 g for 10 min). Non-labeled EVs and antibodies suspended in filtered PBS were used to discriminate positive and negative populations. A total of 100,000 events were acquired. Calibration beads (Megamix-Plus FSC, Stago, France) suspended in PBS were used to validate the capacity to discriminate between 200, 300 and 500 nm particles using the FSC parameter. The data analysis was performed with FlowJo software 10.4.1.

2.1.13 Quantitative Real-Time PCR – Exosome Biogenesis

The expression of genes linked to cellular vesiculation was analyzed in resting and primed MSCs (n=6 per group) by real-time PCR using a custom RT^2 Profiler PCR Array (SABiosciences, Qiagen, Hilden, Germany). This "Vesiculome Array" was provided by Dr. Janusz Rak. P4 MSCs expanded in 75 cm^2 flasks to 80% confluence in complete medium, washed with PBS and cultured for an additional 72 hours in exosome collection medium with or without cytokine priming. TRIzol reagent (Thermo Fisher Scientific, Waltham, MA) was used as a lysis buffer to extract total RNA from MSCs. Purified RNA was obtained using Direct-zol™ RNA MiniPrep (Zymo Research, Irvine, CA) and quantified using BioDrop µlite spectrophotometer (Harvard Bioscience, Holliston, MA). Reverse-transcription (RT) was performed using 1 µg of purified RNA and QuantiTect reverse transcription kit (Qiagen, Hilden, Germany) according to manufacturer's instructions. Following RT, the complementary deoxyribonucleic acid (cDNA) was combined with RT^2 SYBR Green qPCR Master Mix (SABiosciences, Qiagen, Hilden, Germany), and 25 µl of this mix was loaded per well of the custom RT^2 Profiler PCR Array. The vesiculome array is composed of 96

wells containing primer sets for controls (housekeeping genes, genomic DNA control, reverse transcription control, and positive PCR control) and genes of interest (Table 7). After sample loading, quantitative real-time PCR was performed using LightCycler® 96 System software (Roche Molecular Systems, Laval, QC) as follows: a 10-min activation step (95°C), followed by a two-step amplification step for 45 cycles (15 s at 95°C and 1 min at 60°C), and a final thermal dissociation step (95°C 10s, 65°C 60s, 97°C 1s). The relative expression of EV-related genes was normalized to the expression of three housekeeping genes (ACTB, GAPDH, YBX1), and calculated using the ΔΔCt method by Schmittgen and Livak [156]. Briefly, the relative change in EV-related gene expression upon MSC priming was calculated using the following equation:

$$2^{-\Delta\Delta Ct} = (\Delta C_T primed\ MSCs - \Delta C_T resting\ MSCs)$$

2.1.14 Proteomic Analysis of MSC Exosomes

Proteomic analysis of MSC exosomes was performed by the Proteomics Platform of The Research Institute of the McGill University Health Centre (RI-MUHC). For each resting or primed MSC exosome preparation (n=6 for each group, 5 µg per sample), a single stacking gel band was reduced with DTT, alkylated with iodoacetic acid and then digested with trypsin. Peptides were re-solubilized in 0.1% aqueous formic acid/2% acetonitrile, loaded onto a Thermo Acclaim Pepmap (Thermo, 75uM ID X 2cm C18 3uM beads) precolumn and then onto an Acclaim Pepmap Easyspray (Thermo, 75uM X 15cm with 2uM C18 beads) analytical column separation using a Dionex Ultimate 3000 uHPLC at 220 nl/min with a gradient of 2-35% organic (0.1% formic acid in acetonitrile) over 3 hours. Peptides were analyzed using a Thermo Orbitrap Fusion mass spectrometer operating at a 120,000 resolution (FWHM in MS1, 15,000 FWHM for MS/MS) with HCD sequencing of all peptides with a charge of 2+ or greater. The raw data was converted into *.mgf format (Mascot generic format), searched using Mascot 2.3 against human sequences

(Swissprot 2017). The database search results were loaded onto Scaffold Q+ Scaffold_4.7.2 (Proteome Sciences) for spectral counting statistical treatment and data visualization. Classification of MSC exosomal cargo by Gene Ontology (GO) cellular component and biological process was performed using the Database for Annotation, Visualization and Integrated Discovery (DAVID) of the National Institute of Allergy and Infectious Disease (http://david.abcc.ncifcrf.gov).

2.1.15 Statistical Analysis

All analyses were performed with GraphPad Prism software (Graph-Pad, San Diego, USA) and presented as box plots. Non-parametric analyses were used in all comparisons. Mann-Whitney test was used to compare two independent groups (e.g., PED vs ATH), whereas Wilcoxon-signed-rank test was used for dependent samples (e.g., resting and primed MSCs from same individual). Kruskal-Wallis test was used to compare three independent non-normally distributed samples (i.e., PED vs OA vs ATH). All hypotheses tests were 2-sided. A p value of <0.05 was considered statistically significant. Statistical significance is indicated by asterisks in the figures.

Chapter 3: Results

3.1.1 aMSCs Fulfill the ISCT Criteria

The aMSCs used for the experiments included in this study fulfilled the minimal criteria for defining multipotent MSCs as proposed by the ISCT [1]. MSCs displayed spindle shaped morphology and adhered to plastic (Figure 1a). In addition, the samples demonstrated multi-lineage differentiation potential as determined by *in vitro* stainings (Figure 1b); Oil Red O, Alizarin Red, and Alcian Blue were used to detect lipid-filled adipocytes, extracellular calcium deposits of mineralized osteoblasts, and sulfated proteoglycans deposits of functional chondrocytes respectively. Analysis using flow cytometry demonstrated that ≥95% of the population expressed positive surface markers CD73, CD90, and CD105, and ≤2% expressed negative markers CD31, CD45, CD34, CD11b, and HLA-DR (Figure 1c).

3.1.2 Cytokine Licensing Increases Soluble Factor and EV Release by MSCs

To assess the relevance of paracrine factors in mediating T cell suppression by MSCs, we compared the suppressive ability of MSCs cultured with activated PBMCs with (contact) or without (transwell) direct cell-cell contact. The lack of differences between the two conditions confirmed that paracrine factors are key mediators of MSC potency (n=6, contact: 86.4±10.4% vs transwell: 87.9±11.0% $CD4^+$ T cell inhibition, p>0.99.) (Figure 5).

We next tested whether transferring MSC CM inhibited T cell proliferation. We obtained CM from 250,000 MSCs/ml under resting and primed (10 ng/ml IFN-γ + 15 ng/ml TNF-α) conditions and transferred them onto activated PBMCs. As previously shown by others, the potency of MSC CM increased after licensing (n=6, resting MSC CM: 23.0±9.2% vs primed MSC CM: 35.8±11.0% $CD4^+$ T cell inhibition; p=0.03) (Figure 6a); demonstrating that pro-inflammatory cytokines trigger the release of soluble immunosuppressive factors by MSCs.

To characterize the soluble factors released by resting and primed MSC CM, we used multispot electrochemiluminescence immunoassays and enzyme-linked immunosorbent assays (ELISA). Our results confirmed that MSCs constitutively secrete more than 30 different cytokines, chemokines and growth factors (Supplementary S2), including key factors involved in immune modulation (i.e., ICAM-1, VCAM-1, MCP-1, IL-8, IL-6, IP-10, IL,10, IL-2 and IL-4) (Figure 6b). Among them, licensing increased the levels of ICAM-1 (8.0 fold), VCAM-1 (7.5 fold), IL-8 (7.5 fold), IP-10 (>9.2 fold), MCP-1 (>1.5 fold), IL-6 (>4.5 fold), IL-10 (4.5 fold), IL-2 (3.7 fold), and IL-4 (2.0 fold) in the MSC secretome (Figure 6b). Consistent with previous studies, the levels of kynurenine in the secretome of primed MSCs were higher than those in resting MSCs (n=6, resting MSC CM: 0 μM kynurenine vs primed MSC CM: 52.9±7.9 μM kynurenine, p=0.003); indicating the enhanced IDO activity of licensed MSCs (Figure 6c). Therefore, IFN-γ and TNF-α aMSC licensing, enhances the release of soluble factors involved in T cell suppression.

We next sought to determine whether EV release was also affected by MSC licensing. To this end, we performed differential centrifugation of resting and primed MSC CM and quantified the concentration of exosomes harvested using NTA. Our data is the first to show that MSCs release higher levels of small EVs (50-150 nm in diameter) in response to inflammatory stimuli (n=6, resting MSC CM: 55.8±20.1x10^9 vs primed MSC CM: 159.1±70.0x10^9 EVs/ml, p=0.03) (Figure 6d). Altogether, our results indicate that MSCs released soluble factors and small EVs in response to pro-inflammatory cytokines.

3.1.3 MSC Exosomes Possess Immunosuppressive Properties

To investigate the contribution of small EVs from the MSC secretome to immunosuppression, we depleted EVs from primed MSC CM using 100 kDa molecular weight cut off (MWCO) filters and transferred the Filtered CM to activated PBMCs. In MI models, the

>1000-kDa fraction of MSC CM (containing EVs) is responsible for the cardioprotective effects of the MSC secretome [157]. We therefore reasoned that filtration of MSC CM with 100 kDa MWCO would remove these vesicles resulting in a reduction of the MSC immunopotency. The success of EV depletion was confirmed by quantifying 50-150 nm particles using NTA after filtering MSC CM (n=11, Control: $9.6\pm5.2x10^9$ EVs/ml vs Filtered: $0.4\pm0.3x10^8$ EVs/ml, p=0.0005) (Figure 7a). When transferred to activated PBMCs, Filtered CM showed a reduced capacity to suppress T cell proliferation (n=11, Control: 40.2±13.9% vs Filtered: 35.7±16.1% $CD4^+$ T cell inhibition, p=0.01) (Figure 7b). These results suggest that both, soluble factors and EVs in MSC CM, mediate T cell suppression.

Next, we assessed specifically the contribution of exosomes released by licensed MSCs to immunomodulation. Following their collection from the CM [103], MSC exosomes were characterized according to the minimal requirements suggested by the ISEV [105]. The majority of the harvested vesicles were 100-150 nm in diameter as determined by NTA, and floated at a density of 1.13 g/ml after separation using an iodixanol gradient (Figure 8a,b). Visualization by TEM showed that these vesicles were homogeneous in size (50-100 nm), and possessed a cup-like morphology, features characteristic of exosomes (Figure 8c). The presence of proteins typically enriched in exosomes (i.e., the ESCRT-associated protein ALIX and tetraspanin protein CD81) as well as the absence of proteins present in other organelles (i.e. the endoplasmic reticulum protein calnexin) was confirmed by Western blot (Figure 8d). Using CytoFLEX, we showed that these vesicles co-express the MSC marker CD90, and tetraspanin proteins CD63 and CD81 (Supplementary Figure S3). All these features indicate that licensing increased the release of exosomes by MSCs.

To determine the suppressive ability of exosomes obtained from licensed MSC CM, we cultured activated PBMCs with increasing concentrations of these vesicles. Primed MSC exosomes inhibited $CD4^+$ T cell proliferation in a dose dependent manner (n=6, 25 μg/ml: 1.6±3.3% vs 125 μg/ml: 11.1±6.0% $CD4^+$ T cell inhibition; p=0.03) (Figure 9a,b). Treatment with exosomes from primed MSCs did not induce T cell death (Figure 9c). Therefore, pro-inflammatory cytokines prime MSCs to secrete exosomes that contribute to the inhibition of $CD4^+$ T cell proliferation; moreover, the inhibitory effects of primed MSC exosomes do not involve T cell apoptosis.

3.1.4 Impact of Licensing on the Proteomic Cargo of MSC Exosomes

To investigate whether the protein composition of exosomes secreted by MSCs was modified after licensing, we analyzed six independent preparations of resting and primed MSC exosomes using mass spectrometry. Equal amounts of exosomal protein from resting and primed MSCs were compared in each experiment; notably, the amount of protein per exosome was similar in both conditions, therefore equal amounts of vesicles were expected to be compared (n=6, resting MSC Exo: $1.64\pm1.3\times10^{-9}$ vs primed MSC Exo: $2.11\pm1.07\times10^{-9}$ μg protein/particle, p=0.68) (Supplementary Figure S4). To assess for differences in the exosomal cargo between resting and primed MSCs (n=6 samples per group), we included in the analysis only proteins that were consistently present in at least 3 out of 6 replicates.

Out of 517 proteins identified in our analysis, 51 were only present in exosomes from resting MSCs, 195 were only present in exosomes from activated MSCs and 271 were shared by both (Figure 10a). Analysis using the DAVID Gene Functional Annotation Tool showed that 83.7% (227) of the shared proteins were associated with extracellular exosomes; these included 29 proteins commonly identified in exosomes according to ExoCarta such as: tetraspanins (CD9,

CD63, CD81), flotillins (FLOT1), MFGE8, ALIX (PDC6IP), syntenin-1 (SDCBP), 14-3-3 proteins, annexins (ANXA1, ANXA2, ANXA5, ANXA6), Rab GTPase (RAB1A), lysosomal-associated membrane proteins (LAMP1, LAMP2), heat shock proteins HSP70 and HSC70 (HSPA5, HSPA8), and transferrin receptor (TFRC) (http://exocarta.org/exosome_markers_new) (Figure 10b). These results validate the nature of the studied sample (i.e., MSC exosomes). The majority of the proteins common to both resting and primed MSC exosomes were involved in functions including but not limited to: cell adhesion, extracellular matrix organization, cellular protein metabolic processes and proteolysis (GO biological process ontologies).

The 51 unique proteins that were found in exosomes from resting MSCs were localized to 'extracellular exosomes' (37 out of 51 proteins, GO cellular components ontologies). Among them, ADAM10 (A desintegrin and metalloproteinase domain-containing protein 10), heterotrimeric G proteins (GNB1, GNB2), EZR (Ezrin) and RAC1 (Ras-related C3 botulinum toxin substrate 1), are proteins commonly found in exosomes according to ExoCarta (Figure 10c). Using the DAVID Functional Annotation Tool, we found that these 51 unique proteins from resting MSC exosomes were involved in signal transduction, cell migration and adhesion (GO biological process ontologies) (Figure 10c).

466 proteins were identified in primed MSC exosomes, 195 of which were not found in resting counterparts. These unique proteins were involved in a wide range of biological processes including but not limited to: protein translation, rRNA processing, cell adhesion, protein stabilization and response to inflammation (GO biological process ontologies) (Figure 10d). Among these processes, we specifically focused on the proteins involved in the inflammatory response. In this category, we identified candidate proteins known to mediate MSC immunopotency. Two proteins, A20 (i.e., tumour necrosis factor-a-induced protein 3 [TNFAIP3])

and TSG-6 (Figure 10d) that we uniquely found in activated MSC exosomes have been implicated in MSC suppression. Knockouts models of these proteins have previously confirmed their relevance for MSC immune modulation [45, 158]. Neither of these proteins have yet been reported in MSC exosomes. We were able show the presence of TSG-6 in primed MSC exosomes by Western blot (Figure 11). The relative amount of TSG-6 in MSC exosomes was higher compared to that in CM from primed MSCs and in primed MSCs (cell extract) (Figure 11). Using similar amounts of MSC exosome protein we were not able to confirm by Western blot the presence of A20. Our results indicate that MSC cytokine licensing induce the release of exosomes containing TSG-6, an anti-inflammatory protein involved in MSC:T cell crosstalk.

3.1.5 Impact of MSC Licensing on Exosome Biogenesis

Next, we assessed mechanisms responsible for the increase in exosome production and changes in the exosomal cargo associated with MSC licensing. The expression of 84 genes associated with exosome biogenesis and/or cargo (i.e., the 'vesiculome') was assessed with a custom RT2 Profiler™ PCR Array in resting and primed MSCs (n=6 per group).

We first compared the expression of genes encoding the ESCRT machinery and associated proteins involved in ILV biogenesis and exosome cargo sorting [159]. Licensing increased the expression of CHMP4B (2.65 fold, p=0.03) in MSCs (Figure 12a). CHMP4B is crucial in the biogenesis of syndecan-CD63-syntenin-containing exosomes [160]. Of relevance, the changes we observed in CHMP4B expression were consistent with the observed enrichment of ALIX, syntenin-1 and CD63 proteins in licensed MSC exosomes in our proteomic analysis. Low levels of CHMP4B was detected in exosomes obtained from primed MSCs only.

Next we compared the expression of Rab GTPases, which control several different steps of vesicle trafficking and release [161]. Rab GTPases act by recruiting specific effector proteins

onto membrane surfaces to drive cargo collection, organelle motility or vesicle docking at target membranes [161]. The Rab proteins included in the vesiculome array were the following: *RAB2A, RAB2B, RAB3A, RAB5A, RAB5B, RAB6B, RAB11A, RAB11B, RAB23, RAB27A, RAB27B, RAB31* and *RAB35*.

Compared to resting MSCs, licensed MSCs expressed higher levels of *RAB27B* (15.4 fold, p=0.03), *RAB5A* (1.5 fold, p=0.03), and *RAB31* (1.6 fold, p=0.03) (Figure 12b). Rab5b regulates early stages of endocytosis and is essential for exosome production [79]; Rab31 plays an essential role in membrane trafficking from the transgolgi network (TGN) to late endosomes [162, 163]; and Rab27b is involved in the transfer and retention of late endosomes to the cell periphery leading to the subsequent release of ILVs as exosomes [164].

We did not observe changes in *RAB11, RAB23,* or *RAB35* expression, suggesting that the enhanced release of exosomes by licensed MSCs was not mediated by recycling endosomes [69, 165, 166]. The expression of *RAB2* was not affected by licensing suggesting that autophagic and endocytic lysosomal degradation did not change [167]. Interestingly, *RAB6B* was downregulated in primed MSCs (4.5 fold, p=0.03) suggesting that the retrograde transport/recycling of vesicles from endosomes to the TGN network is downregulated in licensed MSCs [168, 169].

To determine whether an accumulation of late endosomes occurred in licensed MSCs, we compared the expression of the early and late endosome markers Rab5 and Rab7 in resting and primed MSCs. Our results showed that Rab5 and Rab7 expression was indeed higher in primed MSCs compared to resting (Figure 13). Altogether our results indicate that licensed MSCs promoted the formation of early and late endosomes which were directed away from the TGN and instead towards the surface to be released as exosomes via Rab27b.

Tetraspanin molecules are enriched in the membranes of MVBs and exosomes. Tetraspanins interact with itself and other transmembrane molecules (e.g. integrins and other adhesion receptors, immunoglobulin-domain-containing factors, growth factor and cytokine receptors and ectoenzymes) and can organize to form tetraspanin-enriched microdomains that participate in ILV biogenesis and the selection of exosome cargo [74, 75, 170-172]. Comparison of tetraspanin gene expression in resting and licensed MSCs showed a significant increase in CD63 (1.9 fold, $p=0.04$) and CD82 (10.7 fold, $p<0.001$) expression after licensing (Figure 12c). MSCs may therefore generate CD82 and CD63-dependent ILVs in response to inflammation [74]. The association between CD82 upregulation and TSG-6 secretion has been previously reported; MSC spheroids optimized to express TSG6 also highly express the tetraspanin protein CD82 [173]. However, further work is necessary to determine the relationship between CD82 expression, and the sorting and/or release of the anti-inflammatory protein TSG6 via exosomes.

3.1.6 Effect of Chronic Inflammation on MSC Exosomes and Vesiculation

Our laboratory has previously reported that the donor's age and diagnoses of chronic inflammatory conditions (i.e., atherosclerosis, diabetes mellitus) reduce the potency of MSCs [27, 36]. We therefore asked whether this was mediated by a reduction in exosome production. To this end, we analyzed MSC exosomes obtained from three groups of patients: (1) healthy pediatric donors undergoing programmed orthopedic surgery, (2) adults with osteoarthritis (OA) undergoing programmed orthopedic surgery ('healthy adults'), and (3) adults with atherosclerosis undergoing coronary artery bypass grafting (ATH). We performed differential centrifugation of primed PED, OA and ATH MSC CM (40ml each) and performed NTA of the harvested exosomes. Our results indicate that PED MSCs produced significantly more exosomes compared to ATH ($n=6$, PED: $2.38\pm0.83\times10^{11}$ vs ATH: $0.93\pm0.45\times10^{11}$ EVs/ml, $p=0.008$) and OA MSCs ($n=6$, OA:

$1.01\pm0.39x10^{11}$ EVs/ml, p=0.01) (Figure 14). These results suggest that donor age impacts the efficiency of exosome production in MSCs. Although, we did not observe significant differences in MSC exosome yield between OA and ATH samples, we do not exclude the possibility that disease status influences vesiculation by MSCs.

The greatest differences in exosome yield were observed in ATH versus PED MSCs. Therefore, for the assessment of MSC exosomal cargo we compared ATH versus PED samples by mass spectrometry. Notably, the protein quantities per exosome in PED and ATH MSC donors were similar (n=6 per group, PED: $1.50\pm1.27x10^{-9}$ vs ATH: $2.03\pm9.5x10^{-9}$ μg protein/particle) (Supplementary Figure S5). Mass spectrometry identified 393, 548, 245 proteins in the three PED MSC exosome preparations and 394, 385 and 311 proteins in the ATH MSC exosome preparations (Figure 15a). Proteins detected in at least two of three exosome preparations from each group were compared (PED: 345 proteins vs ATH: 312 proteins). From all detected proteins in primed MSC exosomes (n=394), the majority (67%) were present in both PED and ATH MSC exosomes (263 of 394 total identified proteins) (Figure 15b). These results suggest that the composition of PED and ATH exosomes were not significantly different. Analysis using DAVID Functional Annotation Tool showed that the majority of the exosome-associated proteins were shared between groups (Figure 15c); these proteins were associated with extracellular matrix organization, cell adhesion, proteolysis and protein stabilization (GO biological process ontologies) (Figure 15d). Fourteen of the shared proteins were classified in the 'inflammatory response' group. Among them, we tested whether TSG-6, a protein involved in immune modulation that was specifically enriched in licensed MSC exosomes, was differentially expressed in PED and ATH exosomes. Indeed, TSG-6 expression was higher in PED compared to ATH MSC exosomes as determined by

Western Blot (n=5 per group, PED:13.7±13.4 vs ATH: 4.0±6.0 TSG-6 expression; p=0.09) (Figure 16).

To explore the mechanisms that could account for the differences in exosome yield and cargo, we compared the vesiculome of resting and licensed MSCs from PED and ATH donors (n=3 per group). Licensed MSCs from PED donors upregulated the expression of *TSG101* and *Rab27B* to a greater extent compared to ATH donors (*TSG101*- PED: 2.7±1.2 vs ATH: 1.4±1.1 fold, p=0.40; *RAB27B*- 30±28.0 vs 14.9±9.0 fold, p=0.40) (Figure 17). Given the role of *TSG101* and *RAB27B* in ILV formation and exosome release, this process may be more efficient in PED than ATH MSCs. Western blot confirmed that PED MSCs expressed higher levels of Rab27b after priming compared to ATH (Figure 18). Further experiments (e.g., monitoring vesicle cycling with FM dyes or vesicle trafficking by fluorescently labelling components of the endocytic pathway [early endosomes, late endosomes, or lysosomes]) would be necessary to determine whether endocytic processes are impaired in ATH MSCs [174, 175]. Interestingly, although not statistically significant due to small sample size, our vesiculome analysis showed that ATH MSCs upregulated the expression of the tetraspanin molecule CD82 to a greater extent than PED MSCs (PED: 31.5±14.8 vs ATH: 54.7±6.5 fold, p=0.10) (Figure 17c). Moreover, preliminary experiments performed in our laboratory using flow cytometry suggest that ATH MSCs have greater intracellular levels of CD82 and lower cell surface levels of that molecule compared to PED MSCs. If confirmed, these results may indicate a defect in CD82 trafficking or recycling in ATH MSCs (Supplementary Figure S6). To investigate this, we plan to silence CD82 (siRNA) to determine the contribution of this protein to exosome production and T cell suppression by licensed MSCs.

Chapter 4: Discussion

The immune modulating properties of MSCs were first reported in 2002, when MSCs were shown to inhibit the proliferation of stimulated T cells in a reversible manner [17]. Since then, a large number of studies confirmed that MSCs can modulate innate and adaptive immune responses and effectively suppress inflammation. The capacity of MSCs to promote tolerogenic immune responses provides rationale for clinical trials investigating their therapeutic use for immune mediated diseases and inflammatory conditions. In 2012, MSCs (Prochymal®; Osiris Therapeutics, Inc., Columbia, MD) received conditional regulatory approval in Canada as the first "off-the-shelf" stem cell therapy for the treatment of steroid-resistant GVHD in pediatric patients [176]. However, this approval was based on positive data from a limited subset of patients, and the results of follow-up phase III trials from Prochymal® were mainly negative. Understanding the mechanisms that underlie the immunomodulatory function of MSCs, and those that could account for the discrepant outcomes between preclinical and clinical trials (e.g. MSC donor, tissue source, passage number, "licensing"), are key to optimizing and ensuring the reproducibility of this type of cell therapy [3].

MSCs are not constitutively immunosuppressive; their anti-inflammatory properties are triggered in the presence of an inflammatory environment (i.e., MSC licensing). This can be mimicked *in vitro* by the addition of inflammatory cytokines, which stimulate the release of several immune response-modulating factors mediating the inhibitory effects of MSCs (paracrine mechanisms) [17, 41, 177, 178]. My work assessed the composition of the aMSC secretome pre- and post- IFN-γ and TNF-α activation. We confirmed that several factors involved in T cell suppression (i.e., MCP-1, IL-10, ICAM-1, VCAM-1, IDO metabolites) were induced post-

priming. Of relevance, no single factor of the MSC secretome has alone been capable of reproducing the immunopotency of those cells. In addition to soluble factors, EVs compose the MSC secretome. Since EVs are key molecules mediating the intercellular signaling involved in immune responses, we investigated the effect of licensing on MSC exosome biogenesis and cargo, as well as their contribution to immunomodulation [57]. If MSC EVs were found functionally equipotent to their cell of origin, they could become a novel cell-free therapeutic with the following advantages compared to cellular therapy: safety, ease of manufacturing, broad availability, limited immunogenicity, protection of cargoes from degradation, high stability in serum and blood, and reduced off-target effects. However, the anti-inflammatory properties of MSC EVs are currently debated and the relative contribution of these organelles to the overall immunopotency of MSCs is unclear [58, 134-136, 179-183]. In a recent report, licensed MSCs have been shown to secrete lower levels of EVs, and these vesicles were not capable of inhibiting T cell proliferation [135]. Contrary to this, herein we provide evidence that licensed MSCs release higher levels of EVs than resting counterparts. Moreover, the EVs from licensed MSCs were enriched in exosomes capable of inhibiting the proliferation of T cells in a dose dependent manner. Notably, the suppressive ability of exosomes was less than that exerted by the parental cells or MSC CM. It is therefore the combination of EVs and soluble factors in the secretome that mediate the immunosuppressive activity of aMSCs. The administration of both soluble factors and EVs from primed MSC CM may be more effective at immune suppression than EVs alone.

Consistent with previous reports, the MSC exosomes we collected contained several ‘exosome-characteristic proteins’ including: tetraspanins (e.g. CD9, CD63, CD81), flotillins (e.g. FLOT1), MFGE8, ESCRT components and associated proteins (ALIX), 14-3-3 proteins,

chaperones (HSP90, HSP70, HSC71), annexins, Rab small GTPases, transferrin receptor and LAMP1; and co-expressed mesenchymal markers (i.e., CD90).

It is known that the contents of EVs change in response to external stimuli. As described in a previous report, CD54 (ICAM-1) was only expressed in exosomes produced by licensed MSCs and CD106 (VCAM-1) was absent [135]. This is of particular interest because a higher surface expression of ICAM-1 on MSC exosomes enhance their tethering and intake by immune effector cells [135]. In our study, the exosomal cargo shifted post-MSC priming and contained a subset of proteins involved in inflammatory response. By proteomic analysis we are the first to show that TSG-6, a key molecule implicated in the immunopotency of MSCs, was integrated into the molecular content of cytokine activated MSC EVs. This finding was confirmed by Western blot. TSG-6 has only been recorded in EVpedia and Vesiclepedia (databases on EV content) in the cargo of EVs from cancer cells (brain, breast, colon, kidney, leukemia, lung and melanoma). Our finding is the first evidence indicating that TSG-6 is also present in EVs from normal cells.

The mechanisms regulating the secretion of EV-associated molecules, and the specific pathways activated upon their interaction with target cells are actively being investigated. There are at least three independent mechanisms responsible for the sorting of exosomal proteins: lipid-mediated, tetraspanin-mediated and ESCRT-mediated [184]. It is suggested that these mechanisms coexist and are responsible for the sorting of different proteins and/or for the loading of different subpopulations of vesicles [185]. Our results suggest that following MSC activation, there is an increase in the expression of Rab GTPases (*RAB5A*, *RAB31, RAB27B*), tetraspanins (*CD63, CD82*), and the ESCRT-III component *CHMP4B*. These genes are involved in several steps of exosome generation.

Among the three Rab small GTPase proteins that were upregulated in licensed MSCs, Rab5b is involved in early endosome biogenesis [79]; Rab31 is involved in trafficking proteins from the TGN to late endosomes [162, 163]; and Rab27b mediates the release of exosomes into the extracellular space [164]. Tetraspanin molecules (such as CD63) are involved in organizing the endosomal membrane and clustering proteins required for ILV formation [186]. Following this step, the ESCRT machinery is recruited. ESCRT-I and II drive membrane budding, whereas ESCRT-III is involved in membrane abscission. CHMP4 is an essential component of the ESCRT-III complex. The upregulation of CHMP4B and CD63 expression in primed aMSCs is in agreement with a previous report demonstrating the importance of CHMP4B in the biogenesis of syndecan-CD63-syntenin-1 containing exosomes [160]. Consistent with this data, in our proteomic analysis, higher levels of ALIX, syntenin-1 and CD63 proteins were detected in primed compared to resting MSC exosomes. MSC licensing may therefore stimulate ILV formation in an ESCRT-dependent manner, and these ILVs might then be released from the cell as exosomes via Rab27; however, further work is necessary to confirm this mechanism. The importance of Rab27-dependent exosome production in immune cell communication and regulating inflammatory response has been recently reported in a study using Rab27a and Rab27b double-knockout mice [187]. These mice are deficient in exosome secretion and display chronic, low-grade inflammation characterized by elevated inflammatory cytokines (TNF-α, IL-6) and myeloproliferation. The importance of Rab27-dependent MSC exosome production in T cell inhibition will be further evaluated by silencing experiments.

Inter-donor variability is a major challenge when investigating the therapeutic effects of MSCs (i.e., ‘not all MSCs are functionally equal’). We recently reported that ATH MSCs with reduced *in vitro* immunopotency have elevated mitochondrial ROS levels due to impaired

mitochondrial function [144]. Since cells modulate the content of exosomes in response to extracellular (extrinsic) cues such as oxidative stress [188], my work evaluated to what extent ATH impacts the content and cargo of MSC exosomes. My data shows that following cytokine activation, pediatric samples secrete higher amounts of exosomes than ATH MSCs. This suggests that the exosomal sorting machinery differentially reacts to extrinsic cues in these two MSC donor groups. Moreover, due to the effect of exosomes promoting T cell suppression, defects in exosome production may contribute to the impaired immunopotency of ATH MSCs. Although, due to the limited sample size, it was not statistically significant, there was a trend towards a decreased expression of *RAB27B* (p=0.40) and *TSG101* (p=0.40) in ATH MSCs. Using mass spectrometry, we compared the proteins identified in PED and ATH MSC exosomes and found that the majority of the detected cargo was shared, and did not observe significant differences between groups. However, by Western blot, we showed quantitative differences in the content of PED and ATH MSC exosomes; more specifically, we found higher levels of TSG-6 present in licensed PED MSC exosomes. These differences in exosome cargo could ultimately contribute to the functional differences in MSCs from patients with chronic inflammatory conditions (i.e., ATH). If these results are confirmed in larger sample sizes, our results would suggest that defects in ILV formation, and MVB transport/release by Rab27b occur in ATH MSCs leading to reduced exosome production. Moreover, interventions aimed at improving exosome biogenesis may enhance the therapeutic effects of MSCs obtained from ATH patients.

We acknowledge that our work has limitations which may affect the accuracy of our comparisons. For example, we were not able to conclude on the effect of age versus disease on MSC exosome yield due to the limited number of MSC samples included in each age group. Follow-up experiments will be continued in our laboratory to increase the sample size of the

experiments included in this thesis. In addition, recent data suggest that sex modifies the miRNA content of synovial fluid exosomes of OA patients [189]. It is unknown whether sex also affects exosome yield or other exosome components. Due to the limited sample size, our study cannot address this issue [146]. Notably, the genders of the donors were matched between PED and ATH groups in our comparison of MSC exosome yield; therefore, we do not expect gender to be responsible for the differences we observed. We recognize that we lack a clearly defined functional distinction between classes of EVs, and that our findings in 'exosome-enriched EVs' in the future might be attributed to a more specific type of vesicle. The development of more refined purification methods, as well as improvements in protein detection techniques will help to characterize the different classes and molecular composition of the vesicles that are co-purified using the current protocols. In addition, part of my work focused on the characterization of the protein content of MSC exosomes. Further work is required to characterize other components of the cargo of MSC exosomes such as miRNA and mRNA due to their potential functional implications. Finally, we cannot state to what extent the results we report in ATH MSCs exosomes are generalizable to other chronic inflammatory diseases with predominant autoimmune features (e.g., rheumatoid arthritis, systemic lupus erythematosus, MS). Although autoimmune and inflammatory diseases share common pathogenic mechanisms, unique functional differences have been described in exosomes in the context of autoimmunity [190-192]. Ongoing work in our laboratory aim to establish the functional relevance of CD82 and TSG-6 in primed MSC exosomes as mediators of immune modulation; the role of Rab27b in MSC vesiculation; and the implications of our results in other chronic immune mediated diseases.

Chapter 5: Conclusion

In this work, we aimed to establish the role of licensing and exosomes in MSC immunopotency. Herein we provide evidence that the composition of the MSC secretome shifts in response to inflammatory stimuli; specifically, licensed MSCs secrete higher levels of soluble factors involved in immunomodulation and exosomes. Licensed MSC exosomes contribute to the suppressive ability of the CM and are alone capable of inhibiting $CD4^+$ T cell proliferation. In addition to assessing the inhibitory capacity of exosomes from licensed MSCs, we demonstrate that licensing changes the cargo of MSC exosomes to contain factors involved in resolving inflammation. We report for the first time that TSG-6 is a component of exosomes obtained from IFN-γ+TNF-α licensed MSCs. This is of utmost importance because TSG-6 is an inflammation-modulating protein proposed to predict the efficacy of MSCs in several inflammation models. We assessed key aspects of the vesiculation process and describe unique features of exosome biogenesis following MSC licensing; which include increased endocytosis (*RAB5A* and Rab7), TGN to endosome trafficking (*RAB31*), ILV formation (*CD63, CD82, CHMP4B*) and exosome release (*RAB27B*). Lastly, we explored whether chronic inflammatory conditions (i.e., 'aging' and atherosclerosis) impact exosome production and cargo of MSCs. Although we did not observe differences in the proteins identified in ATH and PED MSC exosomes, there was a significant reduction in the quantity of exosomes and the content of anti-inflammatory TSG-6 within the exosomes released in the context of chronic inflammation. These differences may be mediated by defects in endocytosis, ILV formation and MVB fusion/release. Altogether, this work adds to a growing body of evidence that the therapeutic effects of MSCs is in part mediated by exosomes; raising the possibility of a cell-free therapy consisting of exosomes for treatment of inflammatory diseases/conditions; and emphasizes the importance of donor selection.

Figures

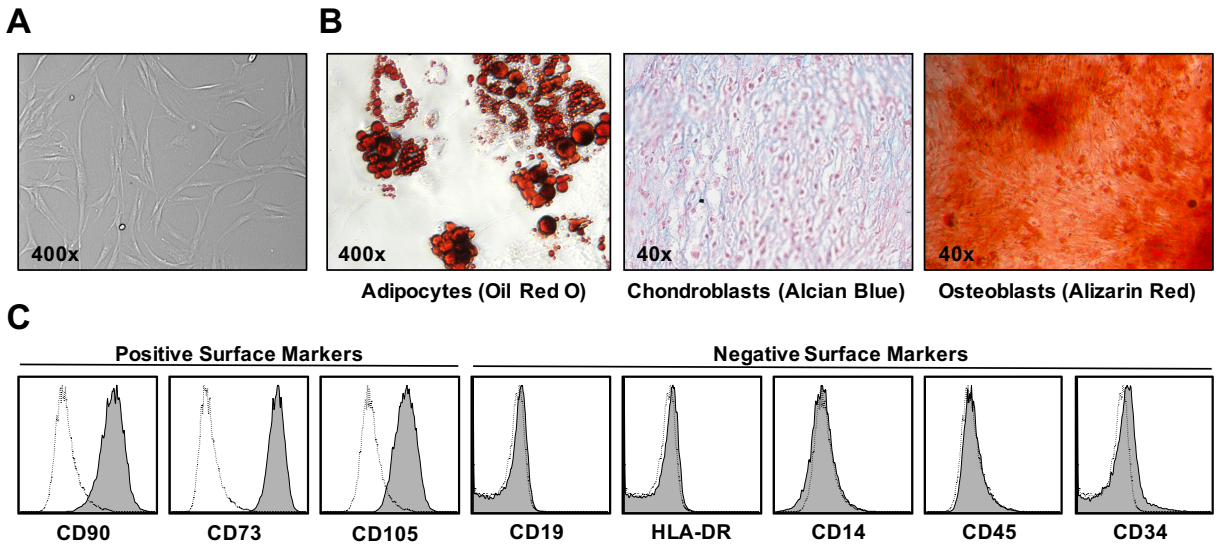

Figure 1: Minimal criteria for defining multipotent MSCs

Human adipose tissue-derived MSCs are **(A)** plastic-adherent when maintained in standard culture conditions and display spindle-shaped morphology; **(B)** differentiate *in vitro* to osteoblasts, adipocytes and chondroblasts; and **(C)** express CD105, CD73 and CD90, and lack expression of CD45, CD34, CD14, CD19 and HLA-DR surface molecules.

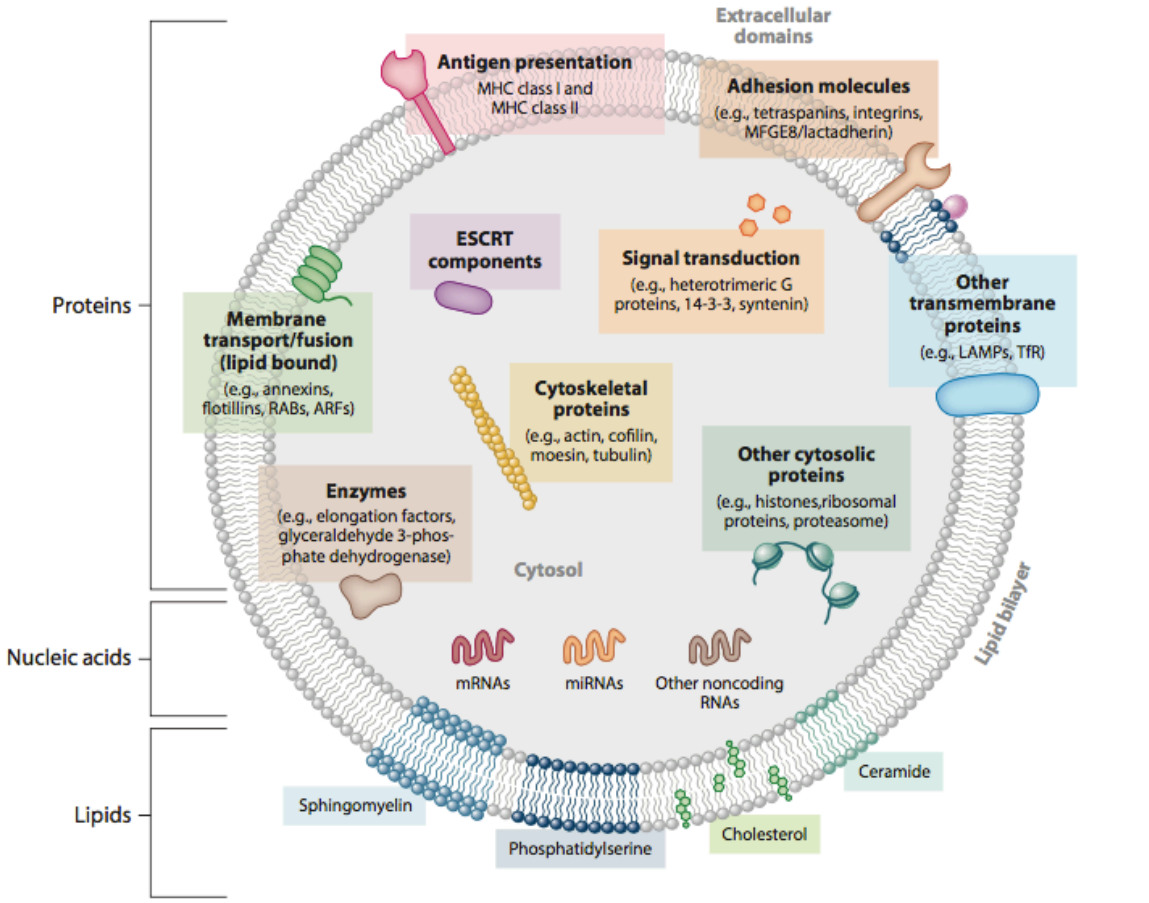

Figure 2: Diagram of a typical EV

This figure shows a schematic depiction of the molecules typically found in the membrane and lumen of a canonical EV. This figure was reproduced from Colombo et al. [193] with permission. Abbreviations- ARF: ADP ribosylation factors; ESCRT: endosomal sorting complexes required for transport; LAMP: lysosomal-associated membrane protein; MFGE8: milk fat globule-epidermal growth factor 8; MHC: major histocompatibility complex; mRNA: messenger RNA; miRNA: microRNA; TfR: transferrin receptor.

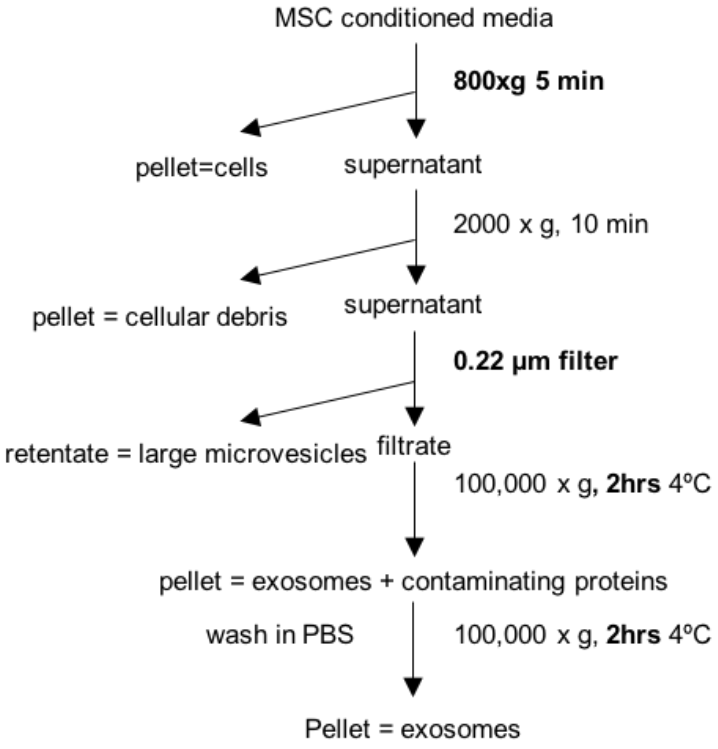

Figure 3: Exosome isolation from MSC CM

Cells and debris were cleared from MSC CM by low speed centrifugation, followed by filtration to remove large MVs (above 220 nm in diameter). To enrich for exosomes, the supernatant was subjected to ultracentrifugation [103]. Abbreviations- MSC: mesenchymal stromal cell; PBS: phosphate-buffered saline.

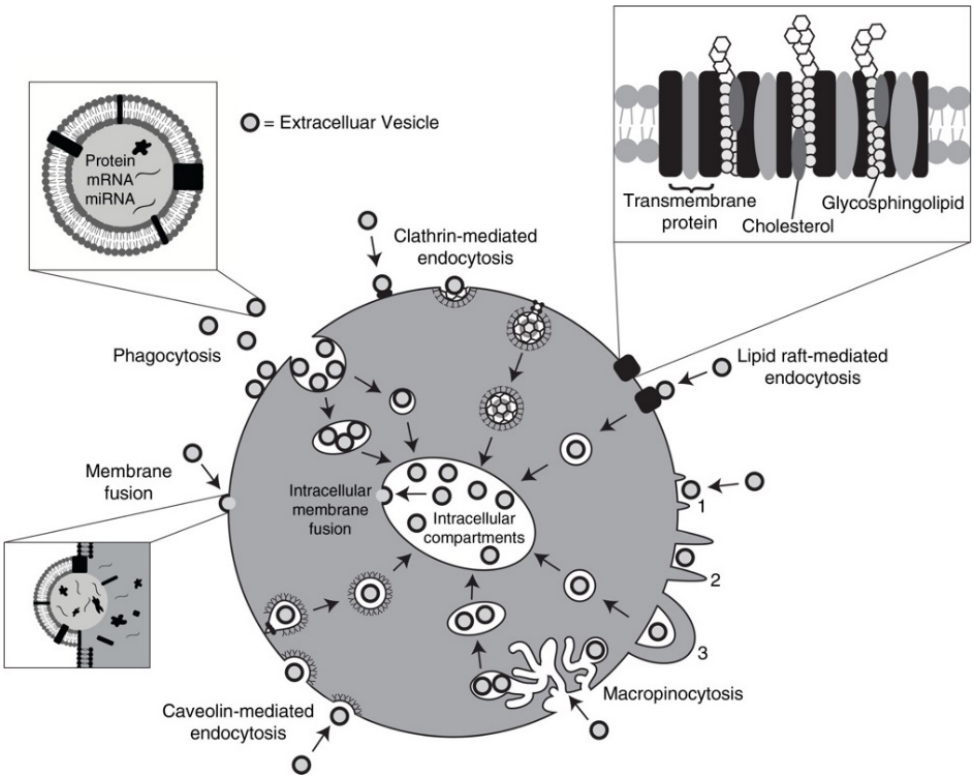

Figure 4: Modes of EV uptake by target cells.

EV are up-taken by recipient cells through a number of different mechanisms, including clathrin, lipid-raft or caveolin-mediated endocytosis; membrane fusion; phagocytosis; and micropinocytosis. This figure was reproduced from Mulcahy et al. [112] with permission.

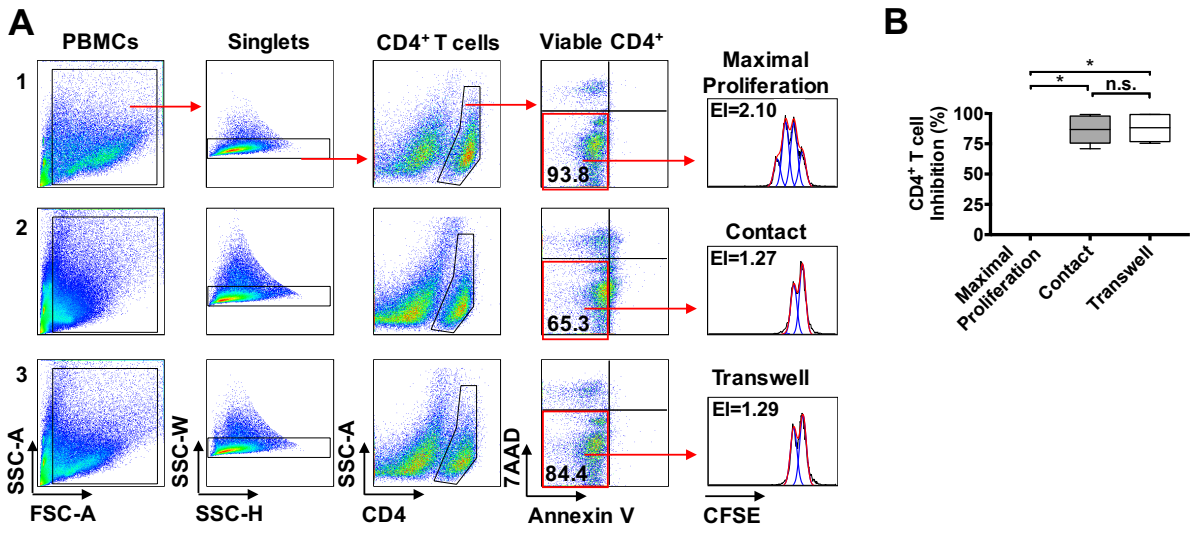

Figure 5: MSCs inhibit T cell proliferation in the absence of cell-cell contact

(A) Representative example of a MSC:T cell suppression immunopotency assay. Anti-CD3 and anti-CD28 antibodies beads were used to stimulate T cell proliferation. Gating strategy and expansion index (EI) of $CD4^+$ T cells **(A.1)** in the absence of MSCs (T cell Maximal Proliferation); or in the presence of MSCs either in **(A.2)** cell-cell contact dependent conditions (Contact) or in **(A.3)** cell-cell contact independent conditions (Transwell). **(B)** MSCs inhibit activated T cell proliferation to a similar extent both in contact dependent and independent conditions. Mean±SD of 6 independent experiments are reported, where (*) represents $p \leq 0.05$. Abbreviations- 7-AAD: 7-Aminoactinomycin D; CFSE: carboxyfluorescein succinimidyl ester; EI: expansion index; FSC-A: forward scatter area; SSC-A: side scatter area; SSC-H: side scatter height; SSC-W: side scatter width.

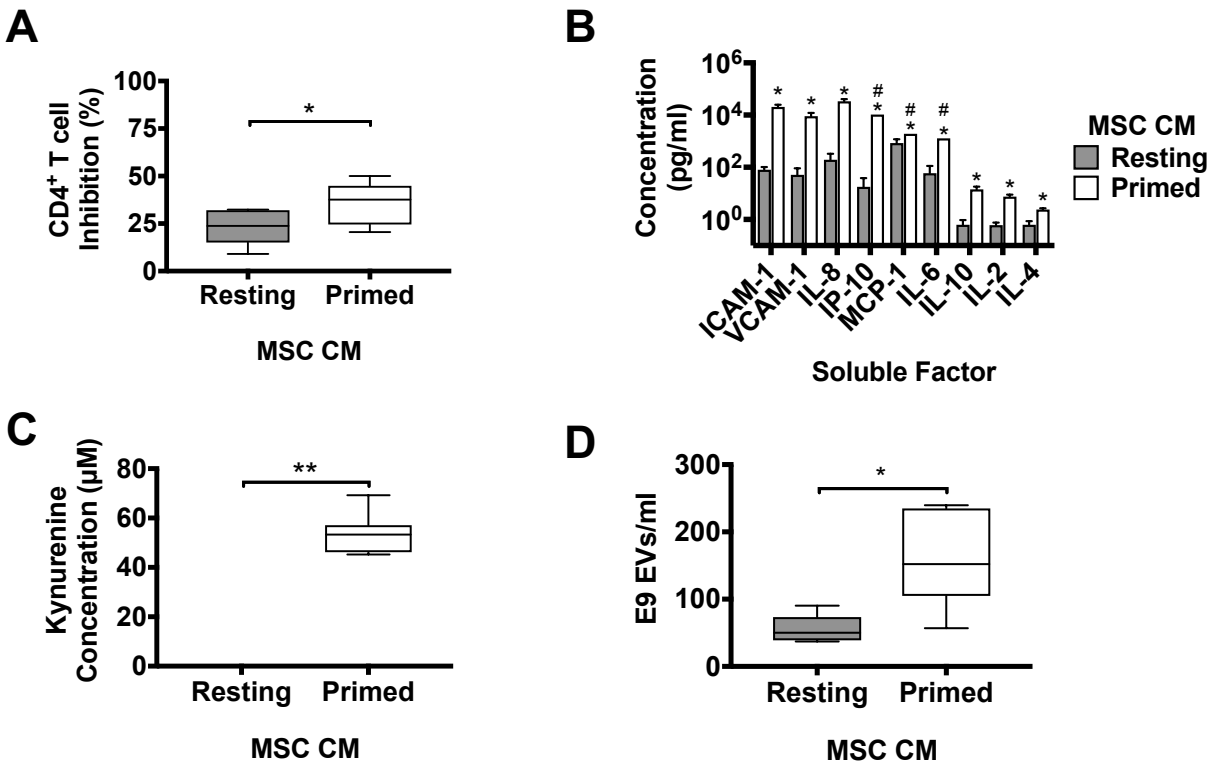

Figure 6: Licensing alters the MSC secretome and enhances immunopotency

The **(A)** inhibition of viable $CD4^+$ T cell proliferation was assessed 3 days following culture with CM obtained from MSCs under resting and primed (10 ng/ml IFN-γ + 15 ng/ml TNF-α) conditions; **(B)** concentration of cytokines and chemokines known to be involved in MSC:T cell suppression was measured using Mesoscale Discovery; **(C)** concentration of kynurenine indicative of indoleamine-2,3-dioxygenase (IDO) activity was measured in CM of resting and primed MSCs with a colorimetric assay; **(D)** total concentration (left) and size distribution (right) of exosomes obtained by ultracentrifugation of resting or primed MSC CM, was determined by nanoparticle tracking analysis (NTA). Mean±SD of 6 independent experiments are reported, where (*) represents $p \leq 0.05$. (#) denotes measurements that were higher than the limit of detection of the assay. Abbreviations- EVs: extracellular vesicles; ICAM-1: intercellular adhesion molecule 1; IL: interleukin; IP-10: interferon gamma-induced protein 10; MCP-1: monocyte chemoattractant

protein-1; MSC CM: mesenchymal stromal cell conditioned media; VCAM-1: vascular cell adhesion molecule 1.

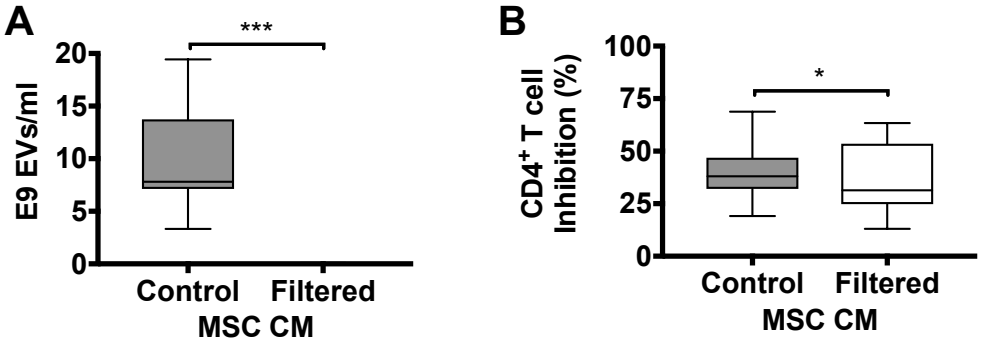

Figure 7: Depletion of EVs reduces the immunopotency of licensed MSC CM

EVs were depleted from licensed MSC CM using 100 kDa MWCO filters. The **(A)** quantity of EVs (50-150 nm) was determined by NTA; **(B)** inhibitory effects on viable $CD4^+$ T cell proliferation was assessed *in vitro*. Mean±SD of 10 independent experiments are reported, where (*) and (***) represent $p \leq 0.05$ and $p \leq 0.001$ respectively. Abbreviations- MSC CM: mesenchymal stromal cell conditioned media; EVs: extracellular vesicles.

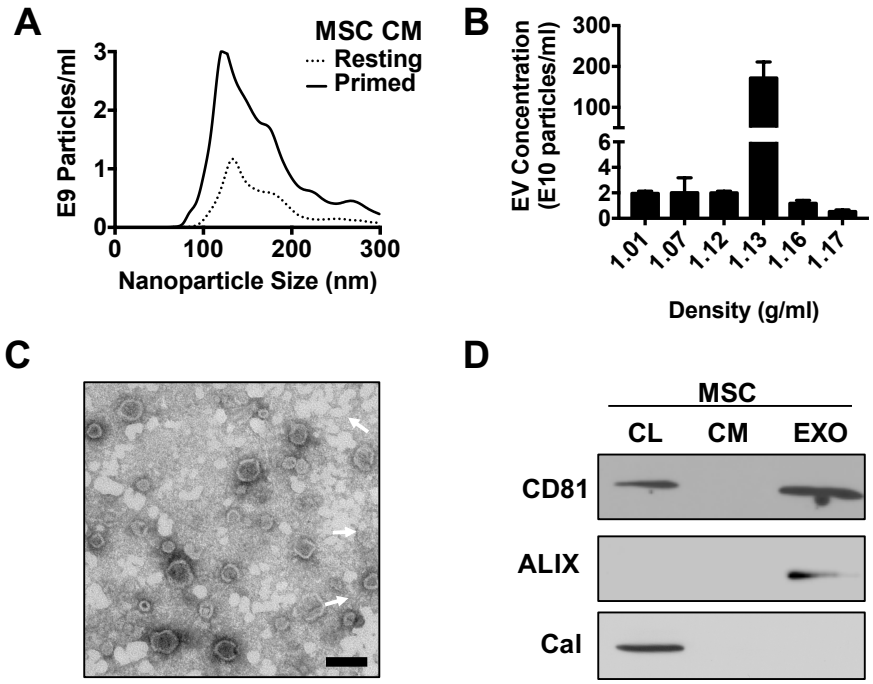

Figure 8: Phenotypic characterization of EVs from licensed MSC CM

(A) Size distribution (NTA); **(B)** flotation densities following fractionation with iodixanol density cushion; **(C)** morphology (TEM through negative staining) (Bar represents 100nm); **(D)** protein composition (Western blot for exosome-enriched proteins [CD81, ALIX] and proteins present in other subcellular organelles [calnexin)]). Abbreviations- Cal: calnexin; CL: cell lysate; CM: conditioned media; EXO: exosomes; EVs: extracellular vesicles; MSC: mesenchymal stromal cell.

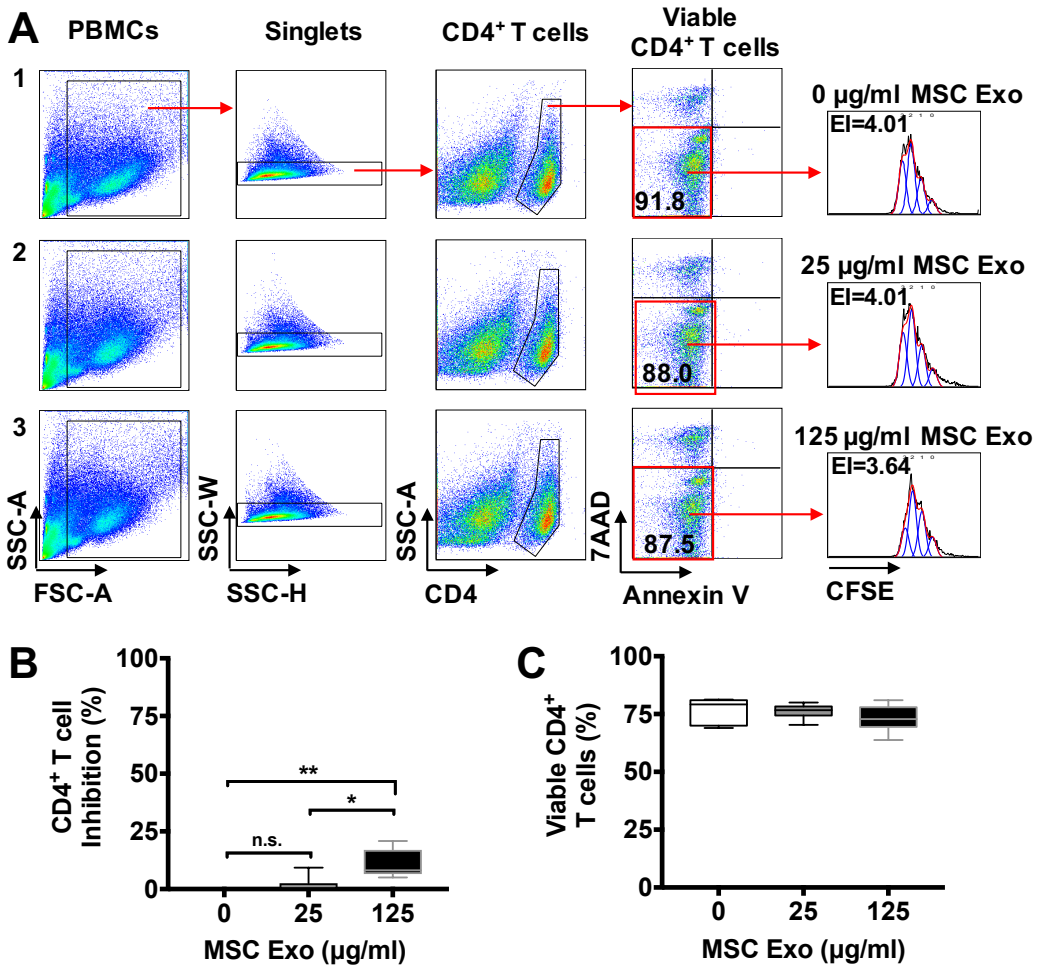

Figure 9: Dose dependent inhibition of T cell proliferation by primed MSC exosomes

(A) Representative example of a T cell suppression immunopotency assay with increasing concentrations of MSC derived exosomes. Gating strategy and expansion index (E.I) of $CD4^+$ T cells **(A.1)** in the absence of MSC derived exosomes **(A.2)** presence of 25 µg/ml or **(A.3)** 125 µg/ml of MSC exosomes. **(B)** Summary graph depicting $CD4^+$ T cell suppression and **(C)** viability in the presence of increasing concentrations of MSC exosomes. Mean±SD of 8 independent experiments are reported, where (**) represents $p \leq 0.01$ and (*) $p \leq 0.05$. Abbreviations- 7-AAD: 7-Aminoactinomycin D; CFSE: carboxyfluorescein succinimidyl ester; FSC-A: forward scatter area; MSC Exo: MSC exosomes; PBMCs: peripheral blood mononuclear cells; SSC-A: side scatter area; SSC-H: side scatter height; SSC-W: side scatter width.

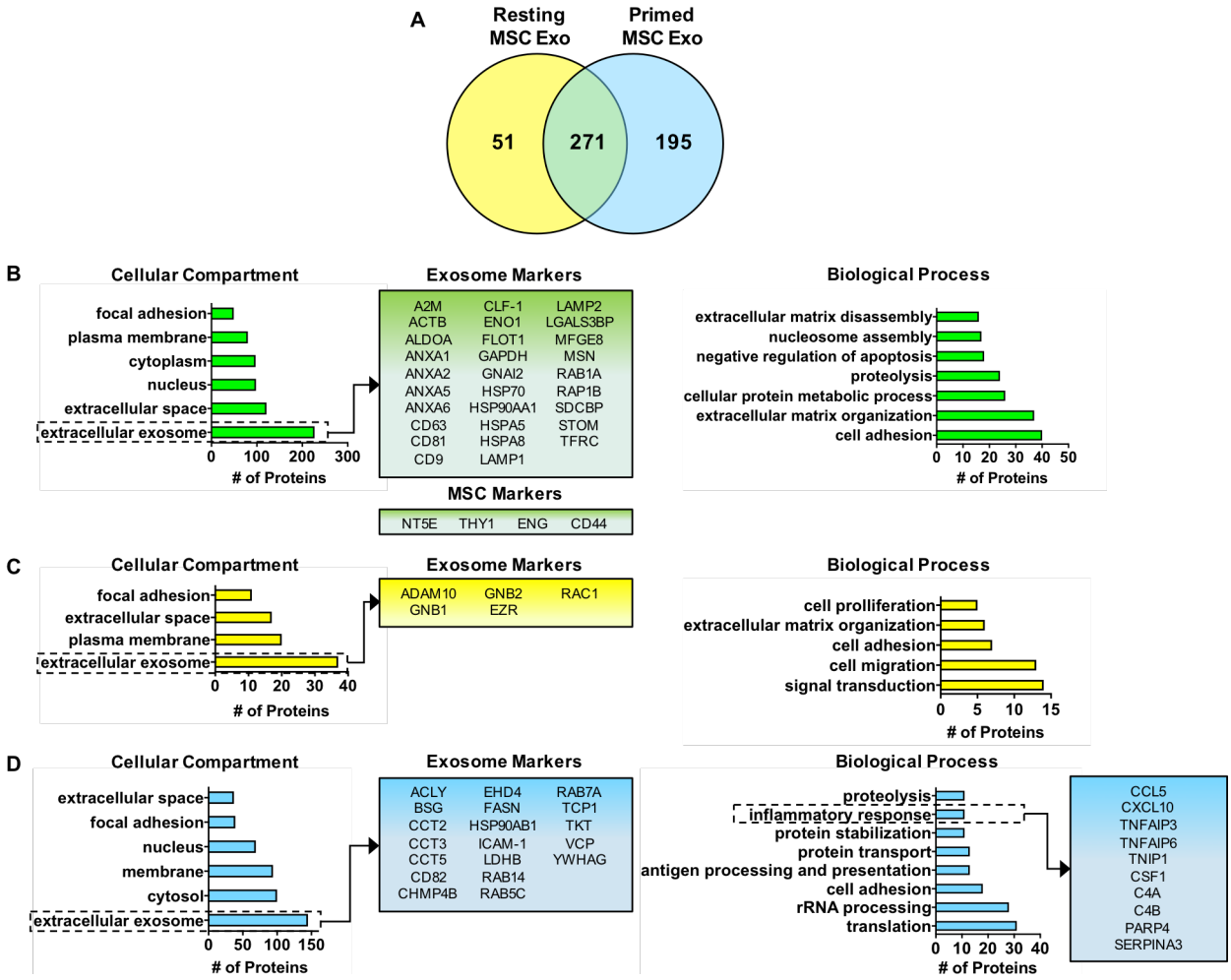

Figure 10: Proteomic comparison of resting and primed MSC exosomes

(A) Venn diagram showing the overlapping proteins in exosomes from resting and primed MSC CM (n=6 per group). A total of 271 proteins overlapped between both groups. The Database for Annotation, Visualization and Integrated Discovery (DAVID) Functional Annotation Tool was used to cluster the **(B)** 271 shared proteins, **(C)** 51 proteins unique to resting MSC exosomes and **(D)** 195 proteins unique to primed MSC exosomes into cellular compartments (left panel) and biological processes (right panel). Proteins included in the list of top 100 proteins identified in exosomes (exocarta.org) are listed in the center panels. Proteins in the 'inflammatory response' category were only expressed in primed MSC exosomes. Among them, TNFAIP6 (TSG-6) and

TNFAIP3 (A20) are the only two proteins reported to be involved in MSCs immunosuppressive function. Abbreviations- MSC Exo: MSC exosomes.

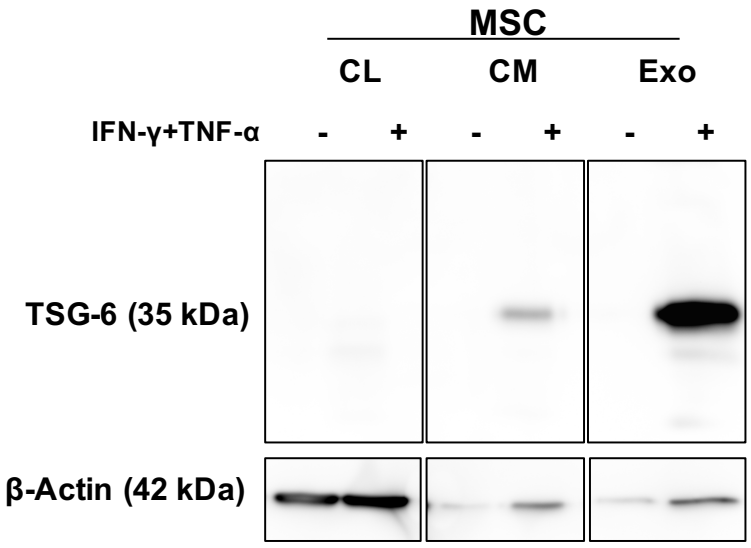

Figure 11: Enrichment of TSG-6 in licensed MSC exosomes

Western blot analysis of 10 µg of resting (-) and licensed (+) MSC lysates (cells), conditioned media (CM), and exosomes (Exo) for human TSG-6. TSG-6 is expressed in CM and exosomes from primed MSCs. The relative amount of TSG-6 to that of other proteins is significantly higher in primed MSC exosomes. Abbreviations- CL: cell lysate; CM: conditioned media; Exo: exosomes; IFN-γ: interferon-gamma; MSC: mesenchymal stromal cell; TNF-α: tumor necrosis factor-alpha TSG-6: tumor necrosis factor-inducible gene 6 protein.

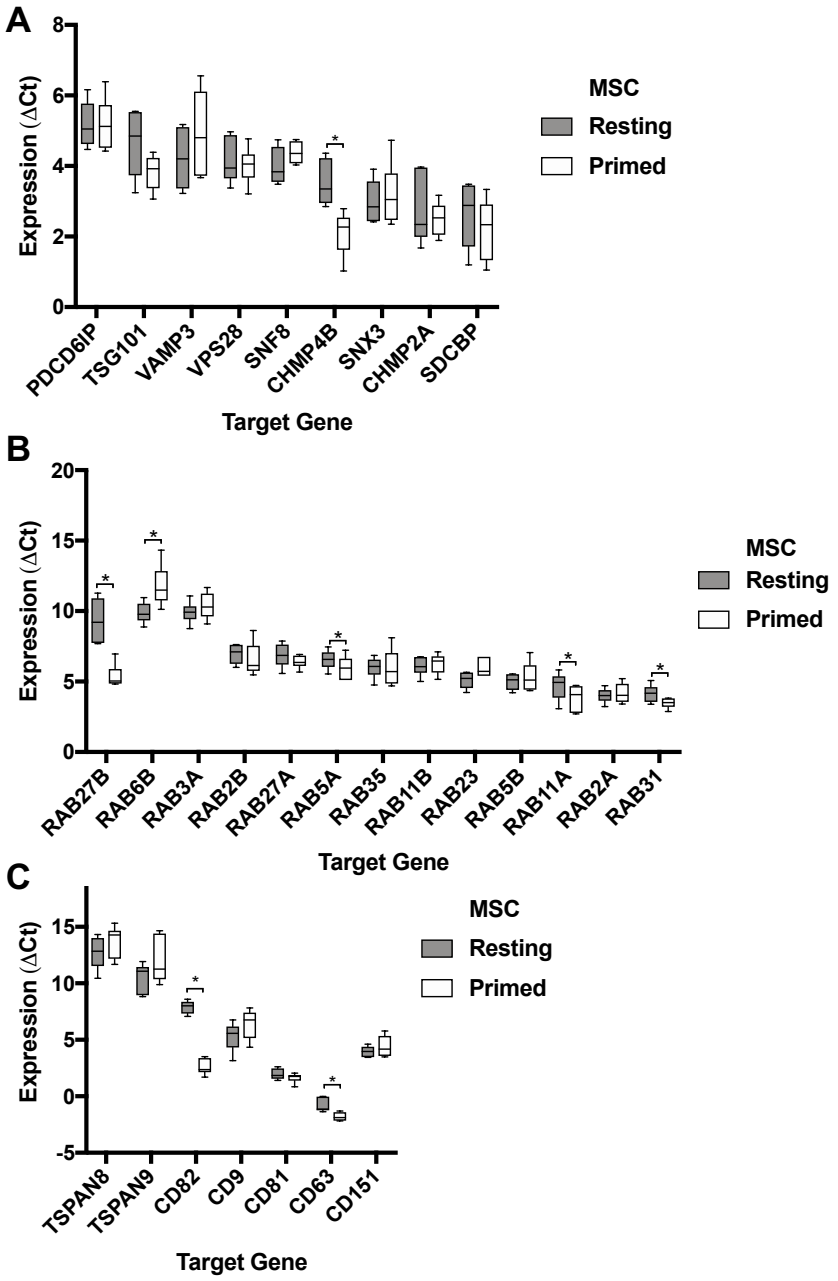

Figure 12: Effect of licensing on MSC vesiculation

A custom RT^2 PCR array was used to measure the expression of **(A)** ESCRT and associated genes; **(B)** Rab GTPases; and **(C)** tetraspanins in resting and licensed MSCs. Mean±SD of 6 independent experiments are reported, where (*) represents $p \leq 0.05$. Abbreivations- Ct: cycle threshold; MSC: mesenchymal stromal cell.

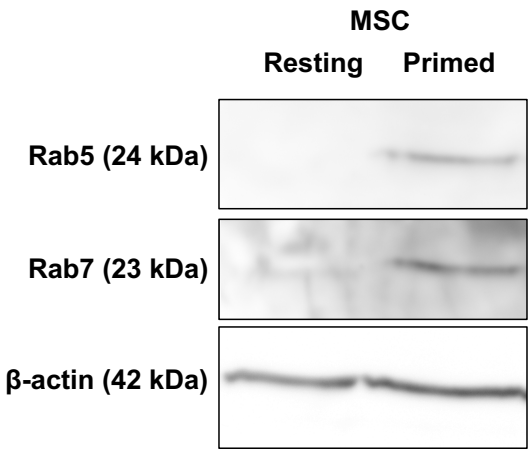

Figure 13: Effect of MSC licensing on endocytosis

Western blot analysis of 50 µg of whole cell lysate prepared from resting and licensed MSCs for Rab5 (early endosome marker) and Rab7 (late endosome marker). Abbreviations- MSC: mesenchymal stromal cell.

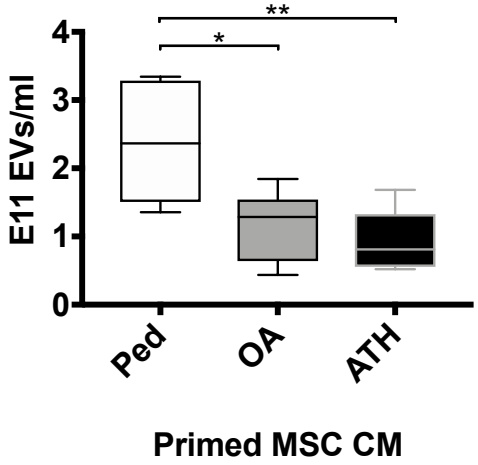

Figure 14: Effect of age and chronic inflammation on exosome production

NTA of exosomes isolated from MSC CM of pediatric (PED), adult (OA), and adults with atherosclerosis (ATH) samples. Mean±SD of 6 independent experiments per group are reported, where (*) and (**) represent $p \leq 0.05$ and $p \leq 0.01$ respectively. Abbreviations- ATH: atherosclerosis; EVs: extracellular vesicles; OA: osteoarthritis; PED: pediatric; MSC CM: MSC conditioned media.

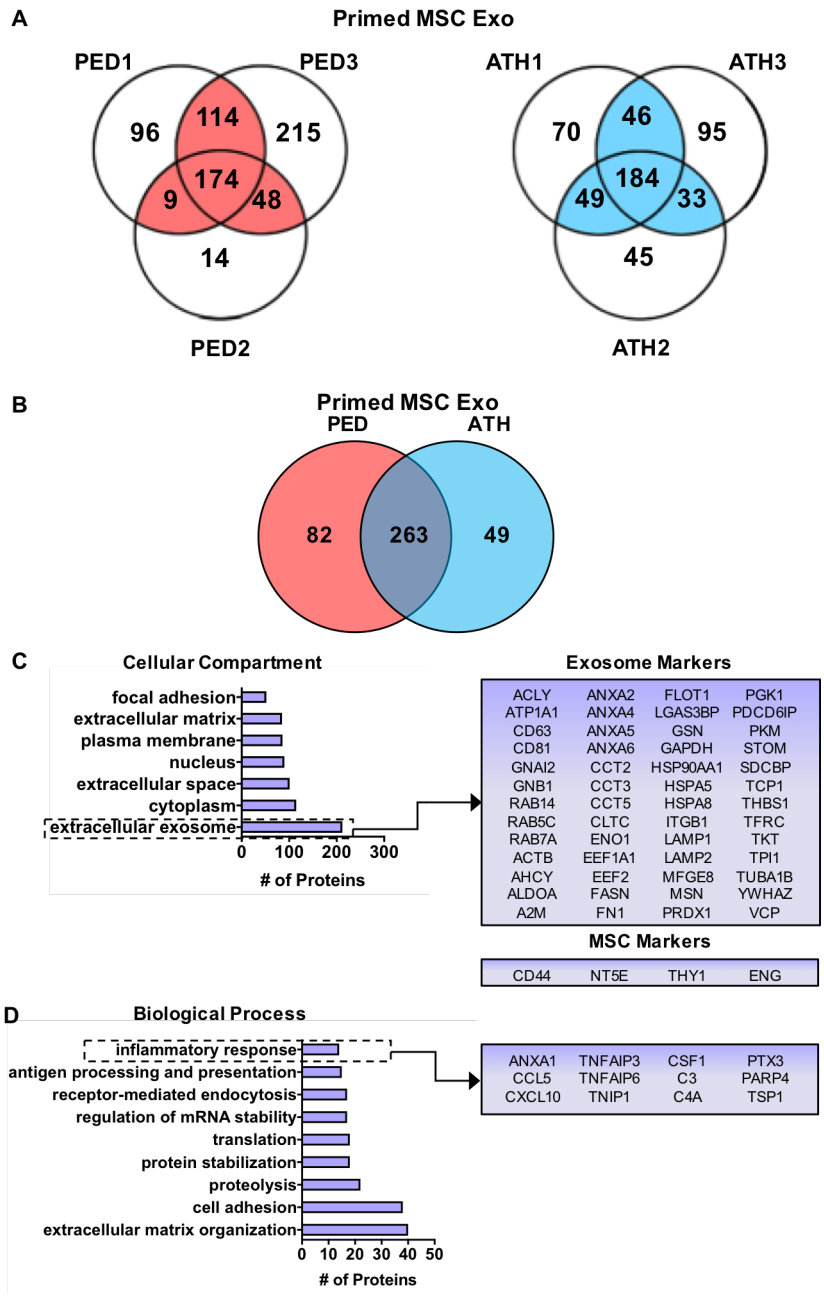

Figure 15: Proteomic comparison of PED and ATH Primed MSC exosomes

(A) Venn diagram showing the overlapping proteins in exosomes from MSC CM of 3 primed PED and ATH donors. **(B)** Overlapping proteins identified in at least two of three PED (345 proteins) or ATH (312 proteins) MSC exosome samples were compared. A total of 263 proteins overlapped between both groups. The Database for Annotation, Visualization and Integrated Discovery

(DAVID) was used to cluster the 263 shared proteins into cellular compartments and biological processes. **(C)** The majority of the proteins common to exosomes from both groups were associated with extracellular exosomes; these included proteins in the list of top 100 proteins identified in exosomes (exocarta.org/exosome_markers_new) (right panel). MSC markers (CD90/THY-1, CD73/NT5E, CD105/ENG, and CD44) were identified in both groups of MSC exosomes. **(D)** Biological processes associated with the shared proteins include extracellular matrix organization, cell adhesion and proteolysis. Proteins involved in inflammatory response were identified in both PED and ATH MSC exosomes (listed in the right panel). Abbreviations: ATH: atherosclerosis; Exo: exosomes; MSC: mesenchymal stromal cells; PED: pediatric.

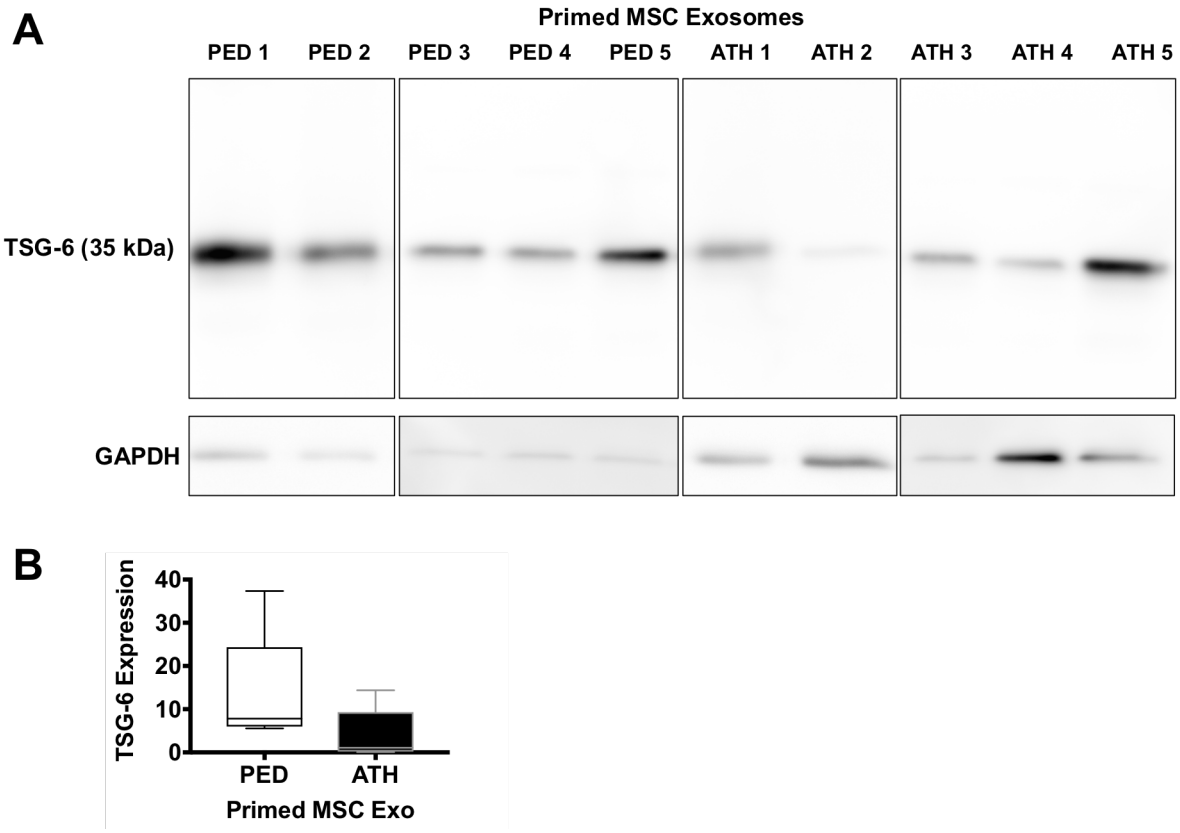

Figure 16: Enrichment of TSG-6 in exosomes from young MSCs

(A) Western blot analysis of 10 μg licensed MSC exosomes from PED and ATH donors, using an antibody specific for human TSG-6; **(B)** Summary of TSG-6 expression in primed MSC exosomes obtained from PED and ATH donors (n=5 per group). Abbreviations- ATH: atherosclerosis; Exo: Exosomes; GAPDH: glyceraldehyde-3-phosphate dehydrogenase; MSC: mesenchymal stromal cells; PED: pediatric; TSG-6: tumor necrosis factor-inducible gene 6 protein.

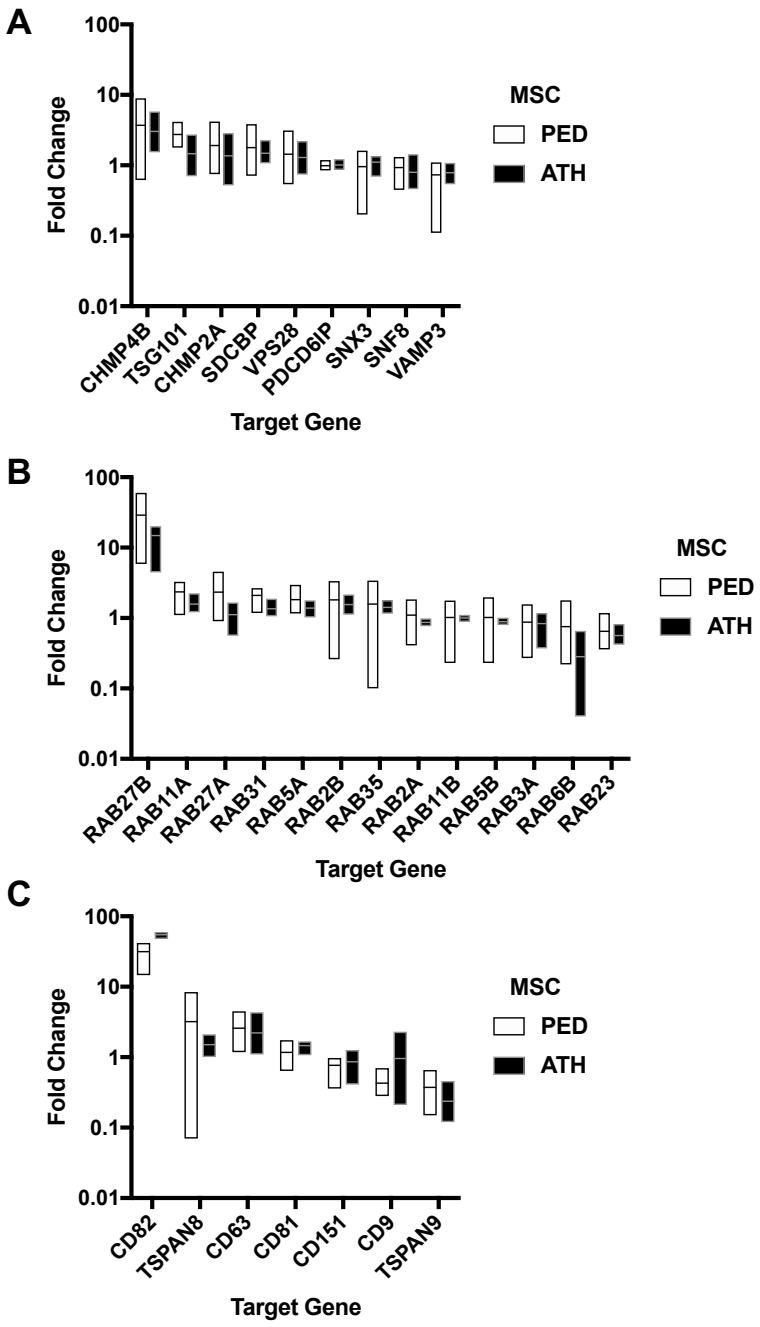

Figure 17: Effect of licensing on PED and ATH MSC Vesiculome

A custom RT^2 PCR array was designed to measure the fold change in the expression of **(A)** ESCRT and associated genes; **(B)** Rab GTPases; and **(C)** tetraspanins in resting and licensed MSCs. Mean±SD of 6 independent experiments (n=3 per group) are reported. Abbreviations: ATH: atherosclerosis; MSCs: mesenchymal stromal cells; PED: pediatric.

Figure 18: Rab27b expression in PED and ATH MSCs

(A) Western blot analysis of 10 µg licensed MSC lysate, using an antibody specific for human Rab27b; **(B)** Summary of Rab27b expression in primed MSC exosomes obtained from PED and ATH donors (n=3 per group). Abbreviations- ATH: atherosclerosis; MSC: mesenchymal stromal cell; PED: pediatric.

Tables

Table 1: Demographic characteristics of study populations

Demographics	PED	OA	ATH
No. of subjects	10	6	9
Sex, (female/male)	6/4	6/0	3/6
Age, mean ± SD years	15.9 ± 1.6	62.8 ± 8.7	65.2 ± 11.9
Ethnicity, %			
African American	10	16	0
Asian	10	0	22
Caucasian	80	83	77
Cardiovascular risk factors, %			
Hypertension	0	33	55
Hypercholesterolemia	0	0	66
Tobacco	0	0	22
Type 2 diabetes	0	0	55

Table 2: Factors involved in MSC:T cell suppression

MSC Source	Cell Responder	Activation	Factor	Findings	Ref
BM, human	Splenocytes, mice	CD3/CD28	TSG6	TSG6 siRNA reduced T cell suppression by MSCs	[45]
BM, mice	Splenocytes, mice	MLR	MCP-1 (CCL2)	CM from WT but not $CCL2^{-/-}$ MSCs reduced IFN-γ release.	[194]
BM, human	PBMCs, human	PHA	PGE_2	Inhibitors of PGE_2 synthesis reduced T cell suppression by MSCs.	[41]
BM, human	PBMCs, human	MLR	IDO	Addition of tryptophan to MSC/MLR co-culture restored T cell proliferation.	[177]
BM, mice	$CD4^+$ T cells, mice	Th-17 polarizing conditions	IL-10	IL-10 neutralizing antibodies blocked Th17 inhibition by MSCs.	[195]
BM, human	PBMCs, human	MLR	TGF-β	TGF-β neutralizing antibodies reversed MSC inhibition of alloreactivity.	[196]
C3H10T1/2 (C3) MSC line, mice	Splenocytes, mice	MLR	IL-6	IL-6 neutralizing antibodies reduced allogenic T cell inhibition by MSCs	[197]
Placenta, human	PBMCs, human	PHA, anti-CD3/CD28	HGF	Knockdown of HGF secretion reduced T cell suppression by MSCs	[178]
BM, human	PBMCs, human	MLR	HLA-G	HLA-G neutralizing antibodies reduced T cell suppression by MSC CM.	[198]

Abbreviations: Bone marrow (BM), C-C motif chemokine ligand 2 (CCL2), conditioned medium (CM), indoleamine 2 3-dioxygenase (IDO), hepatocyte growth factor (HGF), human leukocyte antigen G (HLA-G), interleukin (IL), monocyte chemotactic protein (MCP), mixed lymphocyte reaction (MLR), peripheral blood mononuclear cells (PBMCs), phytohemagglutinin (PHA), prostaglandin E2 (PGE_2), recombinant human (rh), transforming growth factor beta (TGF-β), regulatory T cells (Treg), tumor necrosis factor-stimulated gene 6 (TSG-6), wild type (WT).

Table 3: Examples of physiological and pathological functions of exosomes

Exosome Source	Target	Function	Reference
Mature reticulocytes	NA	Transferrin recycling during reticulocyte maturation; Disposal of unwanted materials	[199, 200]
Mature DCs	T cells	Induce strong antigen-specific T cell proliferation	[109]
Regulatory T cells	$CD4^+$ T cells	Inhibit polyclonal T cell proliferation via CD73 mediated adenosine production	[201]
Glia	Cortical neurons	Increase the survival of cortical neurons under oxidative stress and ischemic conditions	[202]
Cardiomyocyte progenitor cells	Endothelial cells	Stimulate the migration of endothelial cells; may enhance cardiomyogenesis and angiogenesis	[203]
Breast milk	Infant	Modulate the infant's immune system by influencing T cell regulation via miRNAs	[204, 205]
Placenta	T cells	Impair T cell mediated responses; may induce maternal tolerance to fetal antigens	[206]
Nef transformed T cells	$CD4^+$ T cells	Nef association with exosomes facilitates T cell depletion - a hallmark of AIDS	[207]
CML cells	BM stromal cells	Increase IL-8 expression leading to increase adhesion, motility and survival of CML cells	[208]

Abbreviations: Acquired immunodeficiency syndrome (AIDS), bone marrow (BM), chronic myelogenous leukemia (CML), cluster of differentiation (CD), dendritic cells (DCs), interleukin (IL), microRNA (miRNA), not applicable (NA), negative regulatory factor (Nef).

Table 4: Characteristics of apoptotic bodies, microvesicles, and exosomes

Characteristics	Apoptotic bodies	Microvesicles	Exosomes
Origin	Cell surface; Blebbing of apoptotic cell membrane	Cell surface; budding of cell membrane	Endolysosomal pathway; ILVs are released from MVBs upon fusion with cell membrane
Morphology	Heterogeneous	Irregular shape, heterogeneous	Cup-shaped (TEM), homogenous
Size	>1000 nm	100–1000 nm	50-150 nm
Sedimentation	1,200xg	10,000xg	100,000xg
Sucrose gradient	1.16-1.28 g/ml	1.04-1.07 g/ml	1.13-1.19 g/ml
Markers	Histones, cellular organelles (cytochrome C, GP96, actinin-4, mitofilin)	Integrins, selectins, CD40, actinin-4, mitofilin, tubulin	Tetraspanins (CD9, CD63, CD81), endosome-associated proteins (ESCRT, Rab GTPases, SNAREs, Annexins Syntenin-1), ADAM10, EHD4

Abbreviations: A disintegrin and metalloproteinase domain-containing protein 10 (ADAM10), charged multivesicular body protein 4A-B (CHMP4A-B), cluster of differentiation (CD), EH domain containing 4 (EHD4), endosomal sorting complexes required for transport (ESCRT), intraluminal vesicles (ILVs), multivesicular bodies (MVBs), ras-related proteins in brain (Rab), transmission electron microscopy (TEM), messenger RNA (mRNA), microRNA (miRNA), ribonucleic acid (RNA), Soluble N-ethylmaleimide-sensitive factor activating protein receptor (SNARE), tumor susceptibility gene 101 (TSG101), vacuolar protein sorting 4 homolog B (VPS4B).

Table 5: Studies evaluating the immunomodulatory properties of MSC exosomes

MSC Source	Priming	Exosome Isolation	Exosome Loaded	Recipient Cell	Stimulation	Assay Length (Days)	T cell Proliferation Inhibition	Treg Induction	T cell Apoptosis	Alters Th1/Th2 Cytokine Release	Ref
Mouse BM	IL-1β	Ultracentrifugation	0, 10 and 20 μg/ml	EAE Murine Splenic Mononuclear cells ($2x10^5$)	MOG_{35-55}	3	Yes	Yes	Yes	-	[134]
Rat BM	None	Exoquick	10 μg/ml	Rat spleen lymphocytes	Anti-CD3	5	Yes	-	-	-	[209]
Human Embryonic Stem Cells (huES9.E MSC)	None	100 kDa MWCO filtration and HPLC	0.1, 1, 4 μg/mL	Mouse splenocytes (5×10^5 cells/mL)	LPS and ConA	3	Yes	Yes	-	Yes	[179]
Human BM	None	Exoquick	0, 5, 10 and 20 μg	Human PBMCs ($2x10^5$)	ConA	3 or 6	No	Yes	Yes	Yes	[210]
Human BM	IFN-γ + TNF-α	Ultracentrifugation	1 to 300 T cell to EV ratio	Human Purified T cells ($2x10^5$)	Anti-CD3/CD28	4	No	-	-	-	[135]
Human BM	None	Ultracentrifugation	From 2, 5, and 10×10^6 MSC	Human PBMCs (10^5)	PHA	3	Yes	-	-	-	[133]
Human BM	None	100 kDa MWCO and Ultracentrifugation	$4.6x10^8$ EVs	PBMCs (5×10^5)	Anti-CD3/CD28	5	No	Yes	Yes	Yes	[181]
Human BM	None	Sucrose Cushion	10, 50 and 100 μg/ml	Human PBMCs (10^5)	Ant- CD3/CD28	6	No	-	-	-	[182]
Human Adipose							No	-	-	-	
Human Adipose	None	Ultracentrifugation	4, 8, and 16 μg per 10^6 PBMCs	Human PBMCs (2×10^5)	Anti-CD2/CD3/CD28	6	Yes	-	-	Yes	[180]
Human Umbilical Cord	None	Size Exclusion Chromatography	From $2.5x10^5$ or $1.25x10^5$ MSCs	Human Purified T cells ($3x10^5$)	Anti-CD2/CD3/CD28	3.5	Yes	-	No	No	[183]
		Ultracentrifugation					No	-	No	Yes	
Human Umbilical Cord Blood	IFN-γ	Ultracentrifugation	Not specified	Human PBMCs (1.5×10^6)	Anti-CD3	4 or 7	Yes	Yes	-	-	[136]

Table 6: Molecular changes in human MSCs during aging

Hallmark	Function	Evidence in MSCs	Ref
Telomere shortening	Telomeres responsible for protecting the chromosome ends from erosion; shortening beyond a critical length leads to genomic instability, DNA damage, and cellular senescence	MSCs obtained from elderly donors possess shorter telomere lengths	[211, 212]
Genomic instability	Genome maintenance systems act to remove and repair damage caused by extrinsic factors such as ROS, UV radiation and environmental mutagens	MSCs from elderly donors show impaired DNA damage response and increased accumulation of DNA damage	[36, 142, 143]
Mitochondria dysfunction	Mitochondria are essential to generate energy for the cell. Mutations in mitochondrial DNA can lead to respiratory chain dysfunction and the accumulation of ROS	There is an age-associated increase of intracellular ROS in MSCs, suggesting a decline of mitochondrial integrity with advancing age	[36, 213]
Dysregulated proteostasis	Defects in proteostasis result in aberrant folding, toxic aggregation and accumulation of damaged proteins, ultimately leading to cellular damage and tissue dysfunction	Age-dependent reduction of heat shock proteins observed in MSCs, suggesting a decline in the heat shock response	[213]
Impaired intercellular communication	"Inflammaging", refers to the chronic proinflammatory state that accompanies aging in mammals; it is characterized by a functional shift in the activity of the innate immune cells, leading to chronic inflammatory cytokine production	MSCs obtained from elderly donors display a pro-inflammatory secretome and an impaired ability to inhibit inflammatory T cell activity	[36, 146]

Abbreviations: Adenosine triphosphate (ATP), deoxyribonucleic acid (DNA) reactive oxygen species (ROS), ultraviolet (UV).

Table 7: Genes included in the custom RT^2 profiler PCR array

Gene Bank	Symbol	Category	Catalogue number
NM_001110	ADAM10	ADAM metallopeptidase domain 10	PPH13517A
NM_00101443	AKT1	v-AKT murine thymoma viral oncogene homolog 1	PPH00088B
NM_001157	ANXA11	annexin A11	PPH06949A
NM_001153	ANXA4	annexin A4	PPH06928F
NM_001155	ANXA6	annexin A6	PPH06922F
NM_001663	ARF6	ADP-ribosylation factor 6	PPH10416A
NM_001025356	ANO6	anoctamin 6	PPH19527A
NM_004707	ATG12	autophagy related 12	PPH15326A
NM_001172895	CAV1	caveolin 1, caveolae protein	PPH00739A
NM_001039490	CD151	CD151 molecule (Raph blood group)	PPH23445F
NM_000610	CD44	CD44 molecule (Indian blood group)	PPH00114A
NM_001040034	CD63	CD63 molecule	PPH21303A
NM_004356	CD81	CD81 molecule	PPH00960A
NM_001024844	CD82	CD82 molecule	PPH01312A
NM_001769	CD9	CD9 molecule	PPH02661A
NM_005507	CFL1	cofilin 1 (non-muscle)	PPH13461F
NM_014453	CHMP2A	charged multivesicular body protein 2A	PPH07827A
NM_176812	CHMP4B	charged multivesicular body protein 4B	PPH19075A
NM_001098209	CTNNB1	catenin (cadherin-associated protein), beta 1	PPH00643F
NM_001042517	DIAPH3	diaphanous-related formin 3	PPH11577A
NM_019074	DLL4	delta-like 4 (Drosophila)	PPH06026A
NM_001144763	EXPH5	exophilin 5	PPH12394A
NM_005232	EPHA1	EPH receptor A1	PPH05727F
NM_005803	FLOT1	flotillin 1	PPH13731A
NM_004475	FLOT2	flotillin 2	PPH08193A
NM_000165	GJA1	gap junction protein, alpha 1	PPH02781E
NM_004712	HGS	hepatocyte growth factor-regulated tyrosine kinase substrate	PPH19788A
NM_002137	HNRNPA2 B1	heterogeneous nuclear ribonucleoprotein A2/B1	PPH14710A
NM_002154	HSPA4	heat shock 70kDa protein 4	PPH01188C
NM_005347	HSPA5	heat shock 70kDa protein 5	PPH00158E
NM_001130106	HSPBP1	HSPA binding protein, cytoplasmic co-chaperone 1	PPH09439A
NM_000201	ICAM1	intercellular adhesion molecule 1	PPH00640F
NM_002205	ITGA5	integrin, alpha 5	PPH00176C
NM_000210	ITGA6	integrin, alpha 6	PPH00177F
NM_000213	ITGB4	integrin, beta 4	PPH00680B
NM_002213	ITGB5	integrin, beta 5	PPH00634F
NM_005561	LAMP1	lysosomal-associated membrane protein 1	PPH05794G
NM_001122606	LAMP2	lysosomal-associated membrane protein 2	PPH14711A
NM_001204426	LIMK1	LIM domain kinase 1	PPH01081A
NM_001111097	LYN	LYN proto-oncogene, Src family tyrosine kinase	PPH01635A
NM_003010	MAP2K4	mitogen-activated protein kinase kinase 4	PPH00195C
NM_002758	MAP2K6	mitogen-activated protein kinase kinase 6	PPH00742B
NM_001098540	HPSE	heparanase	PPH01060E
NM_001114614	MFGE8	milk fat globule-EGF factor 8 protein	PPH07218A
NM_001162429	PDCD6IP	programmed cell death 6 interacting protein	PPH07704C
NM_001159542	POU5F1B	POU class 5 homeobox 1B	PPH66786A

NM_001145847	PROM1	prominin 1	PPH02400A
NM_001206836	RAB11A	RAB11A, member RAS oncogene family	PPH05835B
NM_004218	RAB11B	RAB11B, member RAS oncogene family	PPH20230A
NM_016277	RAB23	RAB23, member RAS oncogene family	PPH10554A
NM_004580	RAB27A	RAB27A, member RAS oncogene family	PPH16394A
NM_004163	RAB27B	RAB27B, member RAS oncogene family	PPH08600A
NM_001242644	RAB2A	RAB2A, member RAS oncogene family	PPH10101A
NM_001163380	RAB2B	RAB2B, member RAS oncogene family	PPH08395A
NM_006868	RAB31	RAB31, member RAS oncogene family	PPH01844A
NM_001167606	RAB35	RAB35, member RAS oncogene family	PPH10546A
NM_002866	RAB3A	RAB3A, member RAS oncogene family	PPH08762B
NM_004162	RAB5A	RAB5A, member RAS oncogene family	PPH02272A
NM_001252036	RAB5B	RAB5B, member RAS oncogene family	PPH10072A
NM_016577	RAB6B	RAB6B, member RAS oncogene family	PPH17626B
NM_001664	RHOA	ras homolog family member A	PPH00305G
NM_005406	ROCK1	Rho-associated, coiled-coil containing protein kinase 1	PPH01966C
NM_001007067	SDCBP	syndecan binding protein (syntenin)	PPH13276A
NM_000543	SMPD1	sphingomyelin phosphodiesterase 1	PPH02494A
NM_003080	SMPD2	sphingomyelin phosphodiesterase 2	PPH09509A
NM_018667	SMPD3	sphingomyelin phosphodiesterase 3	PPH15917A
NM_001171083	SMPD4	sphingomyelin phosphodiesterase 4	PPH10549B
NM_006714	SMPDL3A	sphingomyelin phosphodiesterase, acid-like 3A	PPH15653A
NM_001009568	SMPDL3B	sphingomyelin phosphodiesterase, acid-like 3B	PPH11648A
NM_003081	SNAP25	synaptosomal-associated protein, 25kDa	PPH01881B
NM_007241	SNF8	SNF8, ESCRT-II complex subunit	PPH11810A
NM_003795	SNX3	sorting nexin 3	PPH07825A
NM_001165903	STX1A	syntaxin 1A	PPH01877A
NM_003569	STX7	syntaxin 7	PPH01862A
NM_001252065	SYT7	synaptotagmin VII	PPH08754A
NM_006292	TSG101	tumor susceptibility 101	PPH06937E
NM_004616	TSPAN8	tetraspanin 8	PPH10294A
NM_001168320	TSPAN9	tetraspanin 9	PPH11091C
NM_004781	VAMP3	vesicle-associated membrane protein 3	PPH06289A
NM_016208	VPS28	vacuolar protein sorting 28 homolog (S. cerevisiae)	PPH19823A
NM_016485	VTA1	vesicle (multivesicular body) trafficking 1	PPH15357A
NM_001002292	WLS	wntless Wnt ligand secretion mediator	PPH16376A
NM_004626	WNT11	wingless-type MMTV integration site family, member 11	PPH02399C
NM_016087	WNT16	wingless-type MMTV integration site family, member 16	PPH02766B
NM_033131	WNT3A	wingless-type MMTV integration site family, member 3A	PPH02772B
NM_001256105	WNT5A	wingless-type MMTV integration site family, member 5A	PPH02410A
NM_004559	YBX1	Y box binding protein 1	PPH09908B
NM_001101	ACTB	actin, beta	PPH00073G
NM_004048	B2M	beta-2-microglobulin	PPH01094E
NM_001256799	GAPDH	glyceraldehyde-3-phosphate dehydrogenase	PPH00150F
NM_007355	HSP90AB1	heat shock protein 90kDa alpha, class B member 1	PPH01201C

Supplementary Figures

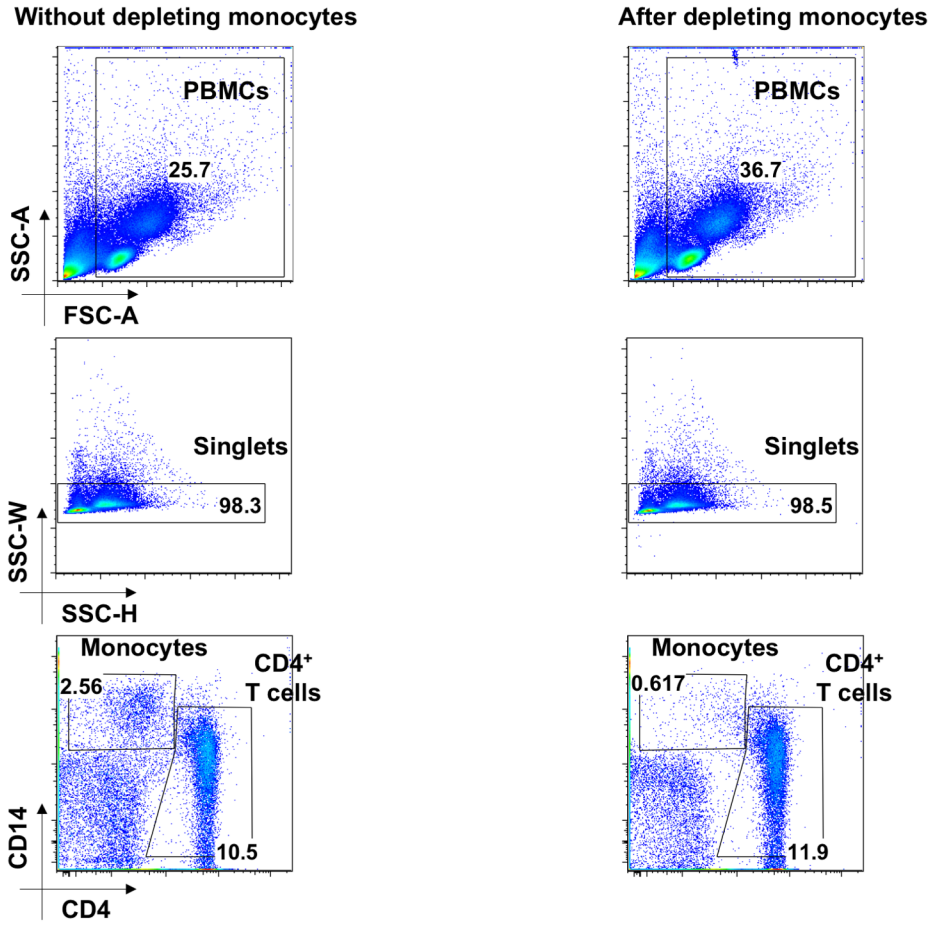

Figure S1: Monocyte depletion from PBMCs

The proportion of $CD14^+$ monocyte and $CD4^+$ T lymphocyte populations in PBMCs were measured by flow cytometry pre- (left panel) or post- (right panel) overnight monocyte depletion. Abbreviations: PBMCs: peripheral blood mononuclear cells; SSC-A: side scatter area; SSC-H: side scatter height; SSC-W: side scatter width.

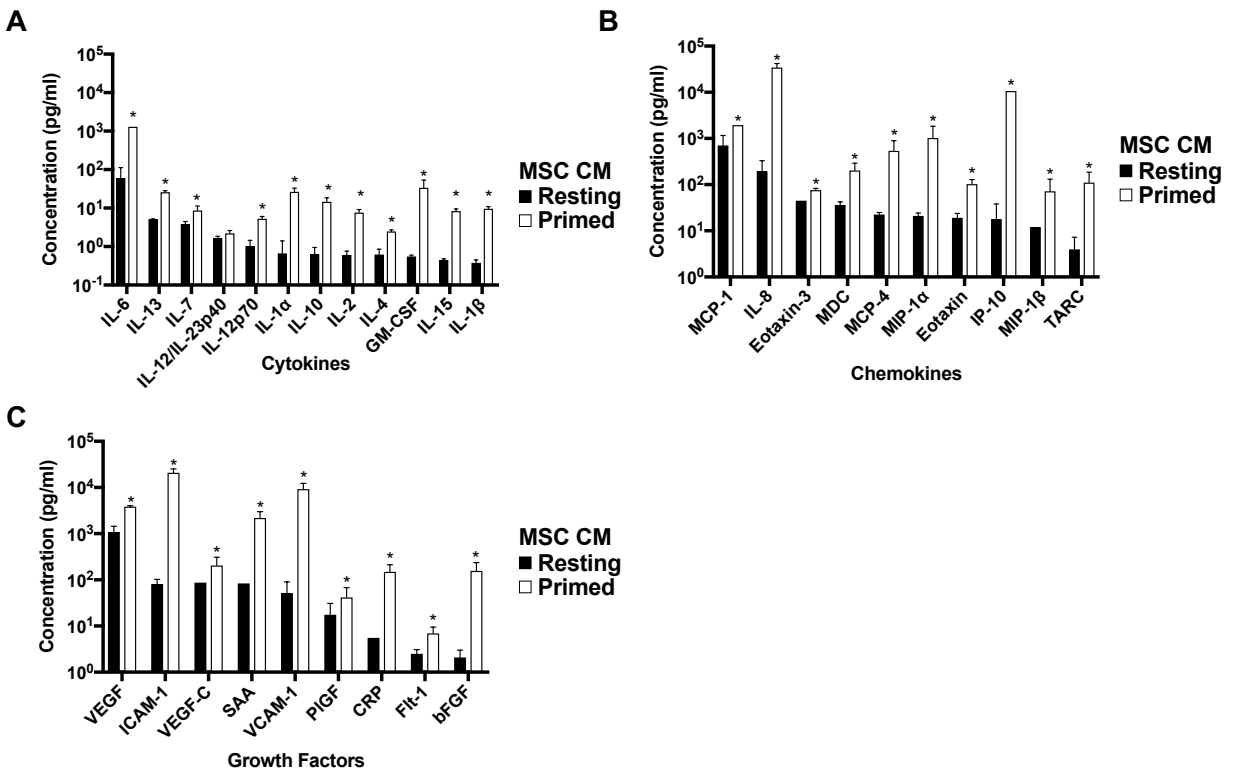

Figure S2: MSC licensing increases cytokine, chemokine and growth factor release

The levels of **(A)** cytokines; **(B)** chemokines; and **(C)** growth factors in the CM obtained from resting and primed MSCs (250,000 cells/ml) was measured using the multiplex platform (Meso Scale Discovery). Mean±SD of 6 independent experiments are reported, where (*) represents $p \leq 0.05$. Abbreviations: bFGF- basic fibroblast growth factor; CRP: C-reactive protein; Flt-1: fms-like tyrosine kinase 1; GM-CSF: granulocyte-macrophage colony-stimulating factor; ICAM-1: intercellular adhesion molecule 1; IL: interleukin; IP-10: interferon gamma-induced protein; MCP-1: monocyte chemoattractant protein-1; MDC: macrophage derived chemokine; MIP: macrophage inflammatory protein; MSC CM: mesenchymal stromal cell conditioned media; PlGF: placental growth factor; TARC: thymus and activation-regulated chemokine; SAA: serum amyloid A; VCAM-1: vascular cell adhesion protein 1; VEGF: vascular endothelial growth factor.

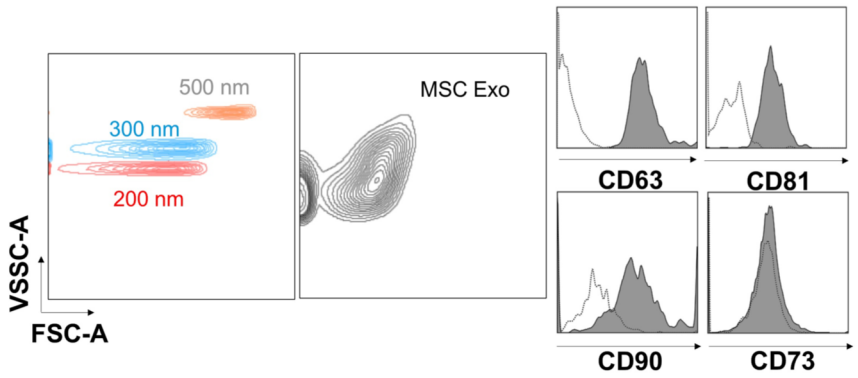

Figure S3: Flow cytometry for surface markers on MSC exosomes

CytoFLEX was used to evaluate the size distribution of MSC exosomes using calibration beads (200, 300 and 500 nm). MSC exosomes were stained with fluorescence-conjugated antibodies to determine the co-expression of exosome (i.e., CD63, CD81) and MSC markers (i.e., CD90, CD73). Abbreviations: FSC-A: forward scatter area; VSSC-A: violet side scatter area.

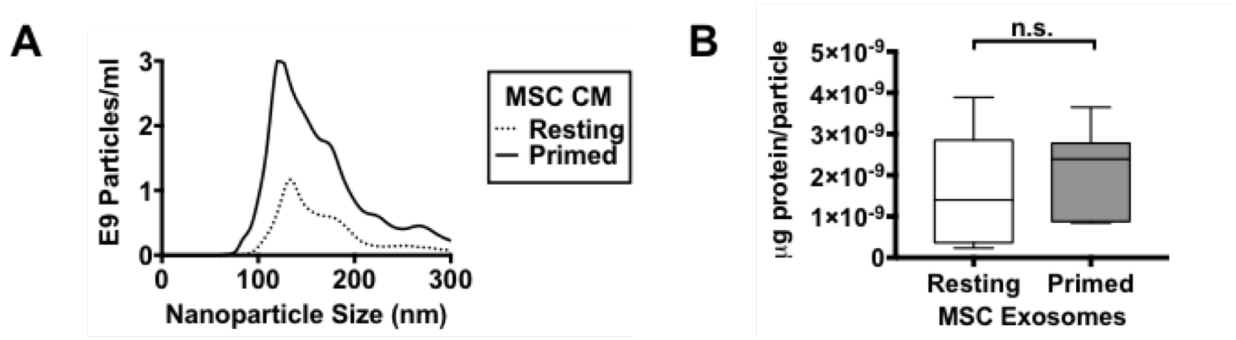

Figure S4: Characterization of exosomes from resting and primed MSCs

Exosomes were harvested from resting or primed MSC CM by differential centrifugation, NTA and MicroBCA was used to compare the **(A)** size distribution of the obtained vesicles and **(B)** the amount of protein per particle. Mean±SD of 6 independent experiments are reported. Abbreviations: MSC CM: mesenchymal stromal cell conditioned media.

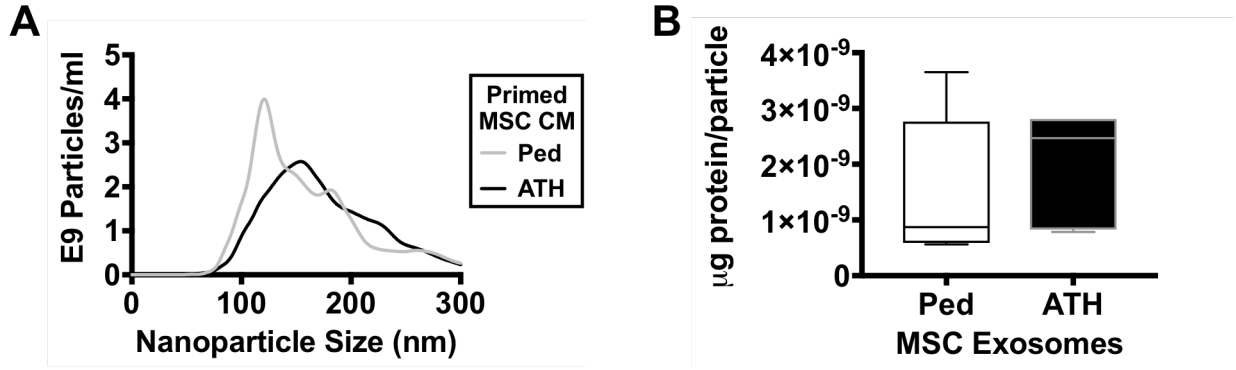

Figure S5: Characterization of exosomes from primed PED, OA and ATH MSCs

Exosomes were collected from primed PED and ATH MSC CM by differential centrifugation, NTA and MicroBCA was used to measure **(A)** particle size distribution, **(B)** amount of protein per particle. Mean±SD of 6 independent experiments are reported. Abbreviations: ATH atherosclerosis; MSC: mesenchymal stromal cells; PED: pediatric.

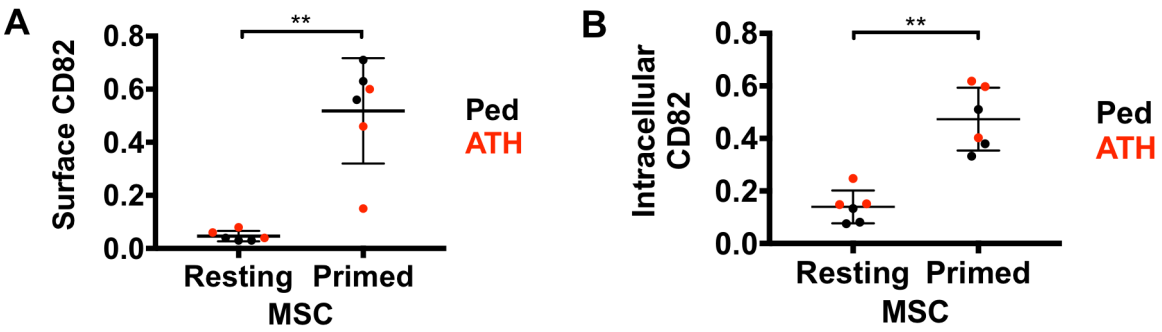

Figure S6: Effect of licensing on surface and intracellular CD82 expression of MSCs

(A) Surface and **(B)** intracellular CD82 expression was measured in resting and primed MSCs (n=6 per group). Mean±SD of 6 independent experiments are reported, where (**) represents $p \leq 0.01$. Abbreviations: ATH: atherosclerosis; MSC: mesenchymal stromal cells; PED: pediatric.

References

1. Dominici, M., et al., *Minimal criteria for defining multipotent mesenchymal stromal cells. The International Society for Cellular Therapy position statement.* cytotherapy, 2006. **8**(4): p. 315-317.
2. Bieback, K., et al., *Critical parameters for the isolation of mesenchymal stem cells from umbilical cord blood.* Stem cells, 2004. **22**(4): p. 625-634.
3. Lee, R.H., et al., *Characterization and expression analysis of mesenchymal stem cells from human bone marrow and adipose tissue.* Cellular Physiology and Biochemistry, 2004. **14**(4-6): p. 311-324.
4. De Bari, C., et al., *Multipotent mesenchymal stem cells from adult human synovial membrane.* Arthritis & Rheumatology, 2001. **44**(8): p. 1928-1942.
5. Scherjon, S.A., et al., *Amniotic fluid as a novel source of mesenchymal stem cells for therapeutic transplantation.* Blood, 2003. **102**(4): p. 1548-1549.
6. Scherjon, S.A., et al., *Isolation of mesenchymal stem cells of fetal or maternal origin from human placenta.* Stem Cells, 2004. **22**(7): p. 1338-1345.
7. Horwitz, E., et al., *Clarification of the nomenclature for MSC: The International Society for Cellular Therapy position statement.* Cytotherapy, 2005. **7**(5): p. 393-395.
8. Marion, N.W. and J.J. Mao, *Mesenchymal stem cells and tissue engineering.* Methods in enzymology, 2006. **420**: p. 339-361.
9. Semedo, P., et al. *Mesenchymal stem cells ameliorate tissue damages triggered by renal ischemia and reperfusion injury*. in *Transplantation proceedings*. 2007. Elsevier.
10. Aziz, M.A., et al., *Therapeutic potential of bone marrow-derived mesenchymal stem cells on experimental liver fibrosis.* Clinical biochemistry, 2007. **40**(12): p. 893-899.
11. Nagaya, N., et al., *Intravenous administration of mesenchymal stem cells improves cardiac function in rats with acute myocardial infarction through angiogenesis and myogenesis.* American Journal of Physiology-Heart and Circulatory Physiology, 2004. **287**(6): p. H2670-H2676.
12. Lai, R.C., et al., *Exosome secreted by MSC reduces myocardial ischemia/reperfusion injury.* Stem cell research, 2010. **4**(3): p. 214-222.
13. Ramasamy, R., et al., *Mesenchymal stem cells inhibit dendritic cell differentiation and function by preventing entry into the cell cycle.* Transplantation, 2007. **83**(1): p. 71-76.
14. Raffaghello, L., et al., *Human mesenchymal stem cells inhibit neutrophil apoptosis: a model for neutrophil preservation in the bone marrow niche.* Stem cells, 2008. **26**(1): p. 151-162.
15. Morrison, T.J., et al., *Mesenchymal Stromal Cells Modulate Macrophages in Clinically Relevant Lung Injury Models by Extracellular Vesicle Mitochondrial Transfer.* American Journal of Respiratory And Critical Care Medicine, 2017(ja).
16. Spaggiari, G.M., et al., *Mesenchymal stem cell-natural killer cell interactions: evidence that activated NK cells are capable of killing MSCs, whereas MSCs can inhibit IL-2-induced NK-cell proliferation.* Blood, 2006. **107**(4): p. 1484-1490.
17. Di Nicola, M., et al., *Human bone marrow stromal cells suppress T-lymphocyte proliferation induced by cellular or nonspecific mitogenic stimuli.* Blood, 2002. **99**(10): p. 3838-3843.

18. Ghannam, S., et al., *Mesenchymal stem cells inhibit human Th17 cell differentiation and function and induce a T regulatory cell phenotype.* The Journal of Immunology, 2010. **185**(1): p. 302-312.
19. Corcione, A., et al., *Human mesenchymal stem cells modulate B-cell functions.* Blood, 2006. **107**(1): p. 367-372.
20. Le Blanc, K., et al., *Treatment of severe acute graft-versus-host disease with third party haploidentical mesenchymal stem cells.* The Lancet, 2004. **363**(9419): p. 1439-1441.
21. Boregowda, S.V. and D.G. Phinney, *Quantifiable Metrics for Predicting MSC Therapeutic Efficacy.* Journal of stem cell research & therapy, 2016. **6**(11).
22. DiMarino, A.M., A.I. Caplan, and T.L. Bonfield, *Mesenchymal stem cells in tissue repair.* Frontiers in immunology, 2013. **4**: p. 201.
23. Krampera, M., et al., *Immunological characterization of multipotent mesenchymal stromal cells—The International Society for Cellular Therapy (ISCT) working proposal.* Cytotherapy, 2013. **15**(9): p. 1054-1061.
24. Xishan, Z., et al., *Comparison of the effects of human adipose and bone marrow mesenchymal stem cells on T lymphocytes.* Cell biology international, 2013. **37**(1): p. 11-18.
25. Fraser, J.K., et al., *Fat tissue: an underappreciated source of stem cells for biotechnology.* Trends in biotechnology, 2006. **24**(4): p. 150-154.
26. Musina, R., E. Bekchanova, and G. Sukhikh, *Comparison of mesenchymal stem cells obtained from different human tissues.* Bulletin of experimental biology and medicine, 2005. **139**(4): p. 504-509.
27. Mancini, O.K., et al., *Age, atherosclerosis and type 2 diabetes reduce human mesenchymal stromal cell-mediated T-cell suppression.* Stem cell research & therapy, 2015. **6**(1): p. 140.
28. Sotiropoulou, P.A., et al., *Characterization of the optimal culture conditions for clinical scale production of human mesenchymal stem cells.* Stem cells, 2006. **24**(2): p. 462-471.
29. Parker, A., et al., *Low serum and serum-free culture of multipotential human adipose stem cells.* Cytotherapy, 2007. **9**(7): p. 637-646.
30. Baer, P.C. and H. Geiger, *Adipose-derived mesenchymal stromal/stem cells: tissue localization, characterization, and heterogeneity.* Stem cells international, 2012. **2012**.
31. Lee, M.W., et al., *Effect of ex vivo culture conditions on immunosuppression by human mesenchymal stem cells.* BioMed research international, 2013. **2013**.
32. Rosova, I., et al., *Hypoxic preconditioning results in increased motility and improved therapeutic potential of human mesenchymal stem cells.* Stem cells, 2008. **26**(8): p. 2173-2182.
33. Koike, M., et al., *Effects of mechanical strain on proliferation and differentiation of bone marrow stromal cell line ST2.* Journal of bone and mineral metabolism, 2005. **23**(3): p. 219-225.
34. von Bahr, L., et al., *Long-term complications, immunologic effects, and role of passage for outcome in mesenchymal stromal cell therapy.* Biology of Blood and Marrow Transplantation, 2012. **18**(4): p. 557-564.
35. Bloom, D.D., et al., *A reproducible immunopotency assay to measure mesenchymal stromal cell–mediated T-cell suppression.* Cytotherapy, 2015. **17**(2): p. 140-151.

36. Kizilay Mancini, Ö., et al., *A Proinflammatory Secretome Mediates the Impaired Immunopotency of Human Mesenchymal Stromal Cells in Elderly Patients With Atherosclerosis.* Stem cells translational medicine, 2017.
37. Galipeau, J., et al., *International Society for Cellular Therapy perspective on immune functional assays for mesenchymal stromal cells as potency release criterion for advanced phase clinical trials.* Cytotherapy, 2016. **18**(2): p. 151-159.
38. Lyons, A.B., *Analysing cell division in vivo and in vitro using flow cytometric measurement of CFSE dye dilution.* Journal of immunological methods, 2000. **243**(1): p. 147-154.
39. Djouad, F., et al., *Immunosuppressive effect of mesenchymal stem cells favors tumor growth in allogeneic animals.* Blood, 2003. **102**(10): p. 3837-3844.
40. Ryan, J., et al., *Interferon-γ does not break, but promotes the immunosuppressive capacity of adult human mesenchymal stem cells.* Clinical & Experimental Immunology, 2007. **149**(2): p. 353-363.
41. Aggarwal, S. and M.F. Pittenger, *Human mesenchymal stem cells modulate allogeneic immune cell responses.* Blood, 2005. **105**(4): p. 1815-1822.
42. Ponte, A.L., et al., *The in vitro migration capacity of human bone marrow mesenchymal stem cells: comparison of chemokine and growth factor chemotactic activities.* Stem cells, 2007. **25**(7): p. 1737-1745.
43. Song, W.-J., et al., *TSG-6 Secreted by Human Adipose Tissue-derived Mesenchymal Stem Cells Ameliorates DSS-induced colitis by Inducing M2 Macrophage Polarization in Mice.* Scientific Reports, 2017. **7**.
44. Qi, Y., et al., *TSG-6 released from intradermally injected mesenchymal stem cells accelerates wound healing and reduces tissue fibrosis in murine full-thickness skin wounds.* Journal of Investigative Dermatology, 2014. **134**(2): p. 526-537.
45. Kota, D.J., et al., *TSG-6 produced by hMSCs delays the onset of autoimmune diabetes by suppressing Th1 development and enhancing tolerogenicity.* Diabetes, 2013. **62**(6): p. 2048-2058.
46. Kemp, K., et al., *Inflammatory cytokine induced regulation of superoxide dismutase 3 expression by human mesenchymal stem cells.* Stem Cell Reviews and Reports, 2010. **6**(4): p. 548-559.
47. English, K., et al., *IFN-γ and TNF-α differentially regulate immunomodulation by murine mesenchymal stem cells.* Immunology letters, 2007. **110**(2): p. 91-100.
48. Hemeda, H., et al., *IFN-gamma and TNF-alpha differentially affect cytokine expression and migration properties of mesenchymal stem cells.* Stem Cells Dev, 2010. **19**: p. 693-706.
49. Jin, P., et al., *Interferon-γ and tumor necrosis factor-α polarize bone marrow stromal cells uniformly to a Th1 phenotype.* Scientific reports, 2016. **6**.
50. Phinney, D.G. and D.J. Prockop, *Concise review: mesenchymal stem/multipotent stromal cells: the state of transdifferentiation and modes of tissue repair—current views.* Stem cells, 2007. **25**(11): p. 2896-2902.
51. Iso, Y., et al., *Multipotent human stromal cells improve cardiac function after myocardial infarction in mice without long-term engraftment.* Biochemical and biophysical research communications, 2007. **354**(3): p. 700-706.

52. Lee, R.H., et al., *Intravenous hMSCs improve myocardial infarction in mice because cells embolized in lung are activated to secrete the anti-inflammatory protein TSG-6.* Cell stem cell, 2009. **5**(1): p. 54-63.
53. Timmers, L., et al., *Human mesenchymal stem cell-conditioned medium improves cardiac function following myocardial infarction.* Stem cell research, 2011. **6**(3): p. 206-214.
54. Gnecchi, M., et al., *Evidence supporting paracrine hypothesis for Akt-modified mesenchymal stem cell-mediated cardiac protection and functional improvement.* The FASEB Journal, 2006. **20**(6): p. 661-669.
55. Spees, J.L., R.H. Lee, and C.A. Gregory, *Mechanisms of mesenchymal stem/stromal cell function.* Stem Cell Research & Therapy, 2016. **7**(1): p. 125.
56. Gnecchi, M., et al., *Paracrine mechanisms in adult stem cell signaling and therapy.* Circulation research, 2008. **103**(11): p. 1204-1219.
57. Lai, R.C., R.W.Y. Yeo, and S.K. Lim. *Mesenchymal stem cell exosomes*. in *Seminars in Cell & Developmental Biology*. 2015. Elsevier.
58. Kordelas, L., et al., *MSC-derived exosomes: a novel tool to treat therapy-refractory graft-versus-host disease.* Leukemia, 2014. **28**(4): p. 970.
59. Ratajczak, J., et al., *Embryonic stem cell-derived microvesicles reprogram hematopoietic progenitors: evidence for horizontal transfer of mRNA and protein delivery.* Leukemia, 2006. **20**(5): p. 847-856.
60. Valadi, H., et al., *Exosome-mediated transfer of mRNAs and microRNAs is a novel mechanism of genetic exchange between cells.* Nature cell biology, 2007. **9**(6): p. 654-659.
61. Elmore, S., *Apoptosis: a review of programmed cell death.* Toxicologic pathology, 2007. **35**(4): p. 495-516.
62. Savill, J., *Recognition and phagocytosis of cells undergoing apoptosis.* British medical bulletin, 1997. **53**(3): p. 491-508.
63. Rubartelli, A., A. Poggi, and M.R. Zocchi, *The selective engulfment of apoptotic bodies by dendritic cells is mediated by the αvβ3 integrin and requires intracellular and extracellular calcium.* European journal of immunology, 1997. **27**(8): p. 1893-1900.
64. Hugel, B., et al., *Membrane microparticles: two sides of the coin.* Physiology, 2005. **20**(1): p. 22-27.
65. Muralidharan-Chari, V., et al., *Microvesicles: mediators of extracellular communication during cancer progression.* J Cell Sci, 2010. **123**(10): p. 1603-1611.
66. Muralidharan-Chari, V., et al., *ARF6-regulated shedding of tumor cell-derived plasma membrane microvesicles.* Current Biology, 2009. **19**(22): p. 1875-1885.
67. Théry, C., M. Ostrowski, and E. Segura, *Membrane vesicles as conveyors of immune responses.* Nature reviews immunology, 2009. **9**(8): p. 581-593.
68. Luzio, J.P., et al., *ESCRT proteins and the regulation of endocytic delivery to lysosomes*. 2009, Portland Press Limited.
69. Stenmark, H., *Rab GTPases as coordinators of vesicle traffic.* Nature reviews Molecular cell biology, 2009. **10**(8): p. 513-525.
70. Antonin, W., et al., *Crystal structure of the endosomal SNARE complex reveals common structural principles of all SNAREs.* Nature Structural & Molecular Biology, 2002. **9**(2): p. 107-111.
71. White, I.J., et al., *EGF stimulates annexin 1-dependent inward vesiculation in a multivesicular endosome subpopulation.* The EMBO journal, 2006. **25**(1): p. 1-12.

72. Glebov, O.O., N.A. Bright, and B.J. Nichols, *Flotillin-1 defines a clathrin-independent endocytic pathway in mammalian cells.* Nature cell biology, 2006. **8**(1): p. 46-54.
73. Trajkovic, K., et al., *Ceramide triggers budding of exosome vesicles into multivesicular endosomes.* Science, 2008. **319**(5867): p. 1244-1247.
74. Van Niel, G., et al., *The tetraspanin CD63 regulates ESCRT-independent and-dependent endosomal sorting during melanogenesis.* Developmental cell, 2011. **21**(4): p. 708-721.
75. Chairoungdua, A., et al., *Exosome release of β-catenin: a novel mechanism that antagonizes Wnt signaling.* The Journal of cell biology, 2010: p. jcb. 201002049.
76. Bianco, F., et al., *Acid sphingomyelinase activity triggers microparticle release from glial cells.* The EMBO journal, 2009. **28**(8): p. 1043-1054.
77. Savina, A., et al., *Exosome release is regulated by a calcium-dependent mechanism in K562 cells.* Journal of Biological Chemistry, 2003. **278**(22): p. 20083-20090.
78. Savina, A., et al., *Rab11 promotes docking and fusion of multivesicular bodies in a calcium-dependent manner.* Traffic, 2005. **6**(2): p. 131-143.
79. Ostrowski, M., et al., *Rab27a and Rab27b control different steps of the exosome secretion pathway.* Nature cell biology, 2010. **12**(1): p. 19.
80. Hsu, C., et al., *Regulation of exosome secretion by Rab35 and its GTPase-activating proteins TBC1D10A–C.* The Journal of cell biology, 2010. **189**(2): p. 223-232.
81. Chaineau, M., L. Danglot, and T. Galli, *Multiple roles of the vesicular-SNARE TI-VAMP in post-Golgi and endosomal trafficking.* FEBS letters, 2009. **583**(23): p. 3817-3826.
82. Nakano, I., et al. *Extracellular vesicles in the biology of brain tumour stem cells–implications for inter-cellular communication, therapy and biomarker development*. in *Seminars in cell & developmental biology*. 2015. Elsevier.
83. Rialland, P., et al., *BCR-bound antigen is targeted to exosomes in human follicular lymphoma B-cells.* Biology of the Cell, 2006. **98**(8): p. 491-501.
84. Saunderson, S.C., et al., *Induction of exosome release in primary B cells stimulated via CD40 and the IL-4 receptor.* The Journal of Immunology, 2008. **180**(12): p. 8146-8152.
85. Lespagnol, A., et al., *Exosome secretion, including the DNA damage-induced p53-dependent secretory pathway, is severely compromised in TSAP6/Steap3-null mice.* Cell Death & Differentiation, 2008. **15**(11): p. 1723-1733.
86. King, H.W., M.Z. Michael, and J.M. Gleadle, *Hypoxic enhancement of exosome release by breast cancer cells.* BMC cancer, 2012. **12**(1): p. 421.
87. Umezu, T., et al., *Exosomal miR-135b shed from hypoxic multiple myeloma cells enhances angiogenesis by targeting factor-inhibiting HIF-1.* Blood, 2014. **124**(25): p. 3748-3757.
88. Skokos, D., et al., *Mast cell-dependent B and T lymphocyte activation is mediated by the secretion of immunologically active exosomes.* The Journal of Immunology, 2001. **166**(2): p. 868-876.
89. Wang, K., et al., *TNF-α promotes extracellular vesicle release in mouse astrocytes through glutaminase.* Journal of neuroinflammation, 2017. **14**(1): p. 87.
90. Pusic, A.D., et al., *IFNγ-stimulated dendritic cell exosomes as a potential therapeutic for remyelination.* Journal of neuroimmunology, 2014. **266**(1): p. 12-23.
91. Rider, M.A., S.N. Hurwitz, and D.G. Meckes Jr, *ExtraPEG: a polyethylene glycol-based method for enrichment of extracellular vesicles.* Scientific reports, 2016. **6**: p. 23978.

92. Gallart-Palau, X., et al., *Extracellular vesicles are rapidly purified from human plasma by PRotein Organic Solvent PRecipitation (PROSPR).* Scientific reports, 2015. **5**: p. 14664.
93. Nakai, W., et al., *A novel affinity-based method for the isolation of highly purified extracellular vesicles.* Scientific reports, 2016. **6**: p. 33935.
94. Böing, A.N., et al., *Single-step isolation of extracellular vesicles by size-exclusion chromatography.* Journal of extracellular vesicles, 2014. **3**(1): p. 23430.
95. Baranyai, T., et al., *Isolation of exosomes from blood plasma: qualitative and quantitative comparison of ultracentrifugation and size exclusion chromatography methods.* PloS one, 2015. **10**(12): p. e0145686.
96. Li, P., et al., *Progress in exosome isolation techniques.* Theranostics, 2017. **7**(3): p. 789.
97. Heinemann, M.L., et al., *Benchtop isolation and characterization of functional exosomes by sequential filtration.* Journal of Chromatography A, 2014. **1371**: p. 125-135.
98. Yamada, T., et al., *Comparison of methods for isolating exosomes from bovine milk.* Journal of Veterinary Medical Science, 2012. **74**(11): p. 1523-1525.
99. Van Balkom, B.W., et al., *Exosomes and the kidney: prospects for diagnosis and therapy of renal diseases.* Kidney international, 2011. **80**(11): p. 1138-1145.
100. Cantin, R., et al., *Discrimination between exosomes and HIV-1: purification of both vesicles from cell-free supernatants.* Journal of immunological methods, 2008. **338**(1): p. 21-30.
101. Gould, S.J. and G. Raposo, *As we wait: coping with an imperfect nomenclature for extracellular vesicles.* Journal of extracellular vesicles, 2013. **2**(1): p. 20389.
102. Witwer, K.W., et al., *Standardization of sample collection, isolation and analysis methods in extracellular vesicle research.* Journal of extracellular vesicles, 2013. **2**(1): p. 20360.
103. Théry, C., et al., *Isolation and characterization of exosomes from cell culture supernatants and biological fluids.* Current protocols in cell biology, 2006: p. 3.22. 1-3.22. 29.
104. Franquesa, M., et al., *Update on controls for isolation and quantification methodology of extracellular vesicles derived from adipose tissue mesenchymal stem cells.* Frontiers in immunology, 2014. **5**: p. 525.
105. Lötvall, J., et al., *Minimal experimental requirements for definition of extracellular vesicles and their functions: a position statement from the International Society for Extracellular Vesicles.* Journal of extracellular vesicles, 2014. **3**.
106. Kalra, H., et al., *Vesiclepedia: a compendium for extracellular vesicles with continuous community annotation.* PLoS biology, 2012. **10**(12): p. e1001450.
107. Denzer, K., et al., *Follicular dendritic cells carry MHC class II-expressing microvesicles at their surface.* The Journal of Immunology, 2000. **165**(3): p. 1259-1265.
108. Stenqvist, A.-C., et al., *Exosomes secreted by human placenta carry functional Fas ligand and TRAIL molecules and convey apoptosis in activated immune cells, suggesting exosome-mediated immune privilege of the fetus.* The Journal of Immunology, 2013. **191**(11): p. 5515-5523.
109. Segura, E., et al., *ICAM-1 on exosomes from mature dendritic cells is critical for efficient naive T-cell priming.* Blood, 2005. **106**(1): p. 216-223.
110. Morelli, A.E., et al., *Endocytosis, intracellular sorting, and processing of exosomes by dendritic cells.* Blood, 2004. **104**(10): p. 3257-3266.

111. Théry, C., et al., *Molecular characterization of dendritic cell-derived exosomes.* The Journal of cell biology, 1999. **147**(3): p. 599-610.
112. Mulcahy, L.A., R.C. Pink, and D.R.F. Carter, *Routes and mechanisms of extracellular vesicle uptake.* Journal of extracellular vesicles, 2014. **3**(1): p. 24641.
113. Tian, T., et al., *Exosome uptake through clathrin-mediated endocytosis and macropinocytosis and mediating miR-21 delivery.* Journal of Biological Chemistry, 2014. **289**(32): p. 22258-22267.
114. Feng, D., et al., *Cellular internalization of exosomes occurs through phagocytosis.* Traffic, 2010. **11**(5): p. 675-687.
115. Parolini, I., et al., *Microenvironmental pH is a key factor for exosome traffic in tumor cells.* Journal of Biological Chemistry, 2009. **284**(49): p. 34211-34222.
116. Raposo, G., et al., *B lymphocytes secrete antigen-presenting vesicles.* Journal of Experimental Medicine, 1996. **183**(3): p. 1161-1172.
117. Zitvogel, L., et al., *Eradication of established murine tumors using a novel cell-free vaccine: dendritic cell-derived exosomes.* Nature medicine, 1998. **4**(5): p. 594-600.
118. Aline, F., et al., *Toxoplasma gondii antigen-pulsed-dendritic cell-derived exosomes induce a protective immune response against T. gondii infection.* Infection and immunity, 2004. **72**(7): p. 4127-4137.
119. Hao, S., et al., *Epigenetic transfer of metastatic activity by uptake of highly metastatic B16 melanoma cell-released exosomes.* Exp Oncol, 2006. **28**(2): p. 126-131.
120. Al-Nedawi, K., et al., *Intercellular transfer of the oncogenic receptor EGFRvIII by microvesicles derived from tumour cells.* Nature cell biology, 2008. **10**(5): p. 619.
121. Valenti, R., et al., *Human tumor-released microvesicles promote the differentiation of myeloid cells with transforming growth factor-β–mediated suppressive activity on T lymphocytes.* Cancer research, 2006. **66**(18): p. 9290-9298.
122. Danzer, K.M., et al., *Exosomal cell-to-cell transmission of alpha synuclein oligomers.* Molecular neurodegeneration, 2012. **7**(1): p. 42.
123. Rajendran, L., et al., *Alzheimer's disease β-amyloid peptides are released in association with exosomes.* Proceedings of the National Academy of Sciences, 2006. **103**(30): p. 11172-11177.
124. Vella, L., et al., *Packaging of prions into exosomes is associated with a novel pathway of PrP processing.* The Journal of pathology, 2007. **211**(5): p. 582-590.
125. Dougherty, J.A., et al., *Potential Role of Exosomes in Mending a Broken Heart: Nanoshuttles Propelling Future Clinical Therapeutics Forward.* Stem Cells International, 2017. **2017**.
126. Willis, G.R., S. Kourembanas, and S.A. Mitsialis, *toward exosome-Based therapeutics: isolation, Heterogeneity, and Fit-for-purpose potency.* Frontiers in Cardiovascular Medicine, 2017. **4**: p. 63.
127. Lai, R.C., T.S. Chen, and S.K. Lim, *Mesenchymal stem cell exosome: a novel stem cell-based therapy for cardiovascular disease.* Regenerative medicine, 2011. **6**(4): p. 481-492.
128. Lai, R.C., et al., *Proteolytic potential of the MSC exosome proteome: implications for an exosome-mediated delivery of therapeutic proteasome.* International journal of proteomics, 2012. **2012**.
129. Kim, H.-S., et al., *Proteomic analysis of microvesicles derived from human mesenchymal stem cells.* Journal of proteome research, 2011. **11**(2): p. 839-849.

130. Anderson, J.D., et al., *Comprehensive proteomic analysis of mesenchymal stem cell exosomes reveals modulation of angiogenesis via nuclear factor-KappaB signaling.* Stem Cells, 2016. **34**(3): p. 601-613.
131. Chen, T.S., et al., *Mesenchymal stem cell secretes microparticles enriched in pre-microRNAs.* Nucleic acids research, 2009. **38**(1): p. 215-224.
132. Arslan, F., et al., *Mesenchymal stem cell-derived exosomes increase ATP levels, decrease oxidative stress and activate PI3K/Akt pathway to enhance myocardial viability and prevent adverse remodeling after myocardial ischemia/reperfusion injury.* Stem cell research, 2013. **10**(3): p. 301-312.
133. Conforti, A., et al., *Microvescicles derived from mesenchymal stromal cells are not as effective as their cellular counterpart in the ability to modulate immune responses in vitro.* Stem cells and development, 2014. **23**(21): p. 2591-2599.
134. Mokarizadeh, A., et al., *Microvesicles derived from mesenchymal stem cells: potent organelles for induction of tolerogenic signaling.* Immunology letters, 2012. **147**(1): p. 47-54.
135. Di Trapani, M., et al., *Differential and transferable modulatory effects of mesenchymal stromal cell-derived extracellular vesicles on T, B and NK cell functions.* Scientific reports, 2016. **6**.
136. Kilpinen, L., et al., *Extracellular membrane vesicles from umbilical cord blood-derived MSC protect against ischemic acute kidney injury, a feature that is lost after inflammatory conditioning.* Journal of extracellular vesicles, 2013. **2**(1): p. 21927.
137. Umezu, T., et al., *Replenishing exosomes from older bone marrow stromal cells with miR-340 inhibits myeloma-related angiogenesis.* Blood Advances, 2017. **1**(13): p. 812-823.
138. Sun, D., et al., *A novel nanoparticle drug delivery system: the anti-inflammatory activity of curcumin is enhanced when encapsulated in exosomes.* Molecular therapy, 2010. **18**(9): p. 1606-1614.
139. López-Otín, C., et al., *The Hallmarks of Aging.* Cell, 2013. **153**(6): p. 1194-1217.
140. Fukada, S.-i., Y. Ma, and A. Uezumi, *Adult stem cell and mesenchymal progenitor theories of aging.* Frontiers in cell and developmental biology, 2014. **2**.
141. O'Hagan-Wong, K., et al., *Increased IL-6 secretion by aged human mesenchymal stromal cells disrupts hematopoietic stem and progenitor cells' homeostasis.* Oncotarget, 2016. **7**(12): p. 13285.
142. Alt, E.U., et al., *Aging alters tissue resident mesenchymal stem cell properties.* Stem cell research, 2012. **8**(2): p. 215-225.
143. Rübe, C.E., et al., *Accumulation of DNA damage in hematopoietic stem and progenitor cells during human aging.* PloS one, 2011. **6**(3): p. e17487.
144. Mancini, O.K., et al., *Mitochondrial Oxidative Stress Reduces the Immunopotency of Mesenchymal Stromal Cells in Adults with Coronary Artery Disease.* Circulation Research, 2017: p. CIRCRESAHA. 117.311400.
145. Kizilay Mancini, Ö., et al., *A Proinflammatory Secretome Mediates the Impaired Immunopotency of Human Mesenchymal Stromal Cells in Elderly Patients with Atherosclerosis.* Stem Cells Translational Medicine, 2017. **6**(4): p. 1132-1140.
146. Siegel, G., et al., *Phenotype, donor age and gender affect function of human bone marrow-derived mesenchymal stromal cells.* BMC medicine, 2013. **11**(1): p. 146.

147. Fan, M., et al., *The effect of age on the efficacy of human mesenchymal stem cell transplantation after a myocardial infarction.* Rejuvenation research, 2010. **13**(4): p. 429-438.
148. Mareschi, K., et al., *Expansion of mesenchymal stem cells isolated from pediatric and adult donor bone marrow.* Journal of cellular biochemistry, 2006. **97**(4): p. 744-754.
149. Choudhery, M.S., et al., *Donor age negatively impacts adipose tissue-derived mesenchymal stem cell expansion and differentiation.* Journal of translational medicine, 2014. **12**(1): p. 8.
150. Mendes, S., et al., *Bone tissue-engineered implants using human bone marrow stromal cells: effect of culture conditions and donor age.* Tissue engineering, 2002. **8**(6): p. 911-920.
151. Yeh Yeo, R.W., *Efficiency of exosome production correlates inversely with the developmental maturity of MSC donor.* 2013.
152. Fafián-Labora, J., et al., *Effect of age on pro-inflammatory miRNAs contained in mesenchymal stem cell-derived extracellular vesicles.* Scientific Reports, 2017. **7**.
153. Dragovic, R.A., et al., *Sizing and phenotyping of cellular vesicles using Nanoparticle Tracking Analysis.* Nanomedicine: Nanotechnology, Biology and Medicine, 2011. **7**(6): p. 780-788.
154. Atayde, V.D., et al., *Exosome secretion by the parasitic protozoan Leishmania within the sand fly midgut.* Cell reports, 2015. **13**(5): p. 957-967.
155. Ramos, T.L., et al., *MSC surface markers (CD44, CD73, and CD90) can identify human MSC-derived extracellular vesicles by conventional flow cytometry.* Cell Communication and Signaling, 2016. **14**(1): p. 2.
156. Schmittgen, T.D. and K.J. Livak, *Analyzing real-time PCR data by the comparative CT method.* Nature protocols, 2008. **3**(6): p. 1101.
157. Timmers, L., et al., *Reduction of myocardial infarct size by human mesenchymal stem cell conditioned medium.* Stem cell research, 2008. **1**(2): p. 129-137.
158. Dang, R.J., et al., *A20 plays a critical role in the immunoregulatory function of mesenchymal stem cells.* Journal of cellular and molecular medicine, 2016. **20**(8): p. 1550-1560.
159. Colombo, M., et al., *Analysis of ESCRT functions in exosome biogenesis, composition and secretion highlights the heterogeneity of extracellular vesicles.* J Cell Sci, 2013. **126**(24): p. 5553-5565.
160. Baietti, M.F., et al., *Syndecan-syntenin-ALIX regulates the biogenesis of exosomes.* Nature cell biology, 2012. **14**(7): p. 677-685.
161. Pfeffer, S.R., *Two Rabs for exosome release.* Nature cell biology, 2010. **12**(1): p. 3-4.
162. Chua, C.E.L. and B.L. Tang, *Engagement of the small GTPase Rab31 protein and its effector, early endosome antigen 1, is important for trafficking of the ligand-bound epidermal growth factor receptor from the early to the late endosome.* Journal of Biological Chemistry, 2014. **289**(18): p. 12375-12389.
163. Rodriguez-Gabin, A.G., et al., *Transport of mannose-6-phosphate receptors from the trans-Golgi network to endosomes requires Rab31.* Exp Cell Res, 2009. **315**(13): p. 2215-30.
164. Ostrowski, M., et al., *Rab27a and Rab27b control different steps of the exosome secretion pathway.* Nature cell biology, 2010: p. 19-U61.

165. Evans, T.M., et al., *Rab23, a negative regulator of hedgehog signaling, localizes to the plasma membrane and the endocytic pathway.* Traffic, 2003. **4**(12): p. 869-884.
166. Kouranti, I., et al., *Rab35 regulates an endocytic recycling pathway essential for the terminal steps of cytokinesis.* Current biology, 2006. **16**(17): p. 1719-1725.
167. Lorincz, P., et al., *Rab2 promotes autophagic and endocytic lysosomal degradation.* J Cell Biol, 2017. **216**(7): p. 1937-1947.
168. Monier, S., et al., *Characterization of novel Rab6-interacting proteins involved in endosome-to-TGN transport.* Traffic, 2002. **3**(4): p. 289-297.
169. Mallard, F., et al., *Early/recycling endosomes-to-TGN transport involves two SNARE complexes and a Rab6 isoform.* The Journal of cell biology, 2002. **156**(4): p. 653-664.
170. Andreu, Z. and M. Yáñez-Mó, *Tetraspanins in extracellular vesicle formation and function.* Frontiers in immunology, 2014. **5**.
171. Perez-Hernandez, D., et al., *The intracellular interactome of tetraspanin-enriched microdomains reveals their function as sorting machineries toward exosomes.* Journal of Biological Chemistry, 2013. **288**(17): p. 11649-11661.
172. Charrin, S., et al., *Tetraspanins at a glance.* J Cell Sci, 2014. **127**(17): p. 3641-3648.
173. Bartosh, T.J., et al., *Aggregation of human mesenchymal stromal cells (MSCs) into 3D spheroids enhances their antiinflammatory properties.* Proceedings of the National Academy of Sciences, 2010. **107**(31): p. 13724-13729.
174. Gaffield, M.A. and W.J. Betz, *Imaging synaptic vesicle exocytosis and endocytosis with FM dyes.* Nature protocols, 2006. **1**(6): p. 2916-2921.
175. Dolman, N.J., J.A. Kilgore, and M.W. Davidson, *A review of reagents for fluorescence microscopy of cellular compartments and structures, part I: BacMam labeling and reagents for vesicular structures.* Current protocols in cytometry, 2013: p. 12.30. 1-12.30. 27.
176. Mills, C., *Osiris therapeutics announces preliminary results for prochymal phase III GVHD trials.* Press Release, 2009. **available at:** http://investor.osiris.com/releasedetail.cfm?ReleaseID=407404.
177. Meisel, R., et al., *Human bone marrow stromal cells inhibit allogeneic T-cell responses by indoleamine 2, 3-dioxygenase–mediated tryptophan degradation.* Blood, 2004. **103**(12): p. 4619-4621.
178. Chen, P.-M., et al., *Induction of immunomodulatory monocytes by human mesenchymal stem cell-derived hepatocyte growth factor through ERK1/2.* Journal of leukocyte biology, 2014. **96**(2): p. 295-303.
179. Zhang, B., et al., *Mesenchymal stem cells secrete immunologically active exosomes.* Stem cells and development, 2013. **23**(11): p. 1233-1244.
180. Blazquez, R., et al., *Immunomodulatory potential of human adipose mesenchymal stem cells derived exosomes on in vitro stimulated T cells.* Frontiers in immunology, 2014. **5**.
181. Del Fattore, A., et al., *Immunoregulatory effects of mesenchymal stem cell-derived extracellular vesicles on T lymphocytes.* Cell transplantation, 2015. **24**(12): p. 2615-2627.
182. Gouveia de Andrade, A.V., et al., *Extracellular vesicles secreted by bone marrow-and adipose tissue-derived mesenchymal stromal cells fail to suppress lymphocyte proliferation.* Stem cells and development, 2015. **24**(11): p. 1374-1376.
183. Monguió-Tortajada, M., et al., *Nanosized UCMSC-derived extracellular vesicles but not conditioned medium exclusively inhibit the inflammatory response of stimulated T cells: implications for nanomedicine.* Theranostics, 2017. **7**(2): p. 270.

184. Villarroya-Beltri, C., et al., *Sorting it out: regulation of exosome loading.* Semin Cancer Biol, 2014. **28**: p. 3-13.
185. Iraci, N., et al., *Focus on Extracellular Vesicles: Physiological Role and Signalling Properties of Extracellular Membrane Vesicles.* Int J Mol Sci, 2016. **17**(2): p. 171.
186. Akers, J.C., et al., *Biogenesis of extracellular vesicles (EV): exosomes, microvesicles, retrovirus-like vesicles, and apoptotic bodies.* Journal of neuro-oncology, 2013. **113**(1): p. 1-11.
187. Alexander, M., et al., *Rab27-Dependent Exosome Production Inhibits Chronic Inflammation and Enables Acute Responses to Inflammatory Stimuli.* The Journal of Immunology, 2017. **199**(10): p. 3559-3570.
188. Beninson, L.A. and M. Fleshner, *Exosomes: an emerging factor in stress-induced immunomodulation.* Semin Immunol, 2014. **26**(5): p. 394-401.
189. Kolhe, R., et al., *Gender-specific differential expression of exosomal miRNA in synovial fluid of patients with osteoarthritis.* Scientific Reports, 2017. **7**.
190. Kimura, K., et al., *Circulating exosomes suppress the induction of regulatory T cells via let-7i in multiple sclerosis.* Nature communications, 2018. **9**(1): p. 17.
191. Wang, Y., et al., *MiR-548a-3p regulates inflammatory response via TLR4/NF-κB signaling pathway in rheumatoid arthritis.* Journal of cellular biochemistry, 2018.
192. György, B., et al., *Improved flow cytometric assessment reveals distinct microvesicle (cell-derived microparticle) signatures in joint diseases.* PloS one, 2012. **7**(11): p. e49726.
193. Colombo, M., G. Raposo, and C. Théry, *Biogenesis, secretion, and intercellular interactions of exosomes and other extracellular vesicles.* Annual review of cell and developmental biology, 2014. **30**: p. 255-289.
194. Rafei, M., et al., *Mesenchymal stromal cells ameliorate experimental autoimmune encephalomyelitis by inhibiting CD4 Th17 T cells in a CC chemokine ligand 2-dependent manner.* The Journal of Immunology, 2009. **182**(10): p. 5994-6002.
195. Qu, X., et al., *Mesenchymal stem cells inhibit Th17 cell differentiation by IL-10 secretion.* Experimental hematology, 2012. **40**(9): p. 761-770.
196. Groh, M.E., et al., *Human mesenchymal stem cells require monocyte-mediated activation to suppress alloreactive T cells.* Experimental hematology, 2005. **33**(8): p. 928-934.
197. Djouad, F., et al., *Mesenchymal stem cells inhibit the differentiation of dendritic cells through an interleukin-6-dependent mechanism.* Stem cells, 2007. **25**(8): p. 2025-2032.
198. Selmani, Z., et al., *Human leukocyte antigen-G5 secretion by human mesenchymal stem cells is required to suppress T lymphocyte and natural killer function and to induce CD4+ CD25highFOXP3+ regulatory T cells.* Stem cells, 2008. **26**(1): p. 212-222.
199. Harding, C., J. Heuser, and P. Stahl, *Receptor-mediated endocytosis of transferrin and recycling of the transferrin receptor in rat reticulocytes.* The Journal of cell biology, 1983. **97**(2): p. 329-339.
200. Pan, B.-T. and R.M. Johnstone, *Fate of the transferrin receptor during maturation of sheep reticulocytes in vitro: selective externalization of the receptor.* Cell, 1983. **33**(3): p. 967-978.
201. Smyth, L.A., et al., *CD73 expression on extracellular vesicles derived from CD4+ CD25+ Foxp3+ T cells contributes to their regulatory function.* European journal of immunology, 2013. **43**(9): p. 2430-2440.

202. Wang, S., et al., *Synapsin I is an oligomannose-carrying glycoprotein, acts as an oligomannose-binding lectin, and promotes neurite outgrowth and neuronal survival when released via glia-derived exosomes.* Journal of Neuroscience, 2011. **31**(20): p. 7275-7290.
203. Vrijsen, K., et al., *Cardiomyocyte progenitor cell-derived exosomes stimulate migration of endothelial cells.* Journal of cellular and molecular medicine, 2010. **14**(5): p. 1064-1070.
204. Admyre, C., et al., *Exosomes with immune modulatory features are present in human breast milk.* The Journal of immunology, 2007. **179**(3): p. 1969-1978.
205. Zhou, Q., et al., *Immune-related microRNAs are abundant in breast milk exosomes.* International journal of biological sciences, 2012. **8**(1): p. 118.
206. Sabapatha, A., C. Gercel-Taylor, and D.D. Taylor, *Specific Isolation of Placenta-Derived Exosomes from the Circulation of Pregnant Women and Their Immunoregulatory Consequences.* American Journal of Reproductive Immunology, 2006. **56**(5-6): p. 345-355.
207. Lenassi, M., et al., *HIV Nef is secreted in exosomes and triggers apoptosis in bystander CD4+ T cells.* Traffic, 2010. **11**(1): p. 110-122.
208. Corrado, C., et al., *Exosome-mediated crosstalk between chronic myelogenous leukemia cells and human bone marrow stromal cells triggers an interleukin 8-dependent survival of leukemia cells.* Cancer letters, 2014. **348**(1): p. 71-76.
209. Teng, X., et al., *Mesenchymal stem cell-derived exosomes improve the microenvironment of infarcted myocardium contributing to angiogenesis and anti-inflammation.* Cellular Physiology and Biochemistry, 2015. **37**(6): p. 2415-2424.
210. Chen, W., et al., *Immunomodulatory effects of mesenchymal stromal cells-derived exosome.* Immunologic research, 2016. **64**(4): p. 831-840.
211. Bernardo, M.E., et al., *Human bone marrow–derived mesenchymal stem cells do not undergo transformation after long-term in vitro culture and do not exhibit telomere maintenance mechanisms.* Cancer research, 2007. **67**(19): p. 9142-9149.
212. Baxter, M.A., et al., *Study of telomere length reveals rapid aging of human marrow stromal cells following in vitro expansion.* Stem cells, 2004. **22**(5): p. 675-682.
213. Stolzing, A., et al., *Age-related changes in human bone marrow-derived mesenchymal stem cells: consequences for cell therapies.* Mechanisms of ageing and development, 2008. **129**(3): p. 163-173.